
DNA-based molecular templates and devices

Stefan Beyer



München 2005

DNA-based molecular templates and devices

Stefan Beyer

Dissertation der Fakultät für Physik
der Ludwig-Maximilians-Universität München

vorgelegt von
Stefan Beyer
aus Gräfelfing

München, den 23.12.2005

Erstgutachter: Prof. Dr. J. P. Kotthaus
Zweitgutachter: Prof. Dr. J. O. Rädler
Tag der mündlichen Prüfung: 20.2.2006

Zusammenfassung der Dissertation

Unter dem Begriff „Nanotechnologie“ sind Bestrebungen verschiedener naturwissenschaftlicher Disziplinen zusammengefasst, Strukturen und Systeme in einer Größenordnung von einem bis einhundert Nanometern zu entwickeln. In der vorliegenden Arbeit werden mit Methoden aus Physik, Biochemie und Mikrosystemtechnik künstliche Systeme aus DNS-Molekülen hergestellt, modifiziert und charakterisiert. Nach einem einleitenden Kapitel über DNS als Konstruktionsmaterial werden im ersten Teil komplexe Strukturen beschrieben, die auf einem Substrat adsorbiert sind. Im zweiten Teil werden nanomechanische und Informations verarbeitende Einheiten in Lösung vorgestellt.

Um selbstorganisierte Oberflächenstrukturen als Grundlage für die nächste Generation von integrierten Schaltkreisen verwenden zu können, müssen einige grundsätzliche Probleme überwunden werden. Hierzu werden in dieser Dissertation zwei Fragestellungen bearbeitet. Erstens ist DNS ein Isolator und muss mit leitfähigem Material modifiziert werden, um als Grundlage für Schaltkreise dienen zu können. Verschiedene Methoden der Synthese von Polyanilin an DNS werden dazu untersucht und die halbleitenden Eigenschaften der entstehenden molekularen Drähte durch Leitfähigkeitsmessungen nachgewiesen. Das zweite Problem ist die Selbstorganisation von periodischen Formen. Dies wird am Beispiel der enzymatischen Herstellung einer linearen Struktur mit Bindungsstellen für Nanopartikel demonstriert. Goldcluster, Proteine oder Halbleiter-Nanokristalle können so einzeln oder kombiniert in exakt definierten Abständen angeordnet werden. Hierzu wurde eine Methode aus der Molekularbiologie erweitert, um die Herstellung dieser Template auf eine einfache und effektive Weise zu ermöglichen.

Im Vergleich zu der weit fortgeschrittenen Miniaturisierung in der Chipindustrie befindet sich die Miniaturisierung von komplexen Maschinen gegenwärtig noch im Anfangsstadium. Andere physikalische Bedingungen und fehlende Manipulationsmöglichkeiten auf der Nanometerskala zwingen dazu, neue Konzepte für deren Erzeugung finden. In der Natur existieren bereits gut funktionierende Vorbilder, die auf Selbstorganisation von organischen Molekülen beruhen: Proteine stellen die funktionellen Einheiten aller lebenden Organismen dar und erledigen Aufgaben von hoher Komplexität. Im Rahmen dieser Arbeit werden zwei aus Nukleinsäuren gebildete nanoskopische Einheiten vorgestellt, die einfache Aktionen ausführen können. Die erste besteht aus einer dreidimensional gefalteten DNS, die spezifisch an ein Protein kann. In diesem so genannten Aptamer wird die Spezifität durch die Basenabfolge des Einzelstranges bestimmt. Es wird untersucht, in wie weit dessen Modifizierung und Erweiterung seine Fähigkeit beeinflusst, das für die Blutgerinnung relevante Protein Thrombin zu binden. Zweitens wird die Konstruktion und Funktion einer aus DNS konstruierten Steuereinheit beschrieben. Ihre Aufgabe ist es, das Schalten von Aptameren unabhängig von deren Basensequenz zu machen. Darüber hinaus kann damit der Funktion des Aptamers eine „Logik vorgeschaltet“ werden, die autonom auf bestimmte Zustände reagiert und die Bindefähigkeit des Aptamers moduliert.

Abstract

The term “nanotechnology” encompasses efforts of different scientific disciplines to develop structures and applications of the size of one to one hundred nanometers. This work presents artificial systems comprised of deoxyribonucleic acid (DNA) molecules that are synthesized, modified and characterized by methods related to physics, biochemistry and micro-engineering.

After an introductory chapter on DNA properties, complex DNA structures that are adsorbed on a surface are described in the first part. The second part introduces nanomechanical and information-processing devices in solution.

Some fundamental problems have to be solved before self-organized surface structures can be used as templates for next generation integrated circuits. First, DNA is an insulating material and has to be modified accordingly to be useful as a building block for an electronic circuit. Different methods of polyaniline synthesis along DNA strands are investigated in this thesis to overcome this problem. The semiconducting properties of the resulting nanowires are verified by conductivity measurements.

The second problem is self-assembly of periodic structures. This is demonstrated with enzymatic synthesis of a linear structure with anchor sites for nano-particles. Gold clusters, proteins or semiconductor nanocrystals can so be accurately aligned, either one kind exclusively or combined with others. A method from molecular biology was expanded to allow the simple and effective synthesis of these templates.

In comparison to the progress of miniaturization in chip technology, the miniaturization of complex machines is still in the beginning stage. Different physical circumstances and the difficult manipulation of objects on the nanometer scale demand to find new concepts for the fabrication of nanodevices. Nature provides well functioning examples of nanomachines that are based on self-assembled biomolecules: Proteins are the functional units of all living organisms and perform tasks of high complexity. In the course of this thesis two nucleic acids-based devices are presented that can conduct simple actions.

The first one consists of a three-dimensionally folded DNA-strand which binds specifically to a protein. The specificity of this so called aptamer is determined by the base sequence of the DNA-strand. To investigate the integration of an aptamer in more complex systems, the influence of modifications to the aptamer on its ability of binding the protein thrombin was analyzed.

The second part describes the construction and function of an aptamer control unit comprised of DNA strands. It was built for the purpose to make the operation of aptamer devices independent from their base-sequence. Furthermore, this control unit can perform simple logical operations which could modulate the binding capability of the aptamer autonomously, based on existing environmental conditions.

Contents

Zusammenfassung	v
Abstract	vii
List of Figures	xii
1 Introduction	1
1.1 Nano-Structures on Surfaces	2
1.1.1 Present Advances and Problems in Si-based Chip Technology	2
1.1.2 A Bottom-up Approach to Surface Structures	3
1.2 Mechanical Devices on Nanometer Scale	4
1.2.1 Miniaturized Machines	4
1.2.2 Self-Assembled Nanodevices	5
1.2.3 Nanomechanical DNA-Devices	5
2 DNA and Self-Assembly	7
2.1 Structure and Physical Properties of DNA	7
2.1.1 The Structure of DNA	7
2.1.2 Optical Properties	9
2.1.3 Mechanical Properties	10
2.1.4 Thermodynamical Considerations	11
2.1.5 Electronical Properties	12
2.2 Self-organization	13
3 DNA Templated Structures	17
3.1 DNA as a Scaffold for Integrated Circuits	17
3.1.1 DNA Metallization	17
3.1.2 Reference [1]: Polyaniline Synthesis Templated by DNA	20
3.2 Complex DNA Structures	21
3.2.1 Synthesis of DNA	23
3.2.2 Reference [2]: Periodic DNA Nanotemplates Synthesized by Rolling Circle Amplification	23

4	DNA Based Mechanical Devices	27
4.1	Aptamers	28
4.1.1	Introduction to Aptamers	28
4.1.2	Reference [3]: Design Variations of an Aptamer-based DNA Nanode- vice	29
4.2	DNA Logic Devices	30
4.2.1	Introduction to DNA Devices	30
4.2.2	DNA Device Overview	31
4.2.3	Allosteric Aptamer Device	33
4.2.4	Reference [4]: A Modular DNA Signal Transducer for the Controlled Release of a Protein by an Aptamer	36
5	Outlook	39
6	Appendix	41
	Reference [1]	A1
	Reference [2]	A7
	Reference [3]	A11
	Reference [4]	A17
	Bibliography	67

List of Figures

2.1	Chemical structure of DNA backbone (left) and bases (right).	8
2.2	Two representations of a B-form DNA double helix.	8
2.3	Set of Wang tiles, sufficient for non-periodical coverage of the 2D plane. . .	14
3.1	To test if metallized DNA is still capable of hybridization, two different strands with sticky ends were prepared from plasmids. One of them was metallized and mixed with an other non-metallized strand, the result was analyzed by gel electrophoresis and atomic force microscopy.	18
3.2	A: AFM image of a platinized DNA strand. B: Agarose gel migration assay comparing the hybridization of platinized and non-platinized DNA fragments.	19
3.3	Structure of an aniline monomer (A) and polyaniline (B).	20
3.4	Topology of double (DX) and triple (TX) crossover building blocks. The grey bars indicate the interwoven double helices.	22
3.5	Principle of the rolling circle amplification process.	24
4.1	Structure of thrombin-aptamer complex, derived from X-ray analysis. The representation of the aptamer on the right side displays the two G-quadruplexes of the armchair-like binding motif.	28
4.2	Design variations of a thrombin-binding aptamer device. The basic aptamer (red) was extended by additional bases (blue) and fluorophores (green). . .	30
4.3	Simplified working principle of the aptamer device. Trigger strand T has to be complementary to the aptamer sequence A (red). A is determined by the shape of the binding motif that is specific to the ligand (yellow), in this case thrombin. Therefore the trigger sequence T can not be chosen freely.	33
4.4	Working principle of the proposed aptamer device. Trigger strand T* (green) induces a conformational change in the binding region, which sets the ligand (yellow) free. T* does not hybridize directly to the protein-specific region (red) and can be of an arbitrary sequence. The aptamer A (black) is different from the aptamer in Figure 4.3 and Figure 4.2.	34
4.5	Gel analysis of the allosteric aptamer device. Lane 1 and 2 contain the enabled aptamer, lane 3 and 4 the disabled aptamer, each without and with thrombin.	35

- 4.6 Principle of the DNA sequence translator. Sequence **T*** can be chosen independently from the aptamer sequence **A** 35
- 4.7 Operation DNA translation device: A short input sequence (**IN**) induces the activation of an actuator strand (**OUT**→**OUT***). 36

Figures contain graphics designed or edited by Denise Chlosta

1 Introduction

Nanotechnology is the superordinate concept of scientific and engineering activities that deal with length scales in the range of 0.1 to 100 nm. In contrast to physics, chemistry and biology, where research on these dimensions has been conducted for years for the sake of increasing knowledge, the goal of nanotechnology is the development of new materials and applications.

Traditional nanotechnology aimed at the miniaturization of structures and machines that already exist in the “non-nano” world. In 1956 Richard Feynman was the first scientist to suggest that these could someday be fabricated on atomic scale. It took till the early 1980s until new analytical techniques like AFM (atomic force microscopy) and STM (scanning tunnelling microscope) allowed visualization of features as small as 1 nm. In the same decade older technologies like SEM and TEM (scanning and transmission electron microscopy) became technically mature and commercially available and also affordable. Decreasing structure sizes led to the incorporation of surface chemistry, necessary for the handling of structures with a high surface-to-volume ratio. With the integration of biological and biophysical methods in the late 1990s, nanotechnology has opened towards medical and pharmaceutical applications. Since then, computer science has become important for the modelling of complex systems and prediction of self-organized structures.

Nanotechnology can be divided into two branches that are defined by their sample preparation strategies. The initial one is called top-down strategy, structures are here defined through removing or changing surface material of large substrates. The present semiconductor industry is based on this technology. It has reached an extremely advanced state but its limitations are becoming visible. The other branch, termed bottom-up, is a constructive approach where the final structure is composed of building blocks. Since these building blocks, which of course have to be smaller than the product, are very difficult to handle, this discipline relies heavily on self-organization.

Deoxyribonucleic acid (DNA) has established itself as the most promising material for the construction of self-organizing building blocks. The introduction of this cumulative thesis sets the background for four publications in the field of DNA nanotechnology. They are put into the context of other key publications and most recent developments of this discipline.

There is a large overlap between top-down and bottom-up strategies and in all likelihood the future of nanotechnology lies in the combination of both. In the following sections they will be compared in the context of structures on surfaces and nano-mechanical devices in solution. The advantages of DNA-based structures will be discussed and compared to other self-organizing materials.

1.1 Nano-Structures on Surfaces

1.1.1 Present Advances and Problems in Si-based Chip Technology

In 2005 the semiconductor industry celebrates the 40th birthday of Moore's law. In 1965 Gordon E. Moore predicted the doubling of the number of components on computer chips every year for the next 10 years. In its revised form of 1975 it is still valid today: Every 24 months the complexity of computer chips is doubled¹.

The most recent advances drive the technology on the tracks of Moore's law towards the feature width of 65 nm, prototypes thereof were presented recently. Layers of strained silicon and so called "high-k" dielectric materials improve the drive current while reducing leakage through transistor gates. Silicon-on-insulator (SOI) architectures insulate the structures electrically against the bulk silicon and further reduce power dissipation.

Other more general advances in chip technology are helping to reduce costs and increase computing power. The introduction of copper as conducting material and the 300 mm wafer technology are important breakthroughs in material science. Conceptual changes like multiprocessor architecture or 64 bit logic increase the computational power. Future generations of semiconductor chips are planned to be based on a 45 nm line width technology, made possible through extreme ultra violet (EUV) lithography with a wavelength of 13 nm. Even though this development casts an optimistic light on the future of semiconductor chip technology, a diversity of problems raise the need for alternative concepts.

The cost per transistor sank dramatically with the advance of chip technology, but the investment cost for new chip production lines almost doubles from one to the next. A similar development in the design costs leads to decreasing numbers of different chip designs every year. Chip manufacturers have to sell larger and larger quantities of the same chips to be profitable.

The technology for the fabrication of structures smaller than 65 nm is prototyped already. It will be based on short wavelength UV (EUV), X-ray lithography will be the next logical step. However this technology is still extremely challenging. Optical components must be made with a higher precision than required for the largest telescopes. The brightness of the light source still requires significant improvement and the lithographic process itself has yet to be developed. New non-diffractive optical systems are necessary when even shorter wavelengths are used for exposure.

¹This value depends on the definition of complexity and can be applied especially to systems, where complexity scales with integration density.

As process technologies advance to 90 nm and below, it is increasingly difficult and time-consuming to achieve design closure using conventional tools. The complex interdependencies of new nanometer effects on signal and power integrity, and on-chip variation cannot be analyzed in conventional ways. The growing design complexity creates enormous capacity and runtime challenges. As a result, turnaround time and costs rise dramatically.

1.1.2 A Bottom-up Approach to Surface Structures

Well proven methods already exist for the fabrication of structures smaller than those of current chip industry. Electron beam and AFM imprint lithography can reliably define structures below 10 nm. Unfortunately these techniques are unsuitable for large scale applications because of their serial character². One feature has to be written after the other, which makes the production of a complex chip extremely time intensive and thus costly. Therefore other, parallel methods need to be developed, like the self-organization of surface bound templates.

Several systems have been under investigation for the self-assembly of surface structures. Most established are so called **block-copolymers**. These linear polymers are composed of linked shorter homo-polymeric chains [5]. The subsections are usually of different polarizabilities, so that for example in aqueous solution, their more hydrophobic parts aggregate and simple structures are formed. Micelles, ordered lamellae, cylinders and other more complex phases exist between completely disordered phases in their phase diagram. By tuning parameters like concentration, chain length or chain composition, the formation of surface structures can be influenced.

Proteins are also candidates for surface patterning with so called **S-layer proteins** as widely used model system. Being components of the outermost layer of the cell wall of many bacteria, they are robust enough to survive the adsorption onto a surface without denaturation [6]. After extraction from the organism and purification, S-layer proteins can recrystallize in square, oblique or hexagonal lattices of long range order. The pore sizes in these lattices range between 1.5 and 8 nm.

Structures with lattice constants below 1 nm self-organize when layers of **small organic molecules** (e.g. trimesic acid, [7]) are deposited on carbon surfaces. High lateral mobility that can be influenced by regulating the substrate temperature leads to the formation of a crystal lattice, which is stabilized by hydrogen bonds between neighboring molecules.

²An exception to this is the IBM “millipede”, an array of 1024 cantilever tips for parallel read/write operations (<http://www.research.ibm.com/journal/rd/443/vettiger.html>).

Carbon nanotubes (CNT) have only poor self-organization capabilities by themselves, but in combination with other materials they have the highest potential to be part of a new type of integrated circuit. CNTs display excellent conductive properties, their synthesis is simple and they can play a dual role as metal-like and semiconducting material in molecular electronics. In the next CPU generation they might be employed as vias, i.e. interconnections between two layers of a chip.

DNA displays a combination of properties that makes it superior to all the other materials mentioned above. Block-copolymers or small organic molecules have only few possible ways of interaction and can therefore assume only a limited number of different shapes. A DNA strand can encode information in up to 10^6 base pairs with a very high information density: One bit comprised of one base pair occupies the volume of roughly 1 nm^3 , this is a prerequisite for the formation of complex structures of nanometer size.

Furthermore the encoded information can also determine the three dimensional shape of a single DNA strand. Proteins have a comparable information content and even wider possibilities for assuming three-dimensional shapes, but their fragility and laborious extraction from cells have prevented scientists from utilizing their full self-assembly capabilities. Not to be underestimated is the fact that DNA has been focus of research and development for a long time. A rich toolbox of enzymes and standard protocols makes this biomolecule accessible even to physicists and computer engineers.

Section 3.2.2 describes the combination of an established protocol from molecular biology and newly developed technologies to produce arrays of nano-particles.

One of the drawbacks of DNA and proteins in the context of molecular electronics is their low electronic conductance. Integrated circuits need semiconducting material for the active elements and metallic wires to connect them. A more detailed description of this problem and possible solutions with the modification of DNA is given in section 3.1.1.

1.2 Mechanical Devices on Nanometer Scale

1.2.1 Miniaturized Machines

The public impression of nanomechanical devices is much influenced by the late 1980s picture of a nano-robot that clears our blood vessels from calcification. It looks like a futuristic submarine with the dimensions of a few 100 nm, but makes no concessions to the physical conditions of the nano-world whatsoever.

Compared to the computer chip industry, miniaturization of devices in other fields of application is slow. The integration density of fluid handling systems made a sudden leap with the introduction of soft polymer materials like PDMS [8]. Miniaturization of mechanical systems is still mostly limited to simple setups like resonators. They find application as filters, acceleration and mass sensors and gyroscopes. Only few actuation units like nano-tweezers [9] have entered the nano-regime in the last decade.

The miniaturization of *complex* machines is still extremely challenging beyond the micrometer scale. So far, our arteries are still not populated with maintenance submarines.

Yet in nature there exist machines for every possible task on a nanometer scale. Proteins cover the whole spectrum of sensors, motors, energy management, chemical synthesis and regulation. Linear motors (actin/myosin or the microtubule/kinesin system), rotors (ATPases or the rotational complex of bacterial flagella) and machines of high complexity (RNA polymerase, the light harvesting complex in chloroplasts, etc) which have been working for millions of years. Simpler “machines” based on nucleic acids supposedly preceded this protein-based world. Almost all enzymatic reactions regarding DNA have been already demonstrated by short RNA strands, so-called ribozymes [10].

1.2.2 Self-Assembled Nanodevices

Current usage of nanodevices falls into two categories. **Proteins** are used widely, in research or commercial applications, either in their natural form or modified by genetic engineering. Enzymes play a big role in food and pharmaceutical industry and gain importance every year. Beer and cheese has been produced for millennia with the help of what we call today nanodevices. This is very convenient with well established processes, but for each new function an already existing protein has to be found, eventually genetically altered, and isolated. So far it is very difficult to manufacture protein-based nanodevices from scratch, because there is no reliable way to predict the three-dimensional structure of a protein from the amino acid sequence alone.

On the other hand, nanodevices can be built bottom-up on an even smaller scale. Prototypes have been developed displaying basic rotational and translational motion. The first structures were based on **rotaxanes** [11], newer designs included **fullerenes** [12]. All these devices are still only of academic interest and their applicability is still unclear.

1.2.3 Nanomechanical DNA-Devices

DNA-based nanodevices are in between these two groups. Most of them are item of basic research, but one class of DNA structures serves as a base for a growing number of commercial applications. Short DNA strands with pronounced tertiary structure, called aptamers, have found to be useful in detection, immobilization and controlled release of proteins, small molecules or ions. They can operate surface bound and in solution. Aptamers cannot be called “device” on their own, but can form the active center of nanometer-sized devices that are operated by short DNA strands [13].

It is clear that for almost all scenarios nanomachines have to work in liquid environment. The forces on the nanometer scale are dominated by dipole and electrostatic interactions, which can only be satisfactorily controlled in solvents. Without control, small mobile elements would aggregate after a short time span according to their polarizability and result in stable nano-piles of junk.

Equally important is the three dimensional diffusion of material that is possible in liquids. Construction material and information has to be brought to the machines, waste needs to be removed.

As mentioned above, DNA is the most promising candidate for the self-assembly of complex structures because of its high information density. For small devices it has an additional advantage: Due to the difference in persistence length of double-stranded and single-stranded DNA, it can be used as structural material and flexible junction simultaneously. DNA also fulfills basic practicability requirements for nanotechnological construction materials: It is sufficiently stable and can be produced and handled without much effort. Proteins have more possibilities for internal interactions like sulfur bonds or hydrophobic interaction, while DNA is limited mostly to the hydrogen bonds between base pairs to form tertiary structures. But this increase in versatility of proteins is curbed by synthesis and handling difficulties and the problem to derive the three dimensional structure from the amino acid sequence.

Two different DNA-nanodevices are presented in chapter 4: The first device is based on an aptamer and can cyclically bind and release the blood-clotting agent thrombin. The second device translates information encrypted in DNA strands into strands that can trigger nanodevices.

2 DNA and Self-Assembly

2.1 Structure and Physical Properties of DNA

The ability of deoxyribonucleic acid (DNA) to store and transmit genetic information from one generation to the next is a fundamental condition for life. Therefore its properties and interaction with other bio-molecules has been intensely investigated in the life sciences. Despite of its unusually high charge density, DNA also serves as a model system in polymer physics. Like no other polymer it can be produced in different lengths spanning five orders of magnitude with a monodisperse length distribution.

A Short History

Friedrich Miescher was the scientist who started the biochemical investigation of the DNA molecule. In 1868 he isolated the acidic substance “nuclein” and suspected a connection between this substance and cellular inheritance, but found no proof. It took until 1944, when Avery, McLeod and McCarty gathered evidence for this theory: Transfer of DNA turned non-virulent bacteria into their virulent form. In the late 1940s, Chargaff isolated nucleotide bases from various organisms and derived several rules for appearance and ratios of bases that formed the foundation for further research on DNA. By tracing radioactively labelled DNA in transfection experiments, Hershey and Chase could disperse still existing doubts about the role of DNA as genetical storage molecule in 1952. In 1953 the complete structure of the molecule was revealed. Franklin and Wilkins performed the first successful X-ray diffraction experiments on DNA fibers. From the diffraction pattern they could deduce that DNA is a helical molecule with two periodicities which were later identified as distance between two base pairs and length of one helix turn. Watson and Crick finished in the same year the three-dimensional picture of the double helix with two antiparallel strands, connected by pairs of complementary bases [14].

2.1.1 The Structure of DNA

Single stranded DNA (ssDNA) is a heteropolymer that consists of nucleoside units linked together via phosphates. The nucleosides are comprised of a monosaccharide, deoxyribose, attached to its 1' carbon atom is one of four so-called bases: adenine, cytosine, guanine or thymine (Fig. 2.1).

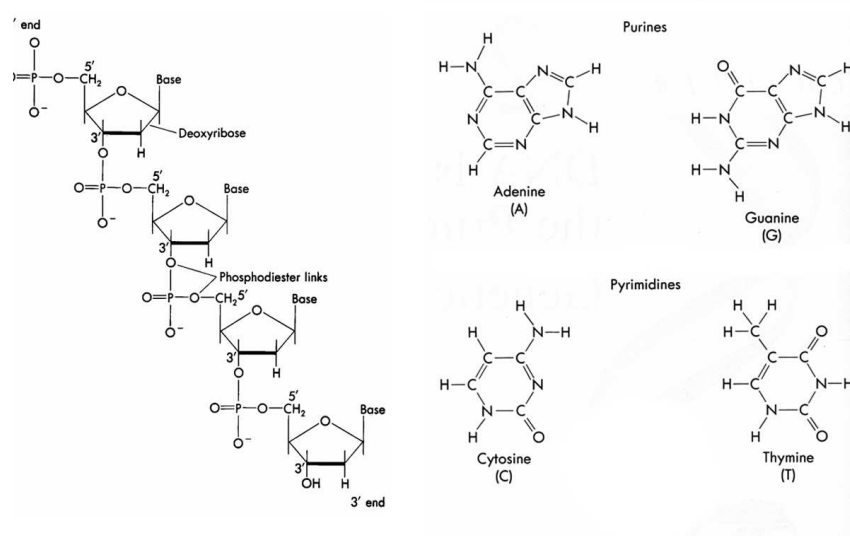


Figure 2.1: Chemical structure of DNA backbone (left) and bases (right).

A direction can be assigned to single DNA strands: One end of the DNA terminates with a hydroxyl group at the 3' C atom (the 3' end), whereas the other end terminates with a phosphate group at the 5' C atom (the 5' end). All sequences of DNA are usually written from 5' to 3' end. Directionality is not only of theoretical interest, most of the enzymes are aware of the direction and act accordingly.

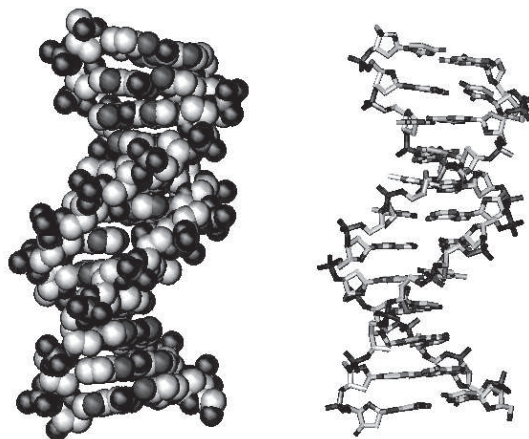


Figure 2.2: Two representations of a B-form DNA double helix.

Two single strands can bind together (hybridize) to form a right-handed double helix (dsDNA), provided that they are complementary, i.e. that every base must find its appropriate Watson-Crick partner (A-T, G-C). Guanine and cytosine can bind with three,

thymine and adenine with two hydrogen bonds, which makes the G-C bonds more stable. When hybridized, the two single strands are always in antiparallel orientation. The offset pairing of the two strands creates a major and a minor groove. Under physiological buffer conditions (pH 7, 100mM monovalent salt) a DNA double helix exists in its “B” form. The diameter of the helix is 2 nm, one turn (10.5 base pairs) stretches over 36 nm, the distance between two adjacent base pairs (bp) is 3.4 Å. Other conformations like an “A” form (righthanded, diameter 2.6 nm, 11 bp per turn) or “Z” form (lefthanded, diameter 1.8 nm, 12 bp per turn) are possible in special buffer or hydration conditions.

2.1.2 Optical Properties

Electronic Absorption

Total absorbance of a polynucleotide depends on the sum of absorbances of the single nucleotides plus the effect of interactions among the nucleotides. These interactions cause a single strand to absorb less than the sum of its nucleotides, a double strand less than the two single strands. This effect is called hypochromism or hypochromicity. The 260 nm absorption peak of DNA is the result of superposition of in-plane transitions between π electrons of the bases ($\pi - \pi^*$). Excitations out of plane of non-binding electrons ($n - \pi^*$) are weaker and negligible for absorption experiments. Sugars and phosphates contribute to the absorbance mainly below 190 nm. This conflicts with the opacity of water below 180 nm and is of no practical importance [15].

Circular Dichroism

Another optical property is based on the chirality of the DNA molecule: Circular dichroism (CD) is the difference in light absorption for incident left and right circularly polarized light. CD spectra can be of the same resolution as absorption spectra, they reveal more information, such as base stacking, but the experimental setup is more sophisticated.

In DNA, chirality is derived from chiral centers of the sugar groups; bases and phosphate groups are identical to their mirror image and do not contribute. Since only *D* isomers of deoxyribose are built into DNA, the chiral character is preserved within the whole strand.

Application: UV/Vis Spectroscopy

The most common practical use of the absorption of DNA is the determination of molar concentration by UV absorption spectroscopy. The optical density A of the sample can be measured and its concentration derived according to

$$A = \varepsilon lc.$$

l is the path length in centimeter through the sample, ε the molar extinction coefficient, which can be calculated for each base sequence. With a path length $l = 1$ cm the average

mass for 1 OD is 50 μg for double stranded, 33 μg for single stranded DNA.

Hypochromicity of DNA can be used to determine the “melting temperature” T_m of DNA strands or constructs (see section 2.1.4). An absorption vs. temperature curve is recorded where the temperature of the sudden rise in absorbance marks the separation of the strands.

2.1.3 Mechanical Properties

Bending

Different models describe the mechanical properties for polymers of different flexibilities. Very rigid molecules or structures like microtubuli can be modelled as cylindrical rods with length L_0 and radius b . Only very short (<50 nm) dsDNA can be described this way. Very flexible polymers are described with the random coil model. Chains of N spherical units of diameter b are attached to each other in a way that allows complete rotational freedom. This leads to the relation between the mean square end-to-end distance L and b :

$$\langle L^2 \rangle = b^2 N$$

Single-stranded DNA can be well characterized in this way.

In between these two extremes, the Worm-Like Chain (WLC) model has been established as the most accurate model for the description of dsDNA. It takes into account the local stiffness and the long-range flexibility of the molecule. Basic parameters are contour length L_0 (length of the stretched polymer) and persistence length a , which equals the distance at which the correlation of two tangent vectors has decreased to $1/e$:

$$\langle \cos(\theta_s - \theta_0) \rangle = e^{-s/a}$$

The persistence length is related to the bending modulus κ_b :

$$a = \frac{\kappa_b}{k_B T}$$

Under normal conditions, 100 mM monovalent salt, 300 K temperature, the persistence length of dsDNA is 50 nm, of ssDNA 1 nm.

Stretching

The behavior of polymers under stretching forces follows Hooke’s law for low forces. The spring constant κ_s can be derived from the respective models for single and double strands. For single strands it equals

$$\kappa_s = \frac{3k_B T}{b}$$

In the case of double strands κ_s depends on the persistence length a :

$$\kappa_s = \frac{3k_B T}{2a}$$

A more detailed description and the behavior in the high force regime can be found in [16].

2.1.4 Thermodynamical Considerations

Entropic Elasticity

The above descriptions of mechanical properties of polymers are incomplete because they do not contain thermal fluctuations and entropic effects [17]. Even though it costs no bending energy, a random coil will resist elongation because of the resulting negative ΔS . In a chain with an end-to-end distance of 10% of the contour length, many more configurations exist than for a 99% stretched state. The result is called entropic elasticity, the relation of force F and extension x can be described with

$$\frac{F a}{k_B T} = \frac{1}{4} \left(1 - \frac{x}{L_0} \right)^{-2} - \frac{1}{4} + \frac{x}{L_0}.$$

L_0 is the contour length of the polymer.

Duplex Formation and Melting Behavior

The mechanisms of the formation of a double helix from two single strands is very complex and thus hard to model quantitatively. Contrary to the common assumption that the formation of hydrogen bonds between the Watson-Crick paired bases is the driving force for hybridization, it plays only a minor role. In aqueous solution the bases already form hydrogen bonds with the water molecules and do not lower the free energy much by the formation of a dimer. Much more important than base pairing is the interaction of bases with their nearest neighbors of the same strand, called base stacking. When locked in a double helix, electrostatic and dipole interactions of two adjacent heterocycles lower the free energy of the system. Water is released, leading to an additional hydrophobic contribution to the interaction. Important for the experimentalist is the influence of electrostatic repulsion of the phosphate backbones. It can be modulated by adjusting the cation concentration of the solvent which is the only way to influence the melting temperature of a duplex.

The melting temperature is defined as the temperature at which half of the amount of DNA is in its duplex form and the other half has been denatured into single strands. For many applications using DNA, but especially for the construction of DNA-based devices and templates, this is the most important parameter of DNA strands. Empirical equations give acceptable results for calculating the melting temperature, depending on the length of the double strand: The simple Wallace Rule [18] is valid for up to 15 bases:

$$T_m = N(AT) \cdot 2^\circ\text{C} + N(GC) \cdot 4^\circ\text{C}$$

$N(AT)$ and $N(GC)$ stands for the number of AT and GC base pairs respectively. A suitable approximation for the melting temperature of longer strands (>60 bp) offers the “GC-content method” [19]. It takes into account the ratio between GC and AT base pairs (%GC) and the total number of base pairs n in the strand. Corrections for the

concentration of monovalent ions $[M+]$, number of mismatches D and formamide content ($\%F$) lead to the extended equation:

$$T_m = 81.5 + 0.41(\%GC) + 16.6 \log [M+] - 500/n - 0.61(\%F) - 1.2D$$

and the GC-content based method for long strands: The nearest neighbor method uses the thermodynamic interaction of nucleotides adjacent in the sequence. It is the most complex and exact method, but only for oligonucleotides between 20 and 60 bases. Change of entropy and enthalpy (ΔS and ΔH) of the melting process are calculated for each dimer in the sequence. In a second step the melting temperature T_m is estimated by the following formula:

$$T_m = \frac{\Delta H}{\Delta S + R \ln c/4} - 273.15^\circ\text{C},$$

where c is the molar strand concentration and R the gas constant. A very detailed description of double strand melting and formation of secondary structures is given in [20].

2.1.5 Electronical Properties

Counterion Condensation

DNA has one of the highest charge densities in the world of polymers. Every phosphate in the backbone is deprotonated above pH 1 and carries one negative charge. This has to be taken into account when investigating interactions with other charged molecules and surfaces.

The equilibrium distribution of ions around a polyelectrolyte can be found with the Poisson-Boltzmann equation. A general solution of it is called Gouy-Chapman model, a widely used linearized and simplified form is the Debye-Hückel theory. It idealizes the discretely charged polymer as a chain with linear charge density and proposes two layers of ions around the DNA strand. Close to the strand is a cloud of condensed counterions, called Stern layer. In the case of DNA it consists of cations, which are free to move along the chain but have to remain within a short distance l_b to it. l_b is called the Bjerrum length, the distance at which coulomb energy of two unity charges equals the thermal energy. The outer layer, called diffuse layer, consists of a cloud of positive and negative ions that still feel the potential of the DNA, but since it is reduced by the Stern layer, they are free to diffuse away. The potential V_s is screened exponentially from its value at the boundary V_0 with the distance x :

$$V_s = V_0 e^{-\kappa x}, \quad \kappa^2 = I \frac{8\pi e^2}{\varepsilon k_B T}$$

with κ^{-1} as the Debye screening length and ionic strength I .

The Bjerrum length and the Debye length are related in this equation:

$$l_b = \frac{e}{8\pi I} \kappa^2$$

In water at room temperature l_b is on the order of 0.7 nm, with a Debye length of 0.9 nm in physiological buffer conditions.

Application: Gel electrophoresis

The interplay between mechanical and electrical properties are the basis for the most common technique for DNA analysis: Gel electrophoresis. DNA samples migrate through an agarose or polyacrylamide gel, driven by a dc voltage. The interaction between DNA strands and gel matrix depends on the strand length and pore size of the gel, longer strands migrate slower than shorter ones. This length separation technique is the most important method for forensic science, genetical engineering and many other fields in molecular biology and biochemistry.

2.2 Self-organization

The theory of self-organization is a vast topic, its detailed description goes beyond the scope of this thesis. The essence of it is that order appears in a system without explicit pressure or involvement from outside. Resulting complexity of the organization is internal to the system and its components. It is important to notice that this cannot occur in a closed system. There must be some interaction with the outside world to compensate for the decrease of entropy due to the creation of order. Simple structures like crystals or the self-organized DNA patterns of this thesis are created when a system relaxes toward a thermodynamically stable state. In 1977 Ilya Prigogine received the nobel prize in chemistry for his research on thermodynamics far from equilibrium, which is the basic instrument for describing complex systems. A permanent non-equilibrium state together with positive and negative feedback loops and multiple interactions of the components can lead to very complex structures, like living organisms or bird and fish swarm behavior.

From the enormous vocabulary of self-organization theory, the word “emergent” is the most important one for this work. It means that the system gains features or properties through the process of self-organization that were not observed there before. An example for this is the assembly of ion channel monomers in a membrane to a functioning protein. One single part of the whole does not have any function related to the final state. The desired function emerges without manipulation from outside by the assembly of the single parts. This makes the idea relevant for applications: By intelligently designing building blocks, we obtain an emerging function while investing less labor than in conventional systems.

The theory most closely related to self-organization, complexity theory or theory of complex systems, is a relatively new field. It bridges many disciplines of science and needs to develop strategies other than the traditional ones. A reductionist or simplification approach is not possible when the whole loses its most important properties when reduced to its parts.

Examples

The concept of self-organization is present in many areas of physics. Creation of ordered structures in space is accomplished in the formation of islands in Stranski-Krastanov-mode of epitaxial growth. Examples of dynamic self-organized structures are Bénard cells in heated liquids and hexagonal pattern of vortices in a superconductor. Order in time can be observed in current oscillations across a Josephson junction with applied bias voltage. The Belousov-Zhabotinsky and Brusselator reactions display order in space and time. All these examples are quite simple and deterministic, more complex examples lead to another class of self-organization. While Josephson oscillations and crystal formation are reproducible under the same circumstances and their origin can be determined by a physical model, the emerging properties of complex, non-deterministic systems can often not be explained. Consciousness arising from a neurophysiological network, life emerging from the special arrangement of bio-molecules or the unpredictable behavior of economical systems result from the self-organizing capabilities of chaotic systems.

Wang Tiles

The applications of self-organization presented here are less complex than most systems found in nature. We operate quasi-closed systems between distinct states of thermodynamical equilibrium instead of manipulating non-equilibrium systems. This makes the problem more manageable but reduces the potential of the technique.

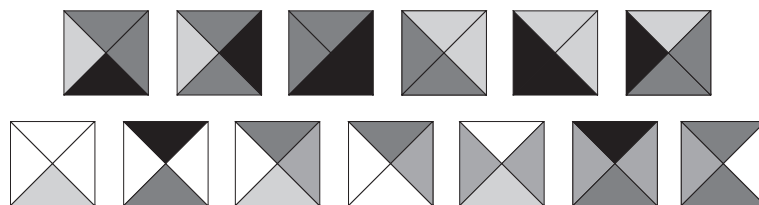


Figure 2.3: Set of Wang tiles, sufficient for non-periodical coverage of the 2D plane.

Theory of self-organization and DNA nanotechnology come closest in the topic of Wang tiles. H. Wang investigated tiling of a two-dimensional plane using squares with colored edges, so that common edges of joined squares are of the same color. Later, during the search for an algorithm for the description of this problem, it was found that Wang tiles have the same computational power as a Turing machine. Winfree et al. used intertwined DNA building blocks as an implementation of Wang tiles [21]. This combination could be used to solve computational problems and for patterning a surface algorithmically and non-periodically, which would be a great advance in the technological use of self-organization. Algorithmic assembly allows the creation of structures with great complexity, that go beyond simple crystals. Only in this way functional nano-circuits can be built.

3 DNA Templated Structures

3.1 DNA as a Scaffold for Integrated Circuits

The suitability of DNA as material for self-organized circuits is severely limited by its electronic properties. The most important function of a molecular wire is to conduct current, the conductance of DNA is too low to be of use. This subject was intensely investigated and controversially debated over the last seven years. The range of classification went from insulator [22, 23, 24] over semiconductor [25] and good conductor [26] to superconductor [27]. Even in similar experiments with identical DNA strands (λ -phage DNA) the observed conductivity varied greatly. This demonstrates that conductivity measurements on bio-materials are heavily influenced by many environmental parameters like substrate surface properties, humidity and residual salt bridges. Today the majority of scientists is in agreement that even though charge transfer across a few base-pairs is possible, the long range conductivity of DNA is not sufficient to be useful as a conductor in electronic circuits.

To exploit its self-organization capabilities in spite of this problem, DNA has to be combined with other, conducting materials. This material can either assume the role of the structural element as in the case of carbon nanotubes [28] or semiconductor nanorods. DNA is then limited to the role of a connector molecule. Alternatively, DNA keeps its function as structural template and is only modified for increased conductivity. This section will explain the second option in detail and present different ways for the synthesis of the semiconducting polymer polyaniline along DNA strands.

3.1.1 DNA Metallization

The most common technique to enhance DNA conductivity is metallization. An obvious but crude way is to evaporate metal on top of the DNA [29]. Since the molecule has to be suspended to prevent short circuits, this is only feasible for very simple designs. A more refined method to achieve higher conductivity is the modification of the nucleotide bases by coordination of a metal atom (Pd, Cu) in the center of a base pair [30, 31]. As an alternative, Zn^{2+} ions can be incorporated into the hydrogen bonds between the bases without prior modification of the strand [32].

Apart from the bases, the DNA backbone is a promising target for metallization. The negative charges of the phosphate groups bind to cationic precursors that can foster the

growth of metal clusters. Several metals have been grown on DNA this way, the procedure is similar for all: First, the precursor ions or complexes bind to the backbone or directly to the bases. A reducing agent in solution or attached to the DNA initializes the formation of small metal islands. In a last step these islands are enlarged to clusters by adding salts of the same or other metals to the solution.

In a pioneering work, Braun et al. [22] combined the molecular recognition of λ -DNA sticky ends with the functionalization with silver clusters to create a conducting wire of 100 nm width between two gold electrodes. Keren et al. [33] improved the method of gold growth through the addition of aldehyde groups to the DNA structure. The results are 50-100 nm long wires with ohmic characteristic. Immobilization of the reducing agent at specific locations along the double strand opens the possibility of patterned metallization [34]. Other metals like Pd and Pt [35] and semiconductors like CdS [36], CuS [37] have been deposited along DNA strands.

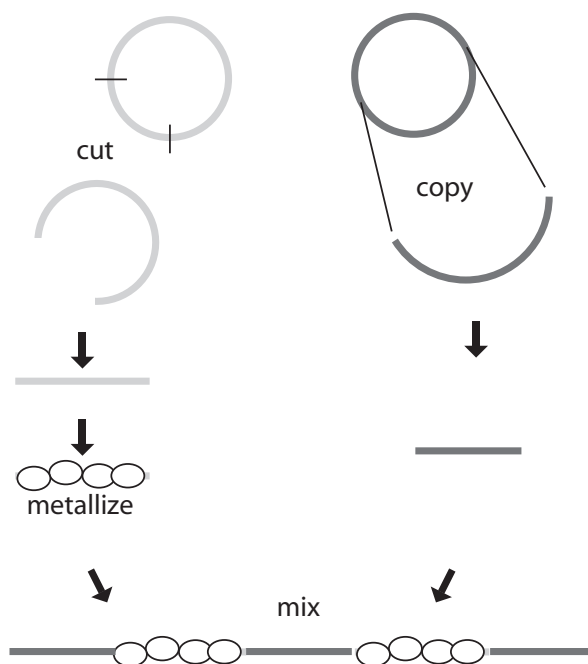


Figure 3.1: To test if metallized DNA is still capable of hybridization, two different strands with sticky ends were prepared from plasmids. One of them was metallized and mixed with an other non-metallized strand, the result was analyzed by gel electrophoresis and atomic force microscopy.

Metallization influences the hybridization properties of DNA by modifying its local charge distribution and preventing sterically the formation of hydrogen bonds. If DNA building blocks are used for the assembly of larger structures, it would be a great advantage to be able to metallize them separately before the assembly. Therefore we investigated the hybridization between DNA complexed with $K_2[PtCl_4]$ and non-modified DNA strands (Fig. 3.1).

Two long double strands with sticky ends were prepared in different ways for this purpose. The first one (blue in Figure 3.1) was created by polymerase chain reaction (PCR), using overhanging primers. The primers are only partially complementary to sites in a plasmid, the non-complementary 5' ends contain restriction sites for *Bam*H I and *Eco*R I endonuclease enzymes. After restriction with the two enzymes the strand had two four base long sticky ends with different sequences. The other strand was cut from a plasmid with the same two endonucleases , resulting in two different sticky ends, compatible with those of the other strand (red).

A fraction of both samples was metallized with $K_2[PtCl_4]$ and mixed to its unmodified counterpart. Since the four bases of the sticky ends were not enough to stabilize the structure at room temperature, ligase was used to link the strands covalently.

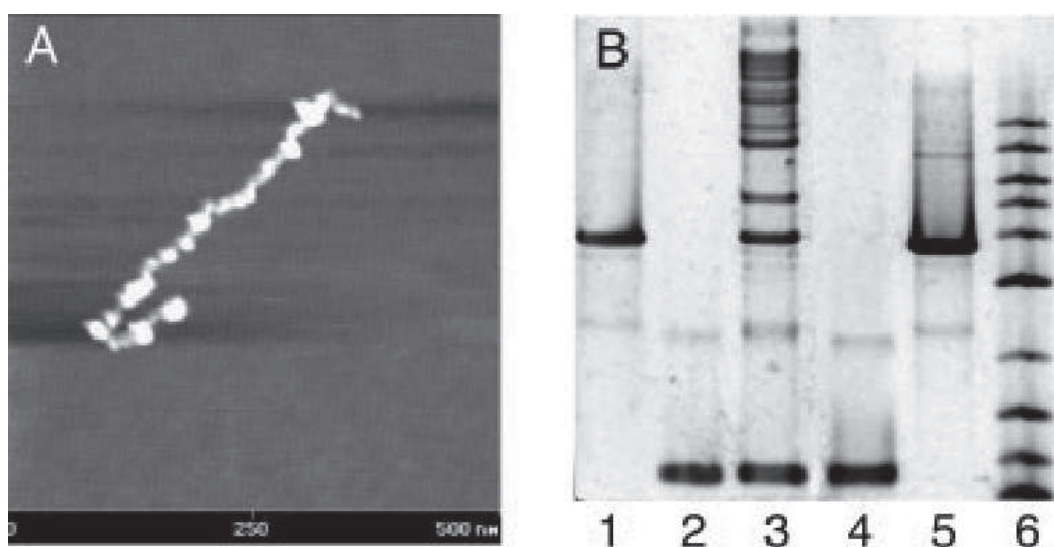


Figure 3.2: **A:** AFM image of a platinized DNA strand. **B:** Agarose gel migration assay comparing the hybridization of platinized and non-platinized DNA fragments.

The gel analysis (Fig. 3.2) shows the strand one (lane 1), and strand two (lane 2) without platin clusters and a typical ladder of two strands that can form chains (lane 3). The platinized strands cannot be visualized in a gel, since the metal-clusters prevent dye molecules, that are needed for detection, from binding. Lane 4 and 5 show the results of the mixture of platinized and non-platinized strands. In lane 4 strand one was platinized, in lane 5 strand two. Here a faint ladder and one darker band with no equivalent in the ladder of lane 3 is visible. This suggests a very weak interaction between the two strands. Lane 6 contains a 1 kbp to 10 kbp base pair size marker. Further extensive AFM analysis of platinized/non-platinized DNA mixtures gave no further proofs of hybridization. This rules out DNA self-assembly strategies where the components are pre-metallized. Either new conducting material or other assembly strategies are needed.

3.1.2 Reference [1]: Polyaniline Synthesis Templated by DNA

All materials that improve the conductivity have to fulfill certain requirements to be useful in the construction of circuits:

- a) The material has to react specifically with DNA. The more sophisticated the design of a circuit is, the higher is the needed specificity to prevent short circuits.
- b) In a continuous chain of clusters the conductivity is more dependent on surface properties at the grain boundaries than on bulk properties of the material. An insulating cluster surface would lead to a tunnel junction that degrades the conductivity by orders of magnitude. This rules out materials that develop insulating surface oxides.
- c) In addition to the previous item, the clusters of the final structure must not be too large. A novel method for nano-patterning cannot be justified if the structures are larger than features that can be produced with conventional techniques.
- d) Two possible scenarios can be distinguished for modified DNA circuits: Either the DNA scaffold is assembled and fixed on a surface, then modified for better conductance, or the modified DNA strands build the scaffold and are then brought to the surface. In the first case, the modification procedure has to work in the proximity of a surface, in the second case the modified DNA strands have to keep their sequence recognition capabilities.

With the aim to create DNA templated circuits, it is even more important to create semiconducting DNA-hybrids than metal-like ones. Metal wires can only transmit information, all functional elements for information processing and storage in electronic circuits are built from semiconducting materials.

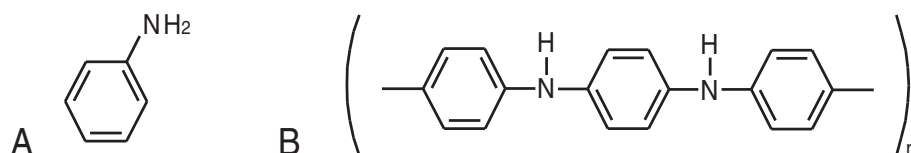


Figure 3.3: Structure of an aniline monomer (A) and polyaniline (B).

The polymer polyaniline (PAni) promises to fulfill all these requirements. The aniline monomer is protonated at low pH-values and can be exchanged as a counter-ion for the negatively charged DNA backbone. The resulting higher concentrations of aniline in the vicinity of DNA provides the necessary specificity. PAni is formed by oxidative polymerization of the monomers, requiring an oxidizing agent. We compared three different methods of polyaniline polymerization along DNA strands. First a relatively mild method based on the protein horseradish peroxidase and hydrogen peroxide (HRP H₂O₂) was applied, to ensure the integrity of the DNA. Second an ammonium persulfate mediated method, and last a photo-oxidation method including ruthenium tris(bipyridinium) (Ru(bpy)₃²⁺) was used.

The polymerization process was monitored by UV/Vis spectroscopy, making use of the fact that the polymer displays absorption peaks at 400nm and 800nm. The topography of the nano-wires and specificity of polymerization was characterized by AFM. To investigate the actual objective, the modification of the electronic properties of DNA, conductivity measurements were performed on gold nano-electrodes on silicon.

The results strongly depended on the different oxidization agents. Ammonium persulfate accounted for the most uniform polymerization, but none of these samples turned out to be conducting. Both HRP H₂O₂ and Ru(bpy)₃²⁺ protocols resulted in samples with semi-conducting behavior, even though Ru(bpy)₃²⁺ treated samples displayed the least uniform polymerization. Horseradish peroxidase turned out to be problematic because of aggregation of the enzyme on the chip surface. Further experiments have to reveal if the electronic properties of DNA-PAni compounds can be enhanced by doping the polymer.

3.2 Complex DNA Structures

This section introduces the current standard construction principles for self-organized DNA structures. In contrast to these building-block related strategies, a simpler method was used by our group for the generation of DNA templates: “Rolling circle amplification” requires only two different short oligonucleotides for the enzymatic synthesis of a 10 000 base single strand with periodic sequence.

The first artificial DNA structures were built in the group of Nadrian Seeman by assembling short single strands step by step. Earliest motifs included three- and four-armed junctions [38], later expanded to five- and six-armed junctions [39]. Objects with the topology of cubes [40], truncated octahedra [41] and Borromean rings [42] were created with the same technique, which is very labor intensive since it requires purification between the single steps. The drastically decreased yield (~1%) in the case of more complicated structures motivated the search for new assembly techniques.

Less ordered structures were created by other groups using plasmid DNA [43] or single stranded DNA with the purpose to assemble gold clusters [44, 45, 46]. In order to measure the conductance of DNA, the first large scale networks were built by Cai and Kawai [25]. Strands containing only adenine (poly dA) or thymine (poly dT) bases self-assembled to an irregular network.

A major breakthrough was the invention of the double crossover (DX) motif [47]: four or five partially complementary single strands form the geometry of two intertwined double strands (Fig. 3.4). Their four sticky ends allow the construction of larger superstructures. Long range order is improved by the increased stiffness of the DX structures due to the connections between helices. Prefabrication of simple building blocks also requires less purification and keeps the number of critical steps limited.



Figure 3.4: Topology of double (**DX**) and triple (**TX**) crossover building blocks. The grey bars indicate the interwoven double helices.

Double and triple [48] crossover (**TX**) tiles are the basic building block for most DNA structures of the recent years. One or two different tiles have been used to construct 2D lattices with long range order [21, 49], octahedra [50], tube-like structures [51, 52] and DNA fibers containing three [53] or six [54] helix bundles. More advanced algorithmic structures like Sierpinski triangles [55] or XOR gates [56] and molecular shadow mask lithography [57] have been implemented with these building blocks. **DX** tiles can be modified from linear to three-armed [58] or four-armed [59] blocks to build mesh grids rather than a solid tiled surface. One purpose of such structures is to provide a regular 1D [60] or 2D [61] array of anchor sites for colloids or proteins.

Constructions that did not use **DX**/**TX** building blocks included DNA streptavidin hybrids [62] or dendrimer-like supermolecules [63]. A RNA jigsaw puzzle was built using the interaction of hairpin loops, so called “kissing loops” [64]. This represents a very promising implementation of Wang tiles. Lattices with long range order are hard to build without stiff building blocks like **DX** or **TX** tiles. It is nevertheless possible, as shown with Holliday junctions [65] or DNA triangles [66].

The challenges of engineering DNA nanostructures go beyond the problems of assembly. Once the structure has self-assembled in solution, it has to be brought onto a surface for analysis, further processing or use. The most suitable materials are single crystalline silicon or cleaved mica, due to their low roughness and controllable surface properties. Both display negative charges in aqueous environment at neutral pH-values. This prevents the likewise negatively charged DNA from adhesion, thus silanes or divalent cations like Mg^{2+} have to be used in a mediating layer.

Critical for the integrity of DNA nanostructures on a surface is the fine tuning of attractive forces. If they are too strong, DNA precipitates onto the surface until it forms a dense layer, inapt for any further use. Insufficient attraction to the surface leads to aggregation of the DNA or the loss of the structures during the drying process. The receding meniscus of the drying liquid exerts strong forces on the surface bound DNA. This can be used in a technique to stretch DNA called molecular combing, but the forces can also destroy the structures or sweep them from the substrate.

3.2.1 Synthesis of DNA

Two methods for the creation of double-stranded DNA building blocks with sticky ends were mentioned above: restriction of plasmids and PCR amplification using overhanging primers. Neither of them utilizes the full capabilities of DNA, any polymer with reactive groups at the ends suits the same purpose.

The advantage of high information content in DNA can only be used if the scientist is in complete control over the sequence of the strand. Furthermore, only single stranded DNA can be considered as a useful basic building block. Once it is completely bound to its complement, no further interaction follows. The single exception is the incorporation of RecA modified DNA [33].

Short single strands can be synthesized base-by-base with a predetermined sequence. Today advanced synthesis chemistry and state-of-the-art parallel DNA synthesizers allow a fast and efficient production of oligonucleotides of almost all sequences. In solid-phase synthesis the desired oligonucleotide sequence is built onto an inert solid support, from which it is cleaved after the synthesis has been completed. The length of the sequence is limited due to the stepwise coupling yields (99.0% to 99.5%) to 120 base pairs. In the early days this method of synthesis was very expensive and time-consuming for the experimenter; the recent commercial availability of nucleic acid sequences based on automated synthesis methods has made DNA nanotechnology possible outside of biochemistry labs.

Enzymatic processes can also be used to create custom periodic strands with the help of either advanced PCR techniques or telomerase reaction [67]. Single strands can easily be copied from a plasmid with the help of DNA polymerase, but then the sequence cannot be predefined. One of the few ways to synthesize a long single strand of determined sequence is rolling circle amplification (RCA).

3.2.2 Reference [2]: Periodic DNA Nanotemplates Synthesized by Rolling Circle Amplification

Even though the positioning of nanoparticles with templates based on DX tiles is possible [60, 61], it requires an elaborate annealing protocol and the precise control of buffer conditions and of the stoichiometry of the single stranded components. These requirements make the whole procedure relatively labor intensive and inflexible for the rapid adaptation to new problems. By modifying Rolling Circle Amplification (RCA), a method known to molecular biologists for many years [68], we avoided the problems of DX-tile synthesis while creating a template of the same quality for the linear assembly of nanoparticles or proteins.

RCA is a simple DNA polymerase reaction with a circular template instead of a linear one. A template strand with 40 to 100 bases is brought into circular form using a primer (15 to 25 bases) that is partly complementary to both ends of the template (Fig. 3.5, A). The resulting nick is closed with a ligase reaction. The circle with the adhering primer is mixed

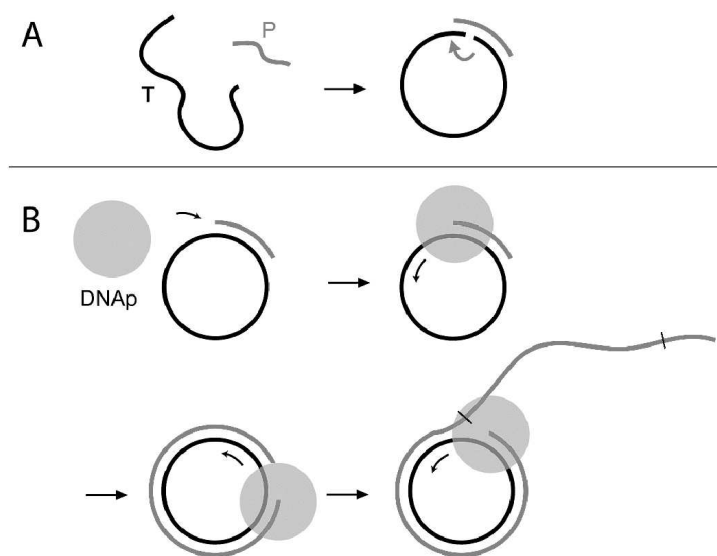


Figure 3.5: Principle of the rolling circle amplification process.

with $\phi 29$ DNA polymerase and dNTPs in an appropriate buffer. The polymerase starts extending the 3' end of the primer, copying the template strand. After less than one turn it encounters the 5' end of the primer and displaces it from the template, which is a special property of $\phi 29$ polymerase (Fig. 3.5, B). In an alternative approach, the Klenow fragment of DNA polymerase I that lacks this strand displacement ability can be used, though not as effectively. If the template is short enough, the bending strain of the emerging double strand is big enough that it is energetically more favorable to split the already synthesized strand from the template. In either way, the polymerase keeps on adding nucleotides along the circle, producing a long single strand with a length of the order of 10 000 bases with a repeating sequence that is complementary to the template.

This method is used by viruses to copy short repeating genetic sequences. In molecular biology it was introduced as a detection method [69, 70]. In presence of the primer sequence, the circle can be closed and the long product strand is polymerized and can easily be detected with gel electrophoresis. Without primer, the polymerization reaction fails. The product strand is up to 500 times longer than the template, which enables the detection of very small amounts of DNA.

The basic idea of our publication [2] is the usage of the long single stranded product not as indicator in a detection protocol, but as a basis for the arrangement of nanoparticles. Oligonucleotides with the same sequence like the template, modified with a functional group at one end, bind to the RCA product and create a linear array of functional groups. These can be either thiol or amino groups or biotin molecules. Alternatively, the material

that needs to be arranged in a chain can be first bound to short single strands and then mixed to the RCA product.

Proof for the generation of long single strands was provided by gel migration analysis. To show that the RCA product actually carries the template sequence, a recognition sequence for a restriction enzyme (*Hind* III) was included into the rolling circle template. By adding the restriction enzyme to the product, the long strand vanishes and short cleavage products appear in the gel.

Alivisatos' group demonstrated the composition of few nano-clusters with the help of short oligonucleotides [45]. The RCA method extends this to the micrometer scale with interspersing precision of few nanometers demanding only little preparative effort. This technology opens the opportunity for the investigation of many interesting physical problems, like the interaction between fluorophores or collective excitation in nanoparticle chains. Gold nanoparticles assembled in a linear regular chain could act as an plasmonic waveguide depending on the size of the particle and the distance between them.

RCA can be the basis for more than the arrangement of gold particles in regular arrays. Many different functional groups at the end of the DNA linker strands can bind even more classes of materials like semiconductor or magnetic nanoparticles, fluorophores and enzymes. Linker strands with the length of a fraction of the repeating sequence make it possible to alternate between different materials. The quenching of fluorophores next to gold particles can be monitored as well as the behavior of redox-centers in the vicinity of conducting polymers. The distance between two active sites can be precisely tuned and has a very narrow distribution throughout the molecule due to the uniformity of the DNA strand.

Since the RCA technology is solely based on DNA biochemistry, all DNA modifications at the bases or backbone that are compatible to polymerization can be applied here. Two further DNA templates based on rolling circle amplification have been published recently [71, 72].

4 DNA Based Mechanical Devices

The development of small functional devices is approached from two opposite sides. From one direction, the miniaturization of already existing and functioning basic machine parts like pumps, valves or rotors is attempted, with the ultimate goal of transferring whole functionalities to the nanometer scale. This is called *top-down* approach. Its challenges are the choice of materials and fabrication techniques, with complications increasing drastically when traditional concepts meet the physical conditions of the nanometer scale: The ratio of the amounts of bulk atoms to surface atoms decreases when an object is scaled down, thus forces related to the mass lose importance against surface interactions. For this reason gravity and inertia does not play a role anymore for structure sizes below $1\ \mu\text{m}$, frictional forces and interactions that are limited to a short range due to screening, like electrostatic and dipole interactions, determine the behavior of the whole system. Entropic effects that do not occur in the operation of large devices cannot be ignored in the design of nanoscale systems. For all devices immersed in solution hydrophobic interaction has to be taken into account, depending on the building materials and solvent. Also the Reynolds number is smaller than one at these dimensions, which implicates a behavior of objects in liquid very different from what we are used to.

The other direction, *bottom-up* construction from a single molecule to the functional device, has the advantage that the products are automatically small. It does not share preparative problems with top-down methods, its main difficulty is the development of new concepts, independent from the “big” world. So far all the devices presented in literature are either objects of basic research or interesting “toys” (like a nanocar [12]), in the best case. The function, not to speak of application, has often to be found in a second step after the device has been built.

This work does not describe a fully functional machine designed for an application, but it documents steps towards a functionality that goes beyond a mere “toy state”. The most advanced products of DNA nanotechnology are so called aptamers, DNA tertiary structures that can bind selectively to ligands. During the last years they have become a new tool for protein immobilization and diagnostics in medical and biomolecular research. Being still an object of basic research but also already used by biomedical companies, aptamers bridge the gap between nano scaled devices and applications of industrial interest.

4.1 Aptamers

4.1.1 Introduction to Aptamers

Aptamers are DNA or RNA single strands that have been selected from random pools based on their ability to bind ligands. Like antibodies, aptamers are highly specific to their targets, and thus have many potential uses in medicine and other areas of technology. The list of targets includes metal ions [73], small molecules like cocaine [74], proteins like streptavidin or thrombin [75], dyes like malachite green [76], and organic superstructures like the HI-virus [77].

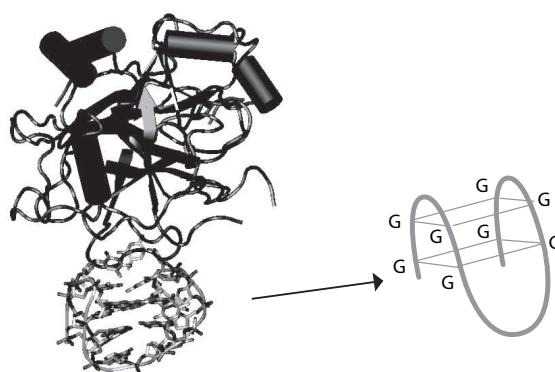


Figure 4.1: Structure of thrombin-aptamer complex, derived from X-ray analysis. The representation of the aptamer on the right side displays the two G-quadruplexes of the armchair-like binding motif.

It is important to mark the difference between classical DNA binding structures and aptamers. DNA binding motifs of proteins or intercalating molecules are shaped to interact with the native B-DNA double strand, while an aptamer uses the affinity of a specially formed tertiary structure of a DNA single strand to an object that does not bind normally to a double helix. This tertiary structures can consist of regular Watson-Crick base pairs or more exotic structures like G-quadruplexes in one of the thrombin aptamers. Even though the secondary structure of a DNA or RNA strand can be derived from its sequence with acceptable accuracy, the development of aptamers is still a matter of trial and error. Interactions of aptamer and target are very hard to predict and in most cases only X-ray or NMR analysis can unveil the structure of the aptamer-target complex. Specific aptamer structures are evolved in a so called SELEX (Systematic evolution of ligands by exponential enrichment) process [78]. A library of nucleic acid sequences is tested for their binding specificity or catalytic function. The most suitable sequences are selectively amplified and the test is repeated with stricter criteria. After several cycles the remaining sequences that were best in the competition are analyzed.

4.1.2 Reference [3]: Design Variations of an Aptamer-based DNA Nanodevice

The main applications for aptamers are immobilization of proteins on a surface and detection or deactivation of proteins in bulk liquid. Immobilization of proteins for detection or synthesis is a key technique for portable analytical devices like proteomics chips, it is a challenging task. Any influence on the fragile structure of the protein can corrupt its function or lead to denaturation. A common method of tethering proteins to a chip surface is to attach a biotinylated protein to a polyethylene glycol (PEG) linker via streptavidin. PEG itself is modified with a silane or thiol group to bind to gold or silicon dioxide substrates. This method requires many elaborate steps, but sometimes it still causes the protein to denature. Together with many other methods, it also has the disadvantage that the link is permanent, the protein cannot be removed easily once it has bound. A better result can be achieved with less effort with the help of aptamers. They can be bound to a gold or silane layer as well and since the binding site and spacer to the surface are parts of the same molecule, no assembly steps are necessary. The only effort is the SELEX process to find the appropriate sequence for every new protein.

Additional to immobilization on a surface, deactivation of proteins in solution can be a task mastered by aptamers. When bound to the active site of the protein or by causing a conformational change it can modulate the function of the protein reversibly. This was demonstrated *in vivo* by Rusconi et al.: The blood coagulation process was influenced by the interaction of an aptamer with a blood clotting factor protein [79]. This way an aptamer can be employed as a switchable drug: It prevents thrombosis when active, but can be turned off to stop uncontrolled bleeding from a wound.

The work presented here aims at the extension of the functionality of the aptamer device previously designed in our lab [13]. The device is based on a short thrombin binding nucleic acid sequence [75]. The binding motif assumes a three dimensional structure with two central G-quadruplexes, stabilized by potassium ions. A “toehold” of 12 bases is attached to the 5’ end of the aptamer to enable the switching to an off state. Without this expansion the operating strand has no leverage to bind and to remove the protein by hybridizing to the aptamer sequence.

To investigate the integration of this aptamer in other devices the influence of modifications of the aptamer on its binding abilities was analyzed in [3]. Dye molecules at the ends of the aptamer are used for detecting the binding of a protein in FRET experiments, but it was not clear, if they change the binding behavior. The other variations were extensions of the strand by additional nucleic acid bases (Fig. 4.2). So far it was known to be uncritical to extend the 5’ end, but in order to obtain an additional handle to be used within an aptamer device it would be necessary to extend the 3’ end as well.

The binding capabilities were tested in gel shift experiments. The binding of thrombin is indicated by the development of an additional band containing the aptamer-protein complex, heavier than the one of the aptamer alone (Fig. 2 in [3]).

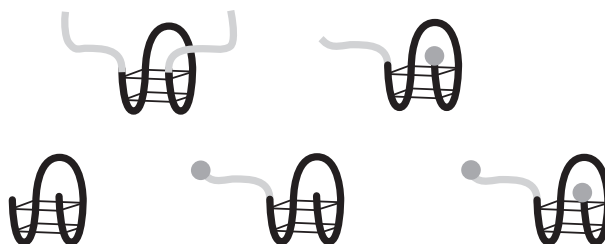


Figure 4.2: Design variations of a thrombin-binding aptamer device. The basic aptamer (red) was extended by additional bases (blue) and fluorophores (green).

It showed that the presence or position of the dye had almost no influence on the function of the aptamer, therefore FRET experiments can be performed without further concern. But while the extension of the 5' end did not influence the binding constant, the addition of 20 bases to the 3' end prevented binding completely. A new design needs to be found if a second arm at the aptamer is needed.

4.2 DNA Logic Devices

4.2.1 Introduction to DNA Devices

The difference in persistence lengths of double-stranded and single-stranded DNA, 50 nm and ~ 1 nm respectively, allow the use of DNA for stiff, structural elements and flexible joints simultaneously. Furthermore, DNA can assume more shapes than a simple double helix. A single strand that is folded back to itself can form structures like loops, bulges and pseudoknots. Interaction of a few strands can lead to a vast variety of shapes, some of which were presented in the previous chapter. We can accordingly determine the shape and function of the device by the design of the base sequence for fixed and flexible parts. Chemical modification of the nucleic acids would expand the range of functionality even further, but is not considered in this work.

DNA devices can be driven by two different mechanisms: The binding of ions or small molecules, or the hybridization of a complementary DNA strand. For a cyclical operation the device has to be switched between two different states of thermodynamic equilibrium. This requires the removal of the ions or molecules in the first of the operation modes and the resetting into the start configuration by a second strand in the other case. After several operation cycles the concentration of waste products increases inevitably, which inhibits the further operations and limits the number of cycles. This mode of operation is inferior to that of protein “nanodevices” in living organisms, which are in a constant thermodynamical disequilibrium state. The local environment of the protein machines is steadily exchanged and recyclable energy sources like ATP and complex regulatory cycles prevent the shutdown through the accumulation of waste products.

4.2.2 DNA Device Overview

In the following description, different DNA structures will be classified according to their function: So called prototypes, that can only change their conformation, devices that process information (computational devices) and devices that come closer to the definition of machines, because they change the position or the state of another DNA structure (DNA machines). The last group contains aptamer-based devices, which release a non-nucleic acid agent. These definitions are arguable and only for structuring purposes. Some devices fall into two of the categories, and it has yet to be defined what a nanomachine has to achieve to earn its name.

Prototypes

The first nanomechanical DNA device was based on a B-Z conformational change triggered by cobalt hexammine [80]. Mao et al. attached double crossover tiles at both ends of a 10 bp double strand, consisting of guanine and cytosine bases. While in the B-DNA conformation under ordinary buffer conditions, this stretch of DNA changes into its Z-form with the addition of cobalt hexammine. The design of the device leads to a turn of 180° which is detectable by FRET.

For a contracting device, Liu and Balasubramanian used non-Watson-Crick base combinations [81]. At low pH-values, C-C+ base-pairs can be formed in cytosine rich regions of the DNA and arrange to a so called “i-motif”. Another device driven by changes in pH uses the transition between a double and a triple helix conformation [82].

A similar approach is the use of G-quadruplexes in the presence of potassium or strontium [83]. Quartets of guanine bases stack to a superstructure until the mediating ion is removed by a chelating agent.

A different set of devices, based on hybridization, was constructed by Yurke et al. at Bell Labs [84]. Driven by consecutive hybridization, a tweezers-like structure was switched between two states. A FRET pair at the ends of the tweezers was used to monitor the movement. It was further improved to resemble a tri-state device [85]. To go beyond the manual addition of the strands, Dittmer et al. used the *in vitro* transcription of a gene to operate a DNA device [86]. The mRNA copied from a DNA template hybridizes to a DNA construct and changes its conformation. This allows the further regulation by inhibitor or inducer proteins and suggests future combination of DNA and protein based logical operations.

Computational Devices

DNA based computing has become a major field of research on its own, so only a fraction of the available concepts will be mentioned here. The information encoding capabilities of DNA can be used to store, transform and read out data.

The most prominent example of DNA computing is Adleman's solution of an instance of the directed Hamiltonian path problem, also known as the "travelling salesman problem" [87]. A small graph was encoded in molecules of DNA, and the "operations" of the computation were performed with standard protocols and enzymes. Stojanovic et al. developed a tic-tac-toe computer based on DNA hybridization [88]. Logic gates comprised of DNA secondary structures [89] evaluated the input that was pipetted to each of the 3x3 fields. An increased fluorescence signal indicated the next move of the "computer".

Another logical XOR gate was implemented with the use of TX tiles [56], an expansion of this technique is the algorithmic assembly of a Sierpinski triangle [55].

With a new concept, Benenson et al. introduced the use of the *FokI* restriction enzyme to perform logical operations similar to a finite state machine [90]. In a second step, the device was extended to release a short drug-DNA strand in the presence of certain mRNAs that indicate prostate cancer [91].

It is clear that nucleic acid based computation is currently no match for the current silicon technology computers. Even though calculations can be performed in a massively parallel way in solution, the information input and readout is very tedious. But in applications where information and actuation is not easily accessible for silicon based technology, DNA based logic can fill the gap. This will be discussed in greater detail in the next section.

DNA Machines

Devices with movable parts that are able to change the state or location of a object that is not part of the device itself can be called machines. An example is a ribozyme based device that repetitively binds, cleaves and releases a short combination of DNA/RNA [92]. One major goal of nano-engineering is the creation of artificial muscles for the actuation of small devices. Prerequisite is the realization of controlled linear movement on a small scale, as it is demonstrated by the organic counterparts, actin/myosin. A DNA "walker" was built by Sherman et al. [93]. Every step of the "biped" device was actuated by adding two short oligonucleotides. The first strand was used to remove the "foothold", the second one to create a new connection further down the track. A similar but simpler device was built by [94]. Subsequent designs realized an autonomous walking device. Either a nicking enzyme [95] or a built-in catalytic ribozyme [96] were used to remove one foot from its toehold¹.

¹It has to be mentioned here that the linear transport of material on a very small scale has been realized for 20 years with the help of microtubuli/kinesin interaction [97]. These adoptions from natural transport mechanisms are easier to implement, but do not allow the precise control of direction and start and stop points like DNA-"walkers" do.

Aptamer-based devices

Despite of the growing interest for aptamers, aptamer-based DNA devices are scarce. An aptamer that can cyclically bind and release thrombin was developed in our lab by Dittmer et al. [13], it is the base for further experiments described in this section. The reverse operation was performed by Nutiu et al. [98]. A short single strand is displaced through the binding of a target molecule, this can be used as a detection method. Similar constructs were built with RNA, in this case an allosteric ribozyme [99]. An advanced design that combines molecular logic with aptamers allows the release of a molecule controlled by boolean calculations [100]. Though not a device, but also a large step in the use of nucleic acids technology is the linear assembly of aptamers at the edges of TX tiles [101].

4.2.3 Allosteric Aptamer Device

To have a switchable linker that can be engineered for almost any type of protein would be very convenient. However, it would be less convenient to be able to release the protein only with one predetermined trigger sequence. This sequence has to be complementary to the protein binding region of the aptamer² and thus cannot be freely chosen (Fig. 4.3).

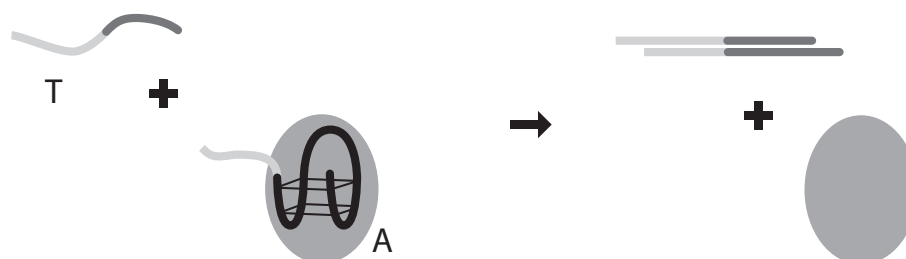


Figure 4.3: Simplified working principle of the aptamer device. Trigger strand **T** has to be complementary to the aptamer sequence **A** (red). **A** is determined by the shape of the binding motif that is specific to the ligand (yellow), in this case thrombin. Therefore the trigger sequence **T** can not be chosen freely.

That implies that a specific switch has to be designed to every aptamer and, worse, one cannot use a given sequence (for instance mRNA) to operate the aptamer. This severely limits the use of aptamers in integrated operations. For example, the “antidote” in Rusconi’s experiment regarding blood clotting [79] has to be applied by the experimenter. An intelligent drug should act autonomously, based on the recognition of a wound by the emerging tissue factor proteins.

²This applies especially to the design of the aptamer device of [13], where only one end of the binding region is accessible for the actuator strand. This may appear to challenge the usefulness of this design, but the approach of [13] is very general and can be used with most aptamers. This is not the case with other switchable aptamer devices, e.g. [100].

A solution to this dilemma is the separation of the binding site from the trigger mechanism. This property is observed for example in allosteric proteins. “Allosteric” stands for an induced conformational change that results in the release of a previously bound compound. We investigated the possibility of using an allosteric mechanism for the operation of the aptamer, the principle is outlined in Figure 4.4.

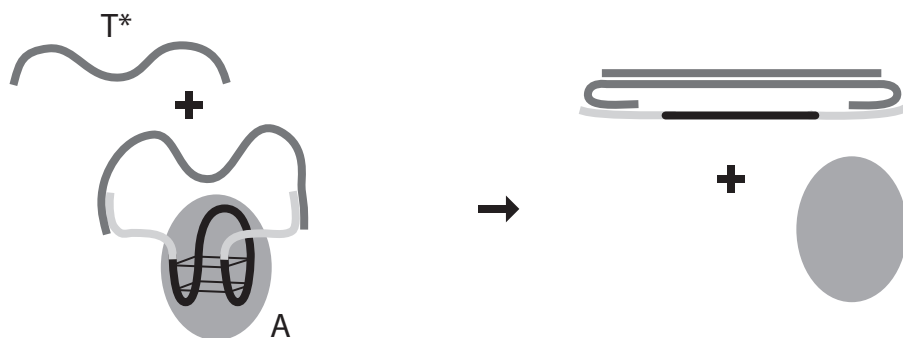


Figure 4.4: Working principle of the proposed aptamer device. Trigger strand T^* (green) induces a conformational change in the binding region, which sets the ligand (yellow) free. T^* does not hybridize directly to the protein-specific region (red) and can be of an arbitrary sequence. The aptamer A (black) is different from the aptamer in Figure 4.3 and Figure 4.2.

A requirement for an allosteric aptamer is that the location of the active sequence is located in the middle of the DNA strand, not at the end as in our original thrombin aptamer. With the design of [3] that is not possible. Tasset et al. developed a DNA aptamer with the specifications mentioned before [102].

Figure 4.4 depicts the mechanism that is supposed to switch the aptamer between a binding and a non-binding state. The two arms of the aptamer are connected by a single strand, which can be stiffened by the trigger strand. This strand can be removed via a toehold (not shown in Figure 4.4), which makes the procedure reversible in analogue to the aptamer of [13].

Figure 4.5 shows a gel analysis of this procedure. The aptamer structure has different conformations that appear as smears in the gel. This makes analysis very difficult and calls for many experiments to gain comparable results. Lane 1 and 2 contain the aptamer in the enabled state without and with thrombin. As expected, binding of the protein shifts the band of the aptamer. Addition of an actuator strand switches the aptamer into a disabled state and also causes the band to shift (lane 3). This should render the binding of thrombin impossible because the binding motif does not exist anymore, bands with and without the protein are supposed to be at the same height now. Nevertheless, when thrombin is added (lane 4), the band shifts: Hybridization of the stretch strand does not remove thrombin from the structure.

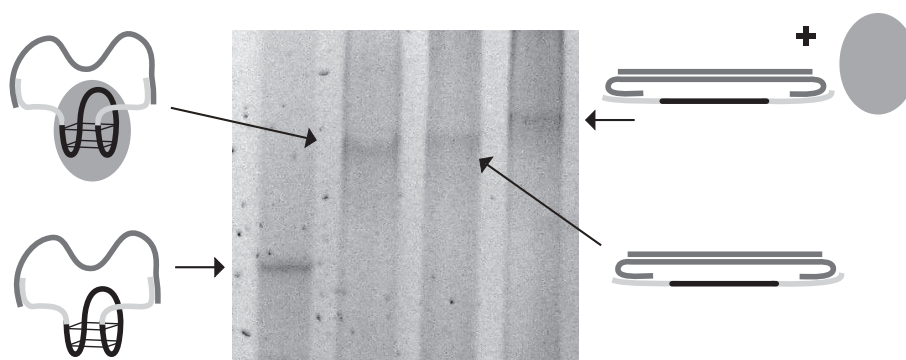


Figure 4.5: Gel analysis of the allosteric aptamer device. Lane 1 and 2 contain the enabled aptamer, lane 3 and 4 the disabled aptamer, each without and with thrombin.

There are several possible reasons why the trigger is not able to remove the protein. Binding of the trigger strand might be either energetically unfavorable because of the strong curvature of its complement (green strand that is attached to the aptamer in Figure 4.4). Or the trigger strand is able to bind, but the resulting double strand is bent rather than tearing open the aptamer structure. A fundamental problem of this design is that every change of parameters (e.g. salt concentration or temperature) that improves the hybridization of the trigger strand also makes it more difficult to change the conformation of the protein binding region of the aptamer. Both mechanisms rely on the same kind of hydrogen bond interaction and cannot be influenced independently. Other designs of allosteric devices contain sections of RNA and covalent bonds between the different strands and can so operate the device by changing buffer conditions [103].

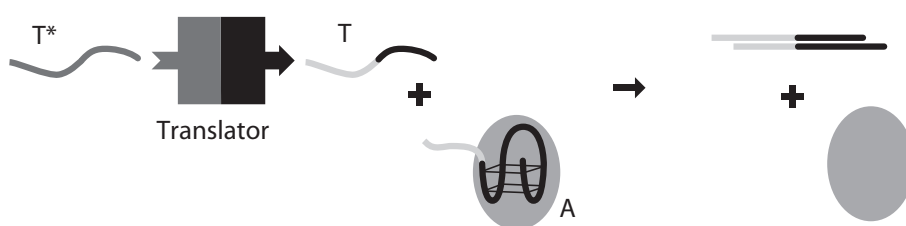


Figure 4.6: Principle of the DNA sequence translator. Sequence T^* can be chosen independently from the aptamer sequence A

To build an aptamer device that can be triggered by generic inputs without chemical modification of DNA, a different approach for the separation of signal recognition and performance of action was chosen (Fig. 4.6). A second device pre-translates specific sequences that should trigger the release of the protein into a second sequence that operates the aptamer as in Figure 4.3.

4.2.4 Reference [4]: A Modular DNA Signal Transducer for the Controlled Release of a Protein by an Aptamer

In 2003, Benenson et al. introduced the use of the restriction enzyme *FokI* as a part of a DNA-based finite state machine [91]. This enzyme recognizes a specific sequence of five base pairs and cuts the double strand 9 and 13 bases downstream, even if the strand in between is not ligated. The presence of the recognition sequence on one side therefore determines if the strands on the other side is cut. This basic principle can be utilized for the construction

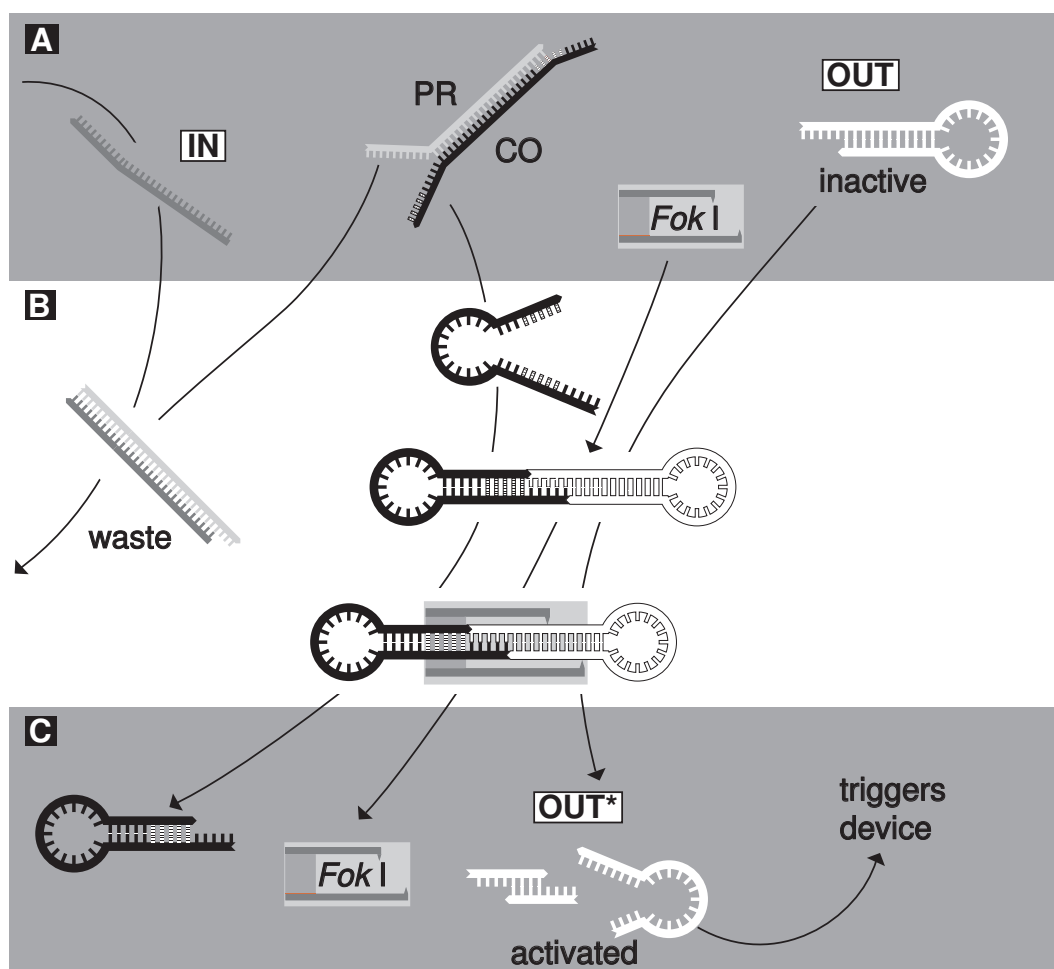


Figure 4.7: Operation DNA translation device: A short input sequence (IN) induces the activation of an actuator strand (OUT→OUT*).

of a sequence independent aptamer trigger. It is comprised of DNA hairpins, secondary structures of single strands with partially self-complementary sequences. The actuator sequence forms initially the loop of a hairpin. In this conformation the interaction with other strands is mostly inhibited (Fig. 4.7, OUT). When a trigger strand (IN) is added to the system, it removes a protection strand (PR) from another hairpin (CO), that contains

a *FokI* recognition site in its stem. Through a short sticky end CO can bind to OUT and *FokI* cuts off the loop of strand OUT. The actuator sequence, now in its linear form, is free to interact with other DNA devices or aptamers.

Using hairpins in this construction opens the opportunity to integrate it with other devices. In comparison with linear single strands, hairpins have the advantage that un-specific interaction between different strands is minimized, because the largest part of a loop-structure is double stranded. The modular design principle furthermore allows for the quick adaptation to different trigger and actuation sequences, without having to redesign the whole device. By operating different modules in parallel or serial, basic logical gates could be built. The feasibility of this was shown in [104]. These basic computational steps could be used to regulate the aptamer state.

The operation of the device was investigated mainly with PAGE gels to show that a short strand is dispatched only in the presence of a trigger. A major part of the work presented here was dedicated to the interactions of the cut and uncut OUT-loops with their target sequences. Even hairpins with long stems display residual binding, which leads to premature triggering of the aptamer. Three designs with different loop sizes and stem lengths were tested, the interactions were monitored in FRET experiments. These showed that it is important to keep the loop as small as possible to prevent unwanted triggering.

The response of the device depends on input strand and enzyme concentrations with the relation between input and output following roughly an sigmoidal curve. A higher enzyme concentration results in higher product output but also an increased false positive rate. This problem can be mitigated by carefully designing the input section of the device. Product output without prior triggering is the result of connector strand dimers that also contain a *FokI* recognition sequence. Protection strands (PR in Figure 4.7) that cover most of the connector sequence prevent this.

This system could be a good example for the future of DNA-based computing. Especially in biological environments where conventional electronic logic has difficulties to retrieve data and perform action, the strength of this new kind of computation become apparent. Electronic devices need power supplies and sophisticated interfaces to biological matter to be able to work autonomously. Devices based on biological matter do not have these requirements and offer the possibility to be integrated in larger device networks to perform more sophisticated tasks.

5 Outlook

Two different facets of DNA nanotechnology have been presented in this thesis: Self-assembled DNA structures on solid substrates and nanomechanical DNA devices in solution.

The DNA surface structures of section 3.1.2 are steps towards DNA templated electronic circuits. A comparison of modification protocols for improving the conductivity of DNA wires was presented. It was shown that the semiconducting polymer polyaniline provides a continuous coating of DNA strands while keeping background deposition of conducting material low. DNA templated circuits do not provide the versatility to replace a CPU chip yet, they are still limited to arrays of straight wires. The simple fabrication of such circuits is a huge advantage when only small number of copies of them is manufactured. This applies especially to research application like setups for detection of quantum effects or creation of novel mesoscopic geometries. In the future simple and highly repetitive commercial chip structures could be templated this way.

In section 3.2.2 a novel method for the synthesis of linear DNA templates was introduced. These templates contain periodically spaced anchor sites for nanoparticles with a distance of 10 to 30 nm extending to a total length of several micrometers. This allows for the controlled alignment of proteins, gold clusters and semiconductor nanocrystals and periodic combinations of these. In its extent and versatility regarding the different types of particles, this is a notable improvement over existing methods. Interesting setups for the investigation of nanoparticle interaction can be created by the alternating arrangement of different kinds of particles. For instance, the quenching of fluorophores in the vicinity of gold clusters or the cooperative function of different catalytic particles can be analyzed with this technique, without direct manipulation of the particles with a scanning probe setup.

The potential of DNA for self-assembled structures has not yet been used to its full extent. Construction of the Sierpinski triangle and basic implementation of Wang tiles are only the beginning of algorithmic self-assembly. New techniques have to be explored to overcome the limitations of the current standard DX and TX building blocks. One possibility is the use of long single strands in a weaving technique as proposed by Yan et al. [105]. For the creation of functional structures, some kind of error detection and correction system will be necessary. Since self-assembly is a statistical process, large scale patterns will always have random errors that affect the functionality of the whole system.

Nature has demonstrated possible error correction schemes with the proofreading and 3' to 5' exonuclease activity of polymerases. Without a mechanism of this kind, DNA templated structures will be either limited to a very small size or has to rely on a more complicated, error tolerant design principle.

One of the most fascinating, nevertheless realistic future application of DNA nanodevices are intelligent drugs. Being a part of the human metabolism, DNA is intrinsically compatible with it. Its interaction with proteins and RNA gives rise to many interesting applications. All steps of protein production in the cell, from transcription over gene splicing to translation could be in principle regulated by DNA-based devices. This opens possibilities to cure viral or hereditary diseases where conventional medication fails. Proteins can be targeted even after their synthesis, as shown in chapter 4. The device that was presented here contains the basic components for an autonomously working drug: detection and actuation based on a logical decision.

But before this new kind of medication can be applied the nucleic acid based devices have to be transferred from their prototype state to *in vivo* tests and medical trials. So far most devices work only *in vitro* under conditions that are very different from those in our body [104]. Another problem that has to be addressed is the reliable and specific delivery of drugs into a target cell. This is not only necessary for nucleic acid based drugs, but for all drugs where side effects play a role and has become one of the most important topics in biotechnology. Packing a highly charged polymer into a small sphere, delivering it to a specific cell type and injecting the drug into the cell are very challenging problems that require interdisciplinary collaboration.

The interaction between electric fields with DNA molecules is another interesting interface between top-down fabricated electrodes and self-assembled nanodevices. Electronically modulated hybridization or actuation would give control over nanodevices that is compatible with current chip technology.

Several different capabilities of DNA nanotechnology have been demonstrated in the last years. It is now time to combine them and find useful applications together with other technologies. A remarkable example is the combination of the sequence recognition capabilities of DNA with the conductance of carbon nanotubes to create a field effect transistor [28]. Semiconductor and metal nano-crystals, proteins and nucleic acids can form together novel materials that exceed conventional ones by far in many aspects. They can be integrated with top-down technology for the assembly of electronic and optical components or sensors, open new possibilities in physics and electrical engineering. The same materials are also interesting for chemists and biologists due to their bio-compatibility. Drugs, implants and detectors for pathogens could be built with their help.

This will not be feasible if scientists of different fields do not look beyond their own area of expertise and start to cooperate. Today it is more important than ever to learn to understand the language and way of thinking of the other sciences. It was the most intriguing detail of my thesis for me to be able to learn and use the techniques of physics, chemistry and biology together for the investigation of new ideas.

6 Appendix

Polyaniline nanowire synthesis templated by DNA

Patrick Nickels, Wendy U Dittmer, Stefan Beyer, Jörg P Kotthaus
and Friedrich C Simmel

Department of Physics and Center for Nanoscience, LMU München
Geschwister-Scholl-Platz 1, 80539 Munich, Germany

Received 7 July 2004, in final form 23 August 2004

Published 10 September 2004

Online at stacks.iop.org/Nano/15/1524

doi:10.1088/0957-4484/15/11/026

Abstract

DNA-templated polyaniline nanowires and networks are synthesized using three different methods. The resulting DNA/polyaniline hybrids are fully characterized using atomic force microscopy, UV–vis spectroscopy and current–voltage measurements. Oxidative polymerization of polyaniline at moderate pH values is accomplished using ammonium persulfate as an oxidant, or alternatively in an enzymatic oxidation by hydrogen peroxide using horseradish peroxidase, or by photo-oxidation using a ruthenium complex as photo-oxidant. Atomic force microscopy shows that all three methods lead to the preferential growth of polyaniline along DNA templates. With ammonium persulfate, polyaniline can be grown on DNA templates already immobilized on a surface. Current–voltage measurements are successfully conducted on DNA/polyaniline networks synthesized by the enzymatic method and the photo-oxidation method. The conductance is found to be consistent with values measured for undoped polyaniline films.

(Some figures in this article are in colour only in the electronic version)

1. Introduction

The highly specific molecular recognition processes between DNA strands with complementary base sequences form the basis of DNA self-assembly. In contrast to other self-assembly strategies, DNA-based approaches offer the significant advantage of sequence programmability and therefore the potential to construct nontrivial assemblies [1, 2]. Whereas conventional self-assembly processes such as the formation of self-assembled monolayers lead to structures with very low information content (periodic assemblies), DNA, in principle, can be used to produce non-periodic and complex structures. A large variety of such DNA-based nanoconstructs have been demonstrated in recent years: for example, geometric objects like cubes [3] and octahedra [4], or various two-dimensional assemblies [5–7]. The power of DNA-based algorithmic self-assembly has recently been shown by the construction of a Sierpinski triangle [8]. Utilizing its mechanical properties, DNA can even be used to build dynamic nanoscale actuators (see e.g., [9–11]).

One of the most challenging goals of molecular nanotechnology is the self-assembly of a molecular computer.

Whereas great progress has been made in the electronic characterization of single molecules, there are only few convincing concepts for the assembly of electronic circuits made from molecules [12]. It is therefore of great interest to explore whether the unique self-assembly properties of DNA can be exploited for the construction of nanoscale electronic circuits. Recent detailed investigations into the conductivity of DNA molecules have shown that DNA is an extremely poor conductor [13–18]. To build electronic circuits with the help of DNA therefore requires attachment of electronically functional materials to DNA [13, 19–31] or an appropriate chemical modification of DNA itself [32–34]. At the same time, the molecular recognition properties of DNA should not be compromised by these modifications. DNA has already been shown to be a template for the directed growth of metals [13, 19–23], semiconductor nanoparticles [24, 25] and conductive polymers [26–30]. Successful electronic transport measurements have predominantly been performed with DNA-templated metal wires so far—with the exception of the ingenious DNA-directed assembly of a carbon nanotube based field effect transistor [31]. Metal wires are only useful as interconnects for electronically functional structures like

diodes or transistors. It is therefore of great importance to the field of DNA-based electronics to find materials with interesting electronic properties which are compatible with DNA technology. Obvious candidates are conductive polymers such as polypyrrole, polyaniline (PAni) [27–30] or poly(phenylenevinylene) (PPV) [26] which are based on cationic monomers or precursors and can therefore potentially be synthesized along the negatively charged sugar–phosphate backbone of DNA. We here present a full comparative study of three different methods for the synthesis of the conductive polymer polyaniline templated on DNA, including I – V measurements. Synthesis is performed both in solution and on a surface. The resulting DNA/PAni complexes are stretched on different substrates (mica and silicon) and characterized using atomic force microscopy (AFM). UV–vis spectroscopy gives spectroscopic evidence for the formation of polyaniline. DC transport measurements performed on undoped DNA/PAni wires yield conductance values consistent with those obtained for weakly conducting polyaniline films.

2. Experimental details

2.1. Template-directed synthesis of polyaniline

Polyaniline is a conductive polymer which can be synthesized by oxidative polymerization from its monomer aniline. At low pH values aniline ($pK_b = 9.4$) is protonated to form the positively charged anilinium ion, and it can be exchanged as a counterion for the negatively charged sugar–phosphate backbone of DNA. Here, three different methods were employed to synthesize polyaniline on DNA. A mild oxidative method using horseradish peroxidase (HRP) and hydrogen peroxide, a photo-oxidation method using ruthenium tris(bipyridinium) ($\text{Ru}(\text{bpy})_3^{2+}$) complexes, and a harsh method using ammonium persulfate (APS) as an oxidation agent. The latter method was also used to polymerize polyaniline along DNA strands immobilized to a substrate. λ -DNA (New England Biolabs) with a length of 16.5 μm (48.5 kbp) was used as the DNA template in all cases. Before modification, the DNA was purified by precipitation in isopropanol. If not stated otherwise, all chemicals were purchased from Sigma-Aldrich and used without further purification. In all cases, polyaniline was synthesized at moderately low pH values of 3–5 to prevent DNA damage.

2.1.1. Horseradish peroxidase/hydrogen peroxide method. This method is adapted from [27]. The biological oxidoreductase horseradish peroxidase (HRP) catalyses the reduction of hydrogen peroxide which is accompanied by the oxidation of another molecule. In the presence of both aniline and hydrogen peroxide, HRP catalyses the oxidative polymerization of polyaniline under relatively mild reaction conditions. To facilitate polyaniline synthesis along DNA templates, λ -DNA ($25 \mu\text{g ml}^{-1}$) was typically incubated for 20–60 min in 100 μl aniline solution (1.92 mM in phosphate buffer, pH = 4.3). This corresponds to a ratio of aniline to DNA phosphate groups of 25:1. To this solution 5 μl HRP (5 mg ml^{-1}) was added, followed by the addition of 16 μl H_2O_2 (0.03% in H_2O). Hydrogen peroxide was added in four aliquots of 4 μl . After 90 min of reaction, the

resulting polyaniline/DNA wires were characterized using UV–vis spectroscopy or stretched on a substrate for AFM imaging and electrical characterization as described below.

2.1.2. Ruthenium tris(bipyridinium) method. This method is adapted from [28, 29]. The ruthenium tris(bipyridinium) ($\text{Ru}(\text{bpy})_3^{2+}$) complex strongly absorbs light of wavelengths around 450 nm. In the photo-excited state it can oxidize other species by oxidative electron transfer. For polyaniline synthesis, DNA was added to a solution of *N*-phenylene phenyldiamine (1 mM in H_2O , adjusted to pH = 3 with HCl) to yield a final concentration of $25 \mu\text{g ml}^{-1}$ and a total volume of 120 μl . To this solution, 1 μl of the ruthenium complex (1 mM in H_2O) was pipetted, followed by mixing. The photo-oxidation was initiated by illuminating the reaction vial with a mercury lamp ($P = 100 \text{ W}$) through a band pass filter ($\lambda = 470$ – 490 nm). The reaction was typically maintained for 60 min.

2.1.3. Ammonium persulfate method. For synthesis of polyaniline on DNA templates immobilized on a chip surface, the chip was first incubated for 20–60 min in a 1–100 mM aniline solution in phosphate buffer (pH = 4.3). After thoroughly rinsing the chip with deionized water, it was incubated in a 1 mM solution of $(\text{NH}_4)_2\text{S}_2\text{O}_8$ for 20 min to polymerize the aniline monomers bound to the DNA. The reaction was stopped by extensive rinsing with deionized water and drying of the chip under a flow of nitrogen gas. This procedure could be applied repeatedly to the chips which resulted in denser coating of the DNA with polyaniline.

Ammonium persulfate was also used to synthesize polyaniline templated by DNA in solution. Typically, to 50 μl of DNA ($50 \mu\text{g ml}^{-1}$ in 10 mM phosphate buffer, pH = 4.3) 50 μl of a 77 μM solution of aniline was pipetted. After 20–60 min, 25 μl of ammonium persulfate solution (185 μM) was added to the reaction mixture. In this procedure, the ratio between phosphates, aniline and $(\text{NH}_4)_2\text{S}_2\text{O}_8$ was 2:1:1.2. When aniline was present in excess, this procedure led to the formation of large amounts of PAni not attached to DNA. On the other hand, at roughly equimolar ratio between aniline and phosphates only incomplete coverage of DNA by polyaniline could be achieved (see the discussion).

2.2. Spectroscopy

UV–vis spectroscopy was used to validate the synthesis of polyaniline wires and to monitor the reaction progress. Polyaniline has strong absorption bands around $\lambda = 350$ – 450 nm and between $\lambda = 750$ – 850 nm [35] whereas DNA has its typical strong absorption peak at $\lambda = 260 \text{ nm}$. For longer π -conjugation lengths, the second peak in the polyaniline absorption spectrum can shift towards longer wavelengths [28]. Spectroscopic measurements were performed on a Jasco UV–vis spectrophotometer V-550.

2.3. DNA immobilization and AFM imaging

Before AFM characterization or for polyaniline synthesis on surface bound templates the DNA wires were immobilized on a solid substrate using molecular combing techniques [36, 37].

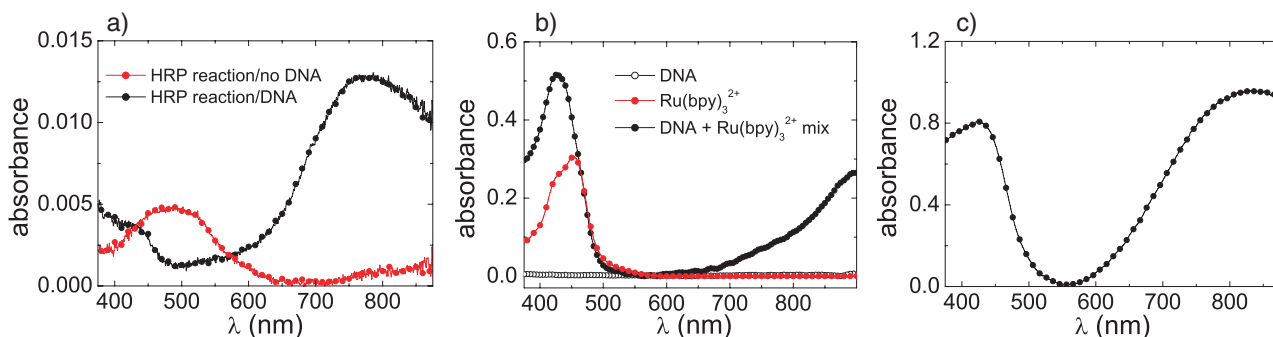


Figure 1. UV-vis spectra of polyaniline synthesized on DNA templates using three different methods. (a) HRP/H₂O₂ method: there is almost no polyaniline formation in the absence of DNA (red/grey curve). The peak at 500 nm is possibly due to the spurious formation of oligomers. In the presence of DNA, polyaniline is synthesized along the template as can be seen by the peaks at 400 and 800 nm. (b) Ru(bpy)₃²⁺ method: the absorbance of the ruthenium complex (red/grey curve) overlaps with the low-wavelength absorbance band of PANi. However, the absorption at higher wavelengths shows formation of the polymer (black curve). (c) Absorbance of PANi synthesized with ammonium persulfate as oxidant.

For AFM characterization, the preferred substrate was mica. To the mica surfaces a 10 μ l drop of a 2 mM aqueous solution of MgCl₂ was added, followed by 10 μ l DNA solution (25–250 μ g ml⁻¹) and another 10 μ l drop of water. After each application of a solution the mica sample was spun on a spin coater for 90 s at 3000 rpm. A final spin for 90 s served to dry the sample. For electrical characterization, the wires were stretched between Au electrodes on a silicon substrate. To facilitate combing on silicon, the chips were treated with trimethylchlorosilane for two minutes and subsequently washed with hexane. A drop of DNA solution (1 μ l) at a concentration of 50–250 μ g ml⁻¹ in MES buffer (2.4 mM, pH = 5.5) was deposited on the chip, left for one minute and then removed using filter paper. The receding meniscus of the droplet stretches and aligns the DNA molecules on the surface. AFM characterization of the immobilized DNA/Pani hybrids was performed in tapping mode with a Digital Instruments scanning probe microscope (Dimension 3100) with Nanoscope IIIa controller hardware.

2.4. Lithography and electronic measurements

Electrode structures were fabricated on n⁺-doped silicon wafers with a 150 nm thick insulating oxide layer (Crystec GmbH, Germany) using standard optical and electron beam lithographic techniques. The optically defined electrodes had a thickness of 75 nm with a 5 nm adhesion layer of nickel–chromium or titanium. The electron beam written structures were 35 nm thick with a 5 nm adhesion layer. The electrical transport properties of the polyaniline/DNA hybrids connected to the electrodes were determined in a dry, temperature-controlled environment on a SUSS PM5 analytical probe system (Suss Microtec, Garching, Germany) in a standard two-point arrangement using a low-noise current amplifier (Femto DLPCA-200) close to the sample.

3. Results and discussion

3.1. Synthesis

UV-vis spectra recorded from the reaction solutions show that all three procedures described above successfully led to the

synthesis of polyaniline (figure 1). The resulting spectra for the HRP/H₂O₂ method are shown in figure 1(a). Without DNA, almost no polyaniline is synthesized. In the presence of DNA, however, a clear absorption signal from polyaniline is observed. No absorption is detected from polyaniline when HRP is not added to the reaction. An absorption spectrum obtained from PANi synthesized by the Ru(bpy)₃²⁺ method is shown in figure 1(b). The PANi absorption peak at \approx 400 nm overlaps with the strong absorption of the ruthenium complex at \approx 450 nm. However, the formation of polyaniline can be judged from the appearance of an absorption band at higher wavelengths. This absorption band is shifted towards 900 nm, which indicates that longer PANi chains are formed than in the other reactions. In figure 1(c), the absorbance of polyaniline synthesized using ammonium persulfate at pH = 4.3 is shown. The low aniline concentrations needed to observe preferential growth along DNA (see the next section) were too low to lead to measurable PANi absorbance values. The absorbance curves in figures 1(b) and (c) were therefore recorded from reaction solutions with higher aniline/oxidant concentrations. Under these conditions, DNA does not act as a template any more, and PANi synthesis takes place uniformly in solution. In contrast to the HRP method, DNA is not required for the formation of PANi using APS. However, due to the higher local concentration of anilinium ions along the sugar–phosphate backbone, DNA still acts as a template at very low reactant concentrations. Accordingly, for AFM imaging and *I*–*V* measurements, the concentrations were chosen much lower (see also the experimental sections). In order to be able to judge whether under low concentration conditions PANi synthesis preferentially took place along DNA templates, DNA/PANI samples were immobilized on surfaces and extensively investigated using atomic force microscopy.

3.2. AFM characterization

AFM images of DNA/PANI hybrids show the formation of polyaniline preferentially along DNA strands for all synthesis procedures adopted. In solution, the ammonium persulfate method could only be applied at low aniline concentrations. Otherwise a large amount of PANi not templated by DNA would be formed. However, working at low aniline concentrations

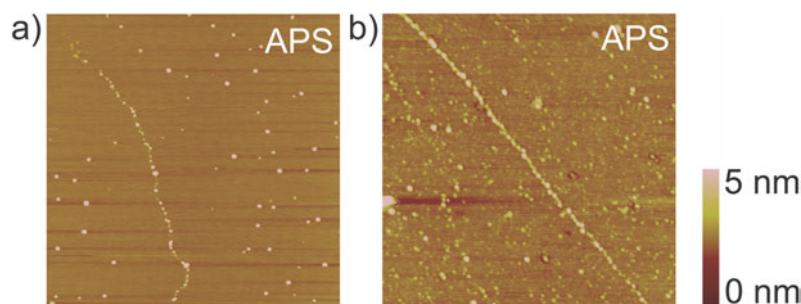


Figure 2. Topographic AFM images of polyaniline synthesized on DNA templates. (a) Synthesis was performed in solution, followed by stretching on mica (the image size is $4\ \mu\text{m} \times 4\ \mu\text{m}$). (b) DNA templates were first combed on a silanized silicon surface, followed by polyaniline synthesis on the substrate (the image size is $2\ \mu\text{m} \times 2\ \mu\text{m}$).

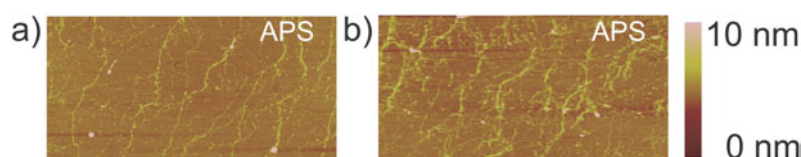


Figure 3. AFM images of polyaniline synthesized on DNA networks: (a) after one reaction cycle, (b) after a second application of the reaction solution to the network shown in (a). The size of the images is $5\ \mu\text{m} \times 2.5\ \mu\text{m}$ in both cases.

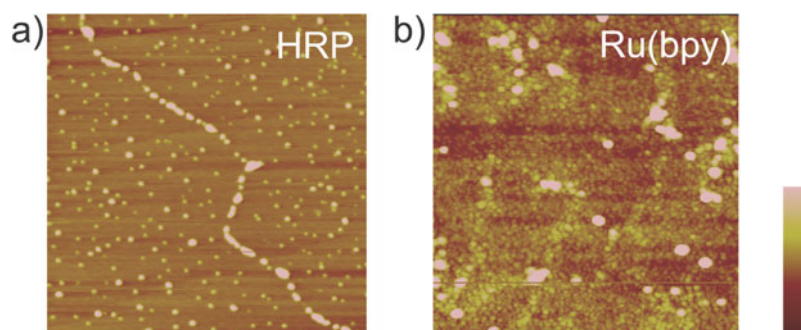


Figure 4. (a) AFM image of DNA/PANI synthesized by the HRP/H₂O₂ method in solution and stretched on a mica substrate. The image size is $2\ \mu\text{m} \times 2\ \mu\text{m}$; the height scale bar ranges from 0 to 5 nm. (b) DNA/PANI network synthesized by the Ru(bpy)₃²⁺ method and stretched on a silicon substrate. The image size is $1.3\ \mu\text{m} \times 1.3\ \mu\text{m}$; the height scale bar ranges from 0 to 10 nm.

led to the formation of only isolated PANI particles along DNA (figure 2(a)). PANI/DNA hybrids could be well distinguished from pure DNA from height measurements. On topographic AFM images, DNA typically appears to be 0.5 nm in height. In contrast, PANI particles and wires were typically 5 nm in height or higher (see figures). One of the advantages of the persulfate method was the possibility to synthesize PANI on pre-immobilized DNA. An example of a chain of PANI particles synthesized along a DNA strand immobilized on a silanized silicon surface is shown in figure 2(b). The figure shows the formation of closely spaced particles of uniform size along the template. There is also some background deposition of PANI. To enhance the coverage of DNA with PANI, the reaction mixture could be applied to immobilized templates several times. This is exemplified in figure 3 with a DNA network which has been imaged after one and two synthesis cycles. Synthesis on a surface is not as effective with the other methods. The HRP/H₂O₂ method is compromised by protein adsorption on the surface. The Ru(bpy)₃²⁺-based method could not be applied as the reaction mixture has to be strongly illuminated to support the photo-oxidation reaction. In solution, however, these methods also successfully led to the

formation of DNA/PANI hybrids. AFM images of DNA/PANI wires synthesized by these methods are shown in figure 4. For the HRP/H₂O₂ method, PANI domains with a typical height of 5 nm formed uniformly along DNA (figure 4(a)) with some background formation of PANI remote from the template. DNA also acted as a template for the formation of PANI using the Ru(bpy)₃²⁺ method; however, the resulting structures were much less uniform in height and tended to agglomerate (figure 4(b)). Stretching DNA/PANI hybrid structures between electrodes turned out to be more difficult than on a bare substrate. The molecular combing technique could not be applied effectively as the receding meniscus of the sample droplet preferentially moved parallel to the electrode gaps and therefore exerted a shearing force to the DNA strands. AFM imaging was difficult due to the large height difference between gold electrodes (40–80 nm) and the DNA/PANI hybrids. Furthermore, AFM images of samples prepared by the HRP/H₂O₂ method suffered from contamination by protein adsorption. Two examples of DNA/PANI networks spanning a $2\ \mu\text{m}$ wide gap between electrodes are shown in figure 5. Whereas the HRP/H₂O₂ sample is highly contaminated, single DNA/PANI wires can be discerned on the AFM image of the

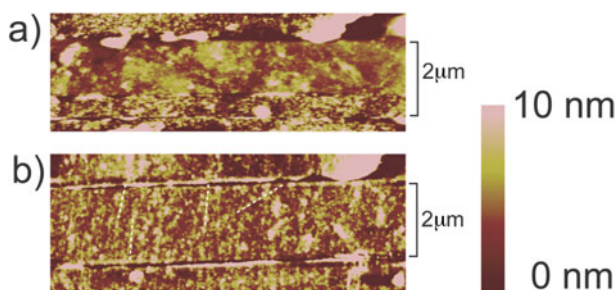


Figure 5. AFM images of polyaniline/DNA networks stretched between two electrodes. (a) Networks synthesized by the HRP/H₂O₂ method, (b) synthesized by the Ru(bpy)₃²⁺ method. The electrode spacing of 2 μm is indicated. The lines in (b) are drawn as a guide for the eye. The height scale is 0–20 nm.

Ru(bpy)₃²⁺ sample. In the case of the HRP/H₂O₂ sample, the excessive protein adsorption is probably mediated by the silanization [38].

3.3. Electronic properties

The electronic properties of the DNA/PAni networks were investigated using samples as shown in figure 5. The samples were extensively washed in deionized water and dried thoroughly after the application of the DNA networks to avoid conduction by water and salt films. All experiments were carried out at room temperature. Control experiments on unmodified DNA performed before PAni synthesis yielded sample resistances >10 TΩ without exception ($I < 1$ pA at $V = 10$ V applied voltage; see figure 6(d)). We were also unable to drive a current through networks prepared by the ammonium persulfate method, even after the application of several reaction cycles to the sample as described in the previous section. Control experiments performed on continuous polyaniline films prepared by the same method with larger amounts of reagents led to the expected conductivity values. We therefore conclude that the APS method in principle could produce polyaniline; however, the coverage of the DNA templates was not dense enough to allow for a current to flow through the network. It is also conceivable that the DNA templates are degraded by the strong oxidation agent, leading to discontinuities in the PAni wires. Typical I – V curves obtained with samples prepared by the other methods are shown in figure 6. All curves show similar, slightly rectifying behaviour with conductances in the range of 2–5 pS (2 μm electrode spacing) and 0.1–1 nS (200 nm electrode spacing) as expected for a weakly semiconducting material. As displayed in figure 6(d), samples prepared by the HRP/H₂O₂ method and the Ru(bpy)₃²⁺ method show nearly identical behaviour in the voltage range between –5 and 5 V. To rule out conduction by other components than the DNA/PAni networks, additional control experiments were performed on HRP films and on Ru(bpy)₃²⁺ solutions applied to the surface. These experiments did not lead to measurable currents. A finite current was only measured when all the components necessary to synthesize polyaniline on DNA were present. It cannot be ruled out, however, that spurious PAni not formed on the DNA templates also contributes to conduction. To compare the results of our measurements with literature values for the conductivity of polyaniline,

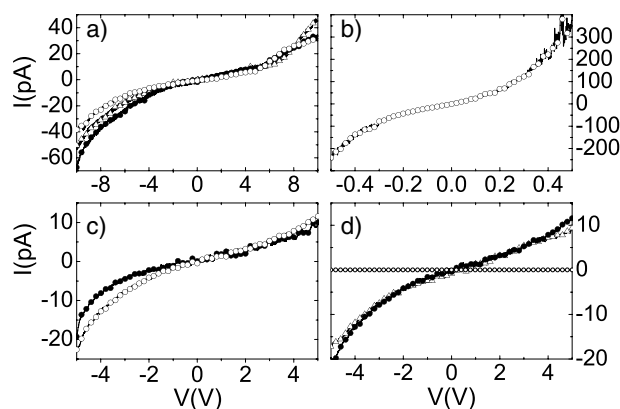


Figure 6. (a) I – V curves measured with three different samples of DNA/PAni networks synthesized by the HRP/H₂O₂ method placed between electrodes with a 2 μm spacing (as in figure 5(a)); (b) as in (a), measured with electrodes with a 200 nm spacing; (c) I – V curves measured on two DNA/PAni samples synthesized by the Ru(bpy)₃²⁺ method (cf figure 5(b)); (d) comparison of I – V curves synthesized by the two methods (triangles: HRP/H₂O₂ method; closed circles: Ru(bpy)₃²⁺ method) and control measurement for unmodified DNA (open circles).

we can make a simple estimate: if we assume that of the order of ~100 wires with ~5 nm diameter connect the two electrodes, a conductance of 1 pS corresponds to a conductivity of $\approx 1 \times 10^{-5}$ S cm⁻¹. The measured conductance values therefore are consistent with values expected for undoped polyaniline base [39]. It is clear, however, that the values measured are not determined by the conduction properties of bulk polyaniline. Current flow will also be strongly affected by discontinuities between conducting domains (see figure 4) and by contact resistances between the networks and the electrodes. This is also expressed in the higher conductance obtained in the measurement with the more closely spaced electrodes (figure 6(b)). Even though the electrodes are only tenfold closer, the conductance increases by a factor of 100. This is probably due to the considerably higher probability of finding a conducting path through the network connecting the electrodes. To further elucidate the conduction mechanisms leading to the currents measured in the experiments described above, additional experiments are required. In particular, the influence of temperature and doping level on the conduction has to be determined. Preliminary attempts to dope the wires using hydrochloric acid did not lead to improved conductance values. It is assumed that subsequent washing with deionized water could ‘undope’ the wires again [40]. One also has to investigate the influence of the contact resistance between the DNA/PAni networks and the electrodes. To improve the contact resistance, it would be important to have a technique to deposit electrodes after the deposition of the networks on the substrate without damaging the PAni. We already performed some preliminary experiments on electroless deposition of gold on top of lithographically defined electrodes coated with DNA/PAni networks following a procedure described by Seidel *et al* [41]. So far, this did not lead to improved conductivity. Another possibility would be to make contact to the samples using electrodes on elastomeric stamps, a technique which has already successfully been used to contact other organic materials [42].

4. Conclusion

We have shown that polyaniline can be synthesized on DNA templates by three different methods. DNA templating seems to work best for polyaniline formed by oxidative polymerization of aniline with ammonium persulfate, both in solution and on templates immobilized on a chip. DNA also is a good template for polyaniline formed by enzymatically catalysed polymerization utilizing horseradish peroxidase. However, immobilization of these structures between contact electrodes is compromised by extensive protein adsorption to the surface. A photo-oxidation method using ruthenium tris(bipyridinium) complexes as photo-oxidant results in less uniform DNA/PAni structures than the other methods. On the other hand, electronic characterization of the resulting DNA/PAni hybrids was only successful for the enzymatic synthesis protocol and the photo-oxidation method. For the DNA/PAni networks investigated, the measured conductance values are consistent with those expected for undoped polyaniline. Additional experiments have to be conducted to improve the conduction properties of the DNA/PAni wires and to possibly utilize the promising protocol for the synthesis of polyaniline on surface-bound DNA templates.

Acknowledgments

This work is supported through the Emmy Noether program of the Deutsche Forschungsgemeinschaft (DFG). WUD acknowledges support by the Alexander von Humboldt foundation.

References

- [1] Seeman N C *et al* 1998 *Nanotechnology* **9** 257–73
- [2] Seeman N C 2003 *Nature* **421** 427–31
- [3] Chen J H and Seeman N C 1991 *Nature* **350** 631–3
- [4] Zhang Y W and Seeman N C 1994 *J. Am. Chem. Soc.* **116** 1661–9
- [5] Winfree E, Liu F R, Wenzler L A and Seeman N C 1998 *Nature* **394** 539–44
- [6] Mao C D, Sun W Q and Seeman N C 1999 *J. Am. Chem. Soc.* **121** 5437–43
- [7] Yan H, Park S H, Finkelstein G, Reif J H and LaBean T H 2003 *Science* **301** 1882–4
- [8] Rothmund P W K, Papadakis N and Winfree E 2004 submitted
- [9] Mao C D, Sun W Q, Shen Z Y and Seeman N C 1999 *Nature* **397** 144–6
- [10] Yurke B, Turberfield A J, Mills A P, Simmel F C and Neumann J L 2000 *Nature* **406** 605–8
- [11] Feng L P, Park S H, Reif J H and Yan H 2003 *Angew. Chem. Int. Edn Engl.* **42** 4342–6
- [12] Heath J R, Kuekes P J, Snider G S and Williams R S 1998 *Science* **280** 1716–21
- [13] Braun E, Eichen Y, Sivan U and Ben-Yoseph G 1998 *Nature* **391** 775–8
- [14] Porath D, Bezryadin A, de Vries S and Dekker C 2000 *Nature* **403** 635–8
- [15] de Pablo P J, Moreno-Herrero F, Colchero J, Herrero J G, Herrero P, Baro A M, Ordejon P, Soler J M and Artacho E 2000 *Phys. Rev. Lett.* **85** 4992–5
- [16] Cai L T, Tabata H and Kawai T 2000 *Appl. Phys. Lett.* **77** 3105–6
- [17] Storm A J, van Noort J, de Vries S and Dekker C 2001 *Appl. Phys. Lett.* **79** 3881–3
- [18] Cai L T, Tabata H and Kawai T 2001 *Nanotechnology* **12** 211–6
- [19] Richter J, Seidel R, Kirsch R, Mertig M, Pompe W, Plaschke J and Schackert H K 2000 *Adv. Mater.* **12** 507
- [20] Richter J, Mertig M, Pompe W, Monch I and Schackert H K 2001 *Appl. Phys. Lett.* **78** 536–8
- [21] Richter J, Mertig M, Pompe W and Vinzelberg H 2002 *Appl. Phys. A* **74** 725–8
- [22] Keren K, Krueger M, Gilad R, Ben-Yoseph G, Sivan U and Braun E 2002 *Science* **297** 72–5
- [23] Richter J 2003 *Physica E* **16** 157–73
- [24] Coffey J L, Bigham S R, Li X, Pinizzotto R F, Rho Y G, Pirtle R M and Pirtle I L 1996 *Appl. Phys. Lett.* **69** 3851–3
- [25] Dittmer W U and Simmel F C 2004 *Appl. Phys. Lett.* **85** 633–5
- [26] Eichen Y, Braun E, Sivan U and Ben-Yoseph G 1998 *Acta Polym.* **49** 663–70
- [27] Nagarajan R, Liu W, Kumar J, Tripathy S K, Bruno F F and Samuelson L A 2001 *Macromolecules* **34** 3921–7
- [28] Uemura S, Shimakawa T, Kusabuka K, Nakahira T and Kobayashi N 2001 *J. Mater. Chem.* **11** 267–8
- [29] Kobayashi N, Uemura S, Kusabuka K, Nakahira T and Takahashi H 2001 *J. Mater. Chem.* **11** 1766–8
- [30] Ma Y F, Zhang J M, Zhang G J and He H X 2004 *J. Am. Chem. Soc.* **126** 7097–101
- [31] Keren K, Berman R S, Buchstab E, Sivan U and Braun E 2003 *Science* **302** 1380–2
- [32] Maeda Y, Tabata H and Kawai T 2001 *Appl. Phys. Lett.* **79** 1181–3
- [33] Lee H Y, Tanaka H, Otsuka Y, Yoo K H, Lee J O and Kawai T 2002 *Appl. Phys. Lett.* **80** 1670–2
- [34] Gu J H, Tanaka S, Otsuka Y, Tabata H and Kawai T 2002 *Appl. Phys. Lett.* **80** 688–90
- [35] Stafstrom S, Bredas J L, Epstein A J, Woo H S, Tanner D B, Huang W S and MacDiarmid A G 1987 *Phys. Rev. Lett.* **59** 1464–7
- [36] Bensimon A, Simon A, Chiffaudel A, Croquette V, Heslot F and Bensimon D 1994 *Science* **265** 2096–8
- [37] Bensimon D, Simon A J, Croquette V and Bensimon A 1995 *Phys. Rev. Lett.* **74** 4754–7
- [38] Sigal G B, Mrksich M and Whitesides G M 1998 *J. Am. Chem. Soc.* **120** 3464–73
- [39] Stejskal J, Hlavata D, Holler P, Trchova M, Prokes J and Sapurina I 2004 *Polym. Int.* **53** 294–300
- [40] Menon R, Yoon C O, Moses D and Heeger A J 1998 *Handbook of Conducting Polymers* ed T A Skotheim, R L Elsenbaumer and J R Reynolds (New York: Dekker)
- [41] Seidel R, Liebau M, Duesberg G S, Kreupl F, Unger E, Graham A P, Hoenlein W and Pompe W 2003 *Nano Lett.* **3** 965–8
- [42] Zaumseil J, Someya T, Bao Z N, Loo Y L, Cirelli R and Rogers J A 2003 *Appl. Phys. Lett.* **82** 793–5

Design variations for an aptamer-based DNA nanodevice

Stefan Beyer, Wendy U. Dittmer, Friedrich C. Simmel
*Center for NanoScience and Sektion Physik, Ludwig-Maximilians-Universität,
Geschwister-Scholl-Platz 1, 80539 Munich, Germany*
(Dated: September 16, 2004)

The performance of DNA nanodevices based on a thrombin-binding DNA aptamer is strongly dependent on chemical modifications and extensions of the protein-binding core sequence. We here give an overview of the influence of fluorescent labeling and extension of the aptamer device sequence on its binding properties. Sequence extension on the 5' end as well as labeling on the 5' or 3' end does not significantly reduce the binding capabilities. Sequence extension on the 3' end completely suppresses binding. This knowledge can be utilized for the construction of a doubly labeled aptamer device which can be operated as a switchable molecular beacon.

I. INTRODUCTION

DNA nanodevices are artificial supramolecular structures composed of DNA which can be controllably switched between different conformations. Switching can be accomplished by changes in buffer composition [1–3] or by the introduction of specific DNA operator strands [4–10]. In the latter case the conformational changes are actively driven by the free energy released from the hybridization between complementary DNA strands. Recently it was shown that a similar operation principle as employed for DNA nanodevices can also be utilized for the construction of a switchable DNA aptamer [11]. Aptamers are DNA or RNA structures which are evolved from a random pool of nucleic acids to bind strongly and specifically to a target molecule [12]. Using the concept of DNA strand displacement by branch migration a DNA aptamer structure can be easily switched between a binding and a non-binding form [11]. The result is a simple DNA nanodevice which can repeatedly bind and release a specific molecule. To apply the branch migration principle to aptamers, DNA address tags which serve as binding sites for DNA operator strands have to be attached to the aptamer structure without significantly deteriorating the binding properties of the aptamer. Furthermore, for the characterization of the devices, the structures have to be fluorescently tagged. In previous studies on aptamer-based fluorescent sensors, the influence of the fluorescent label on the binding properties of aptamers has already been investigated [13–17]. From selection experiments it is well known that only slight alterations of aptamer sequences can significantly deteriorate the performance of the aptamers. We here specifically investigate the influence of fluorescent labeling positions and sequence extensions on the binding properties of a switchable DNA nanodevice based on a thrombin-binding aptamer. The device is labeled at the 5' and the 3' end as well as on both ends. It is found that labeling does not have a significant impact on the binding properties of the aptamer. We present evidence that labeling at the 3' end slightly decreases the affinity of the device for thrombin, whereas extension and labeling at the 5' end does not seem to hinder binding to thrombin. By contrast, with an exten-

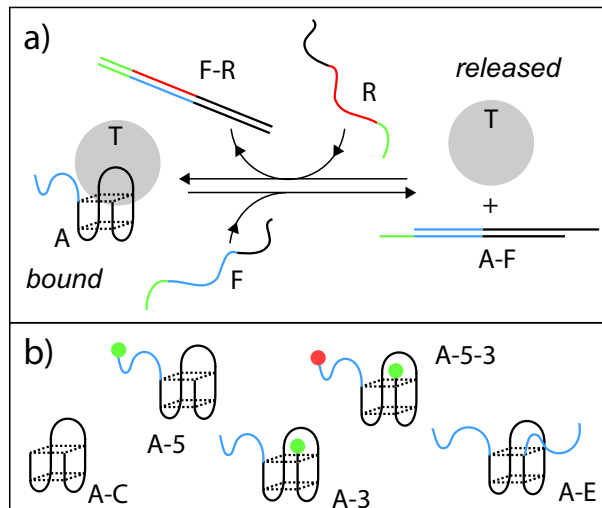


FIG. 1: a) Operation principle of a thrombin-binding DNA device. On the left hand side the aptamer device A is folded into a chair-like conformation which results from two stacked G quartets. In this conformation it binds to the protein thrombin (T). The addition of F destroys this conformation by duplex formation with A and releases the protein (right hand side). This process can be reversed by the addition of the strand R which displaces F from A and therefore allows A to assume its thrombin-binding conformation again. b) Variants of the aptamer devices investigated in this study. Devices are labeled or extended at the 5' or 3' ends as indicated.

sion of the base sequence on the 3' end the device loses its binding properties altogether. This result is particularly important for the development of surface-bound devices and for the incorporation of aptamers into DNA supramolecular structures.

II. OVERVIEW

The operation principle of the device is schematically shown in Fig. 1(a). On the left hand side, the protein thrombin is bound to the folded DNA device A based on the well-known anti-thrombin aptamer [18]. Upon addi-

Name	Sequence
A-C	5'- GGTTGGTGTGGTTGG -3'
A-0	5'-TAAGTTCATCTCG GGTTGGTGTGGTTGG -3'
A-5	5'-OG488-TAAGTTCATCTCG GGTTGGTGTGGTTGG -3'
A-3	5'-TAAGTTCATCTCG GGTTGGTGTGGTTGGT -OG488-3'
A-5-3	5'-Cy3-TAAGTTCATCTCG GGTTGGTGTGGTTGGT -OG488-3'
A-E1	5'-CCTCATCAACAGACAGCGT GGTTGGTGTGGTTGGC AGATATGCGTCAGGACATG
A-E2	5'-CCTCATCAACAGACAGCGTGCCATACG GGTTGGTGTGGTTGGA ATCCTAGCAGATATGCGTCAGGACATG-3'
F	5'-CACACCAACCGAGATGAACTTACGGCGTTG-3'
R	5'-CAACGCCGTAAGTTCATCTCGGTTGGTGTG-3'

TABLE I: Sequences of the DNA strands used. The aptamer core sequence is shown in bold letters. OG488 stands for the fluorescent label Oregon Green 488 (Molecular Probes, Oregon), Cy3 is the fluorescent dye indocarbocyanine.

tion of a DNA strand F which can attach to the “toehold” section of the device (blue), thrombin is displaced from the device. In the released state (right hand side), the aptamer is forced into a double-helical conformation (A-F) which cannot bind the protein. Assisted by a second toehold section (green), the strand F can be removed from the device again by branch migration, a principle which has been previously employed for other DNA nanomechanical devices. The free aptamer device can refold and bind to thrombin again and a “waste” product F-R is released. The operation of the device depends critically on the blue toehold section which significantly increases the speed of the protein release. Also, for characterization purposes and in biosensing applications, fluorescent labeling is usually necessary. In the present study, we investigate several variants of the aptamer device which differ in labeling position or in an extension of the core aptamer sequence by single-stranded arms. The various devices are depicted in Fig. 1(b). The core device (A-C) consists of just the original 15 base long thrombin-binding aptamer sequence [18]. Devices A-5, A-3 and A-5-3 are extended with a random 12 base toehold section on the 5' end and labeled at the 5' position, the 3' position or on both positions, respectively. The 3' labels have been attached through an additional thymine spacer base. A-0 is the device with a 12 base toehold without any label. In some applications for a switchable aptamer device it would be important to immobilize the device and still have a free operator (toehold) section for the release process. In this case, the core aptamer would have to be extended on both 5' and 3' ends as in device A-E. We investigated two devices (A-E1 and A-E2) with extensions of 20 and 28 bases on each end, respectively.

III. METHODS

Experimental. The DNA sequences of the devices in Fig. 1 b) and of the fuel and removal strands F and R are given in Table 1. All oligonucleotides were synthesized, labeled and purified by biomers.net, Ulm, Germany.

Other chemicals were obtained from Sigma-Aldrich, Germany, unless stated otherwise, and used without further purification.

The buffer used for all experiments was a modified physiological buffer consisting of 20 mM Tris HCl, 150 mM NaCl, 10 mM MgCl₂ and 10 mM KCl at pH 8.5. Polyacrylamide gel electrophoresis was performed on a 12% native gel in TBE buffer (89 mM Tris HCl, 89 mM boric acid) with 10 mM KCl and run for 1 h with a field of 10 V/cm at 24°C. Gels were stained using the nucleic acid stain SYBR gold (Molecular Probes). The binding affinity of the aptamer device variants to thrombin was assayed in gel shift experiments in which the concentration ratio between device strands and thrombin was varied. The concentration of aptamer devices was between 0.5 μM and 1 μM in each lane and constant within each titration experiment.

The doubly labeled device A-5-3 can also function as a switchable, thrombin-binding molecular beacon and was further characterized in fluorescence resonance energy transfer (FRET) experiments. In FRET, an excited fluorescent “donor” dye can transfer its energy to an “acceptor” chromophore in its neighborhood whose absorption overlaps with the emission of the donor. The distance over which this process is effective, the Förster radius, is typically on the order of a few nanometers [19, 20]. In the case of the OG488-Cy3 pair it is ≈ 6 nm. FRET experiments were carried out on a Fluorolog-3 fluorescence spectrometer (Jobin Yvon Horiba, France). The excitation monochromator was set to λ=488 nm with a slit width of 5 nm. Emission was detected λ=521 nm through a slit with width 5 nm. The temperature for the FRET experiments was 37°C regulated with a Peltier-thermostated sample holder. The concentration of device strands was 100 nM in all cases, strands F and R were added stoichiometrically. Thrombin was added at 2.5-fold excess over the device strands.

Gel analysis. Depending on their quality, some of the gels were amenable to a more quantitative analysis. Band intensities were quantified with a homemade image analysis program. After subtraction of background signal, the

amounts of DNA in the upper and lower bands were determined by integration of the band intensities. As the intensity of the lower band usually saturated at a finite value even at the highest thrombin concentrations, we assumed that a certain amount of the devices was misfolded and therefore unable to bind to the protein at all. This was corrected for by subtraction. The ratio of the concentration of unbound device to the total concentration $[A]/[A]_0$ was then determined as the ratio of the intensity of the corrected lower band to the corrected total intensity.

IV. RESULTS AND DISCUSSION

Polyacrylamide gels resulting from three representative gel titration experiments are displayed in Fig. 2. In each gel, the added thrombin amount increases from left to right (see figure caption). The binding of the devices to the protein results in the appearance of a high molecular weight band, accompanied by the disappearance of the lower band from the unbound device. It is found that the devices A-E1 and A-E2 do not seem to bind thrombin at all. Devices A-5 and A-0 bind similarly well to thrombin as the core sequence A-C. In a direct comparison of A-5 and A-3, device A-5 binds more strongly to thrombin than the device labeled on the 3' end (see Fig. 3). For some gels, the binding affinity could be further quantified by the analysis of the band intensities (compare Methods). The result of this procedure is shown for three of the devices in Fig. 4, in which the ratio between bound and total device $Y = 1 - [A]/[A]_0$ is plotted against the initial thrombin concentration $[T]_0$. Fits of a theoretical binding curve to the data were used to determine the binding affinities of the various aptamer devices to thrombin. From the definition of the dissociation constant

$$K_d = \frac{[A][T]}{[C]}, \quad (1)$$

where $[C]$ denotes the concentration of the aptamer-thrombin complex, one obtains the theoretical binding curve

$$Y = \frac{1}{2[A]_0} \left\{ [A]_0 + [T]_0 + K_d - \sqrt{([A]_0 + [T]_0 + K_d)^2 - 4[A]_0[T]_0} \right\}. \quad (2)$$

This function can be fit to the data using K_d as the single fit parameter. A fit to the data obtained for the 3' labeled device A-3 yields a K_d of 280 nM, whereas the device A-5-3 has an apparent dissociation constant of 540 nM. The fit to the data obtained for the unlabeled A-0 yields an unexpected higher K_d of 850 nM. Whereas these values are in the same range as those obtained for the original aptamer sequence by other groups [16], their exact quantitative value is probably not reliable. Our results varied between 200 nM and 2.5 μ M with no

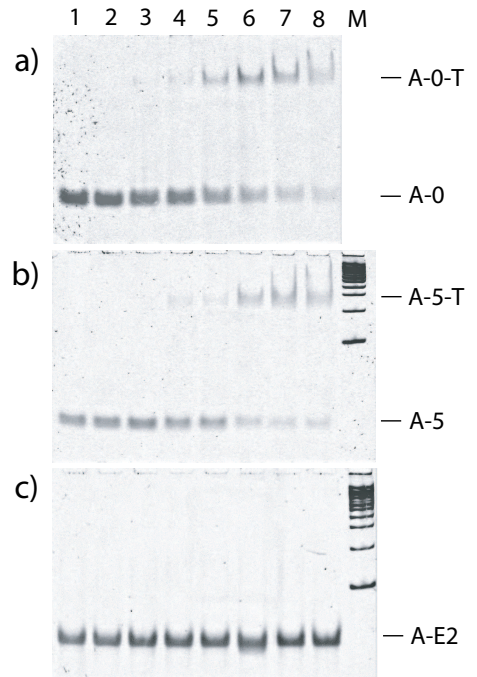


FIG. 2: Gel shift experiments with the aptamer devices: The first lane contains no thrombin. The ratio between initial concentrations of thrombin and aptamer devices is 0.5:1,1:1,1.5:1,2:1,3,5:1,7:1, and 10:1 from lanes 2 to 8. Lane M in gel b) and c) contains a 100 bp marker ladder for comparison. Gel a) contains the unlabeled device A-0, b) the 5' labeled device, and gel c) contains the extended device A-E2. Binding to thrombin can be judged from the appearance of a high molecular weight band (marked with A-0-T and A-5-T, respectively) in the gels. A-0 and A-5 bind comparatively well to the protein, whereas A-E2 does not seem to bind to thrombin at all.

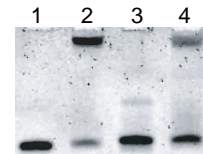


FIG. 3: Direct comparison of A-5 and A-3. Lane 1: 1 μ M A-5, no thrombin. Lane 2: 1 μ M A-5, thrombin in fivefold excess. Lane 3: 1 μ M A-3. Lane 4: 1 μ M A-3, thrombin in fivefold excess. A-5 binds more strongly to the protein than A-3, as can be judged from the stronger high molecular weight band for the bound complex.

clear dependence on the labeling position. In particular, we were unable to quantify the conclusion drawn from Fig. 3 as the K_d obtained for A-5 was unreasonably high. The quantitative analysis of the gels was compromised by several factors: The smearing of the higher molecular weight band for the device-protein complex made a determination of the intensity difficult. It is also unclear, whether dye labeling of the DNA strands

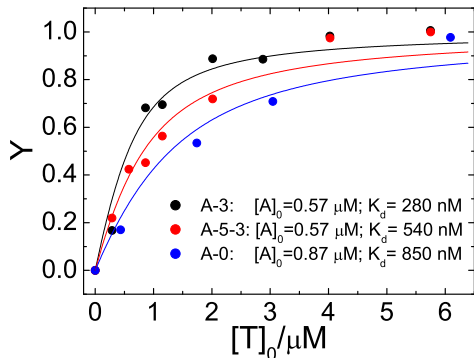


FIG. 4: Plot of the binding ratio Y against the total thrombin concentration for the devices A-3, A-5-3 and A-0. Data points are plotted as dots and fits to the data are continuous lines.

is efficient – and linear in the concentration – for the DNA-protein complex. We also suspect that some of the original complexes decay in the gel due to heating or other effects. In a different set of experiments using fluorescence correlation spectroscopy, we obtained a much lower K_d for A-5 of 10 nM which seems to be a more reasonable value [21].

We have previously demonstrated that A-3 and A-5 can be used for the characterization of the behavior of the aptamer devices in fluorescence resonance energy transfer experiments [11]. We here show that this can also be done in a molecular beacon configuration as employed in A-5-3. In Fig. 5 (a), fluorescence traces recorded for A-5-3 in the presence and in the absence of thrombin are presented for one operation cycle. With the addition of thrombin, the fluorescence signal decreases slightly (see Fig. 5 (b)). The binding of thrombin stabilizes the chair-like conformation of the aptamer core of the device which changes the mean distance between the fluorescent labels at the ends of the device strand. The effect is not as dramatic as in aptamer-based fluorescent sensors as the device is not specifically constructed for sensing purposes. With the addition of fuel strand F, the device A-5-3 is forced into a stretched duplex conformation (compare Fig. 1 (a)). This is accompanied by a sharp increase in the fluorescence signal as the FRET acceptor Cy3 is now far apart from the donor OG488. The same fluorescence level is attained in the absence as in the

presence of thrombin. However, the transition from the low fluorescence to the high fluorescence state is less rapid in the presence of thrombin as the bound protein slows down the formation of the stretched duplex (Fig. 5 (c)). Addition of the removal strand R removes F from the duplex A-5-3-F and A-5-3 returns into the folded state. In the presence of thrombin, the fluorescence of A-5-3 again is lower than in the absence of thrombin, indicating the repeated binding of the protein to the device.

V. CONCLUSIONS

We have investigated a variety of DNA nanodevices based on a thrombin-binding aptamer structure. The devices differ in fluorescent labeling and extensions of the aptamer core sequence on the 5' and 3' end. In gel titration experiments it is found that long sequence extensions on both the 5' and 3' ends destroy the protein binding capability of the device. Extension at the 5' end alone as well as fluorescent labeling does not reduce the binding affinity of the devices significantly. For the devices which retain their binding ability, apparent dissociation constants derived from the titration experiments are on the order of a few hundred nM. These values are probably systematically overestimated. The fact that the aptamer device can be labeled at both 5' and 3' end is utilized for the construction of a switchable aptamer beacon which can sense the presence of thrombin and also repeatedly bind and release it. Our findings have important consequences for the immobilization of our aptamer-based devices or their incorporation into larger DNA nanostructures [22, 23]. Any incorporation has to be made over the 5' end of the sequence. In particular, it will not be possible to attach the device over a spacer on the 3' end and simultaneously add an operator sequence for switching on the 5' end.

VI. ACKNOWLEDGMENTS*

This work was supported through an Emmy Noether grant by the Deutsche Forschungsgemeinschaft. W. U. D. gratefully acknowledges financial support by the Alexander von Humboldt foundation.

-
- [1] C. D. Mao, W. Q. Sun, Z. Y. Shen and N. C. Seeman, *Nature* 397, 144 (1999)
 [2] C. M. Niemeyer, M. Adler, S. Lenhart, S. Gao, H. Fuchs and L. F. Chi, *ChemBiochem* 2, 260 (2001)
 [3] D. S. Liu and S. Balasubramanian, *Angew. Chem. Int. Ed.* 42, 5734 (2003)
 [4] B. Yurke, A. J. Turberfield, A. P. Mills, F. C. Simmel

- and J. L. Neumann, *Nature* 406, 605 (2000)
 [5] H. Yan, X. P. Zhang, Z. Y. Shen and N. C. Seeman, *Nature* 415, 62 (2002)
 [6] J. W. J. Li and W. H. Tan, *Nano Lett.* 2, 315 (2002)
 [7] P. Alberti and J. L. Mergny, *Proc. Nat. Acad. Sci. USA* 100, 1569 (2003)
 [8] L. P. Feng, S. H. Park, J. H. Reif and H. Yan, *Angew.*

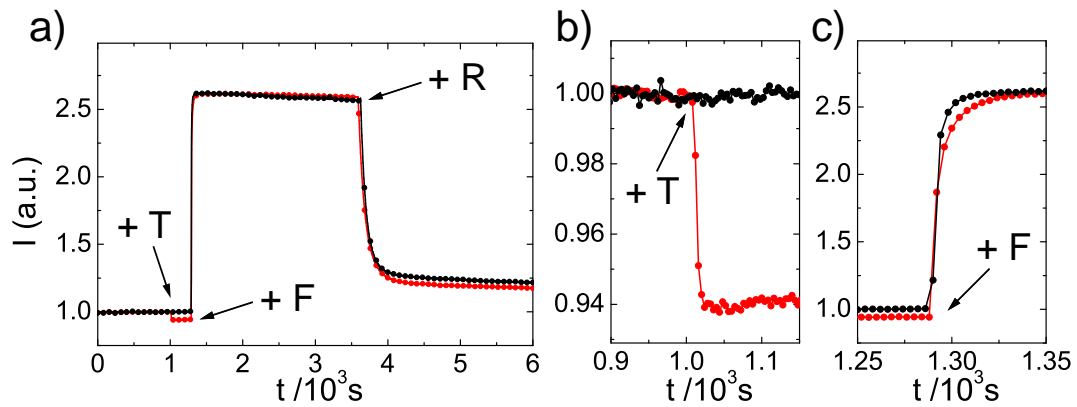


FIG. 5: FRET characterization of the beacon-like aptamer device A-5-3. a) The device is opened and closed by the addition of operator strands F and R. In the case of the red trace, the protein thrombin (T) is added at the point indicated in the graph. Conformational transitions result in changes in the energy transfer efficiency between the donor and acceptor dyes attached to A-5-3 which can be monitored by the fluorescence intensity. The binding to thrombin stabilizes the chair-conformation of A-5-3 leading to a slight decrease in fluorescence intensity. This “sensor action” is shown more clearly in b). The maximum fluorescence is measured for the completely stretched device (after the addition of F) and is independent of the presence of thrombin. After removal of F by R, the fluorescence of A-5-3 is lower in the presence of thrombin, as it again binds to the protein. b) Similarly to aptamer beacon sensors, A-5-3 responds to the presence of thrombin. c) The opening kinetics of the device is slowed down by the presence of thrombin.

Chem. Int. Ed. 42, 4342 (2003)

- [9] Y. Chen, M. S. Wang and C. D. Mao, *Angew. Chem. Int. Ed.* 43, 3554 (2004)
- [10] Y. Chen and C. D. Mao, *J. Am. Chem. Soc.* 126, 8626 (2004)
- [11] W. U. Dittmer, A. Reuter and F. C. Simmel, *Angew. Chem. Int. Ed.* 43, 3550 (2004)
- [12] D. S. Wilson and J. W. Szostak, *Ann. Rev. Biochem.* 68, 611 (1999)
- [13] S. Jhaveri, M. Rajendran and A. D. Ellington, *Nature Biotech.* 18, 1293 (2000)
- [14] S. D. Jhaveri, R. Kirby, R. Conrad, E. J. Maglott, M. Bowser, R. T. Kennedy, G. Glick and A. D. Ellington, *J. Am. Chem. Soc.* 122, 2469 (2000)
- [15] N. Hamaguchi, A. Ellington and M. Stanton, *Anal. Biochem.* 294, 126 (2001)
- [16] J. W. J. Li, X. H. Fang and W. H. Tan, *Biochem. Biophys. Res. Comm.* 292, 31 (2002)
- [17] R. Nutiu and Y. F. Li, *J. Am. Chem. Soc.* 125, 4771 (2003)
- [18] L. C. Bock, L. C. Griffin, J. A. Latham, E. H. Vermaas and J. J. Toole, *Nature* 355, 564 (1992)
- [19] T. Förster, *Ann. Phys.* 2, 55 (1948)
- [20] L. Stryer and R. P. Haugland, *Proc. Nat. Acad. Sci. USA* 58, 719 (1967)
- [21] A. Reuter, W. U. Dittmer, and F. C. Simmel, in preparation (2004).
- [22] N. C. Seeman, *Sci. Am.* 290, 64 (2004)
- [23] H. Y. Li, S. H. Park, J. H. Reif, T. H. LaBean and H. Yan, *J. Am. Chem. Soc.* 126, 418 (2004)

Periodic DNA Nanotemplates Synthesized by Rolling Circle Amplification

Stefan Beyer, Patrick Nickels, and Friedrich C. Simmel*

*Department of Physics and Center for Nanoscience,
Ludwig-Maximilians-Universität München, Geschwister-Scholl-Platz 1,
80539 München, Germany*

Received January 25, 2005; Revised Manuscript Received March 3, 2005

ABSTRACT

Rolling circle amplification (RCA) is an elegant biochemical method by which long single-stranded DNA molecules with a repeating sequence motif can be readily synthesized. In RCA, small circular single-stranded oligonucleotides serve as templates for the polymerization of the complementary strand. A DNA polymerase with an efficient strand displacement activity can copy the circular template without stopping. This results in a long DNA strand with periodic sequence. We here demonstrate that this method, using DNA recognition and biotin–streptavidin binding, provides a simple procedure for DNA-directed nanoscale organization of matter. As an example, a 74 nucleotide (nt) long circular DNA molecule is amplified into a sequence-periodic single strand with a length up to several micrometers. Hybridization of this long periodic DNA template to the biotinylated complement of the sequence motif results in a long DNA duplex with a periodic arrangement of biotin binding sites. On this duplex, streptavidin-coated particles can be organized into one-dimensional arrays. The resulting DNA constructs are characterized by gel electrophoresis and atomic force microscopy.

Biomolecular nanotechnology aims at the construction of complex nanoscale structures using self-assembly and self-organization strategies adopted from biological systems. One of the most prominent examples of biomolecular self-assembly is the molecular recognition between two single strands of DNA with complementary base sequences. These base-pairing interactions have already been used for the construction of a variety of geometric objects^{1–4} and also of complex two-dimensional lattices.^{5–8}

Only in a few cases these complex DNA nanostructures have also been utilized as scaffolds for the directed assembly of nanoparticles⁹ or proteins.¹⁰ There is a considerable body of work on DNA-directed organization of nanoparticles into simpler architectures,^{11–17} while other work concerned with functionalization of DNA with nanoparticles¹⁸ or conductive materials^{19–22} did not explicitly make use of the base-pairing interactions – even though this is the prime motivation for the usage of DNA in nanoconstruction. Instead, for convenience usually phage DNA (such as λ -DNA) was used. One notable exception is the development of sequence-specific lithography by Keren et al.^{23,24} which is based on homologous strand exchange assisted by the recombination protein RecA.

For many applications it would be desirable to produce a long one-dimensional DNA substrate with a designed DNA

sequence rather than having to work with a “random” phage genome. Oligonucleotides of arbitrary sequence can be synthesized base-by-base, but the yield of automated synthesis notoriously is very low for sequences much longer than 100 bases. Long DNA duplexes can be produced with some effort using PCR techniques,²⁵ but without periodic functionalization these DNA duplexes cannot be easily used for the arrangement of nanoobjects. In particular, a periodic duplex is not readily available for hybridization to a target sequence.

We here show how a simple enzymatic technique, rolling circle amplification (RCA), can be used to produce long single strands of DNA which have a repeating sequence with a designed repeat unit on the order of 100 bases. These repeat units can be addressed by hybridization to their complementary DNA sequence. We exemplify the utility of RCA for nanoconstruction by the organization of periodic one-dimensional assemblies of gold nanoparticles.²⁶

Rolling circle amplification^{27,28} is a variation of the standard DNA polymerization procedure and is used for signal amplification in mutation detection^{29–32} and in immunoassays.^{33,34} It also occurs naturally, e.g., during replication of viral RNA (cf. ref 35). In RCA, a single-stranded circular DNA (or RNA) substrate serves as the template for a DNA (or RNA) polymerase. The polymerase makes a copy of the circular template, but after completion of the first round it continues to copy the template sequence without stopping.

* Corresponding author. E-mail: simmel@lmu.de; Fax: (+49) 89 2180 3182.

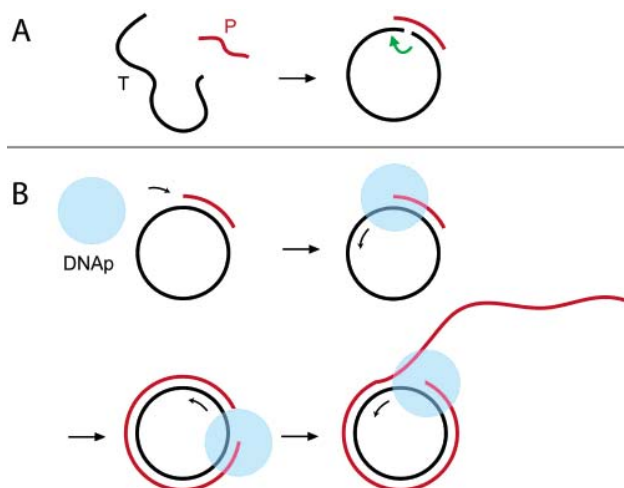


Figure 1. Rolling circle amplification. (A) A circular template is formed by the strands T and P. P holds together the ends of T for ligation and serves as a primer for the polymerization step. (B) A DNA polymerase starts copying the strand T at the primer P. After completion of one round it displaces the newly synthesized strand and starts another polymerization round. Several polymerization rounds lead to the formation of a long single strand with a repeating sequence. The basic repeat unit is the complement of the original template T.

Depending on the reaction conditions and the strand displacement capabilities of the polymerase, this can lead to the synthesis of a long single strand with a repeating sequence that is the complement of the circular template sequence.

The RCA procedure for our particular application is summarized in Figure 1. The circular template is created by hybridizing a 22 base long oligonucleotide P with the 74 nt long strand T. T carries a 5' phosphate and can be transformed into a circular molecule by T4 ligase (Figure 1 A). The strand P was designed to have one larger (16 bases) and one shorter (6 bases) overlap with T, the latter with a melting temperature higher than room temperature. By this construction, ring formation was favored over linear polymerization of several T strands joined by P strands. After ligation, P acted as a primer for the RCA procedure. The RCA reaction itself was carried out using DNA polymerase from phage $\phi 29$. This polymerase has exceptional strand displacement properties which is important for an efficient RCA.^{29,36} As depicted in Figure 1 B the polymerase starts to synthesize the complement of the template T at the primer P. After one round of polymerization it displaces the newly synthesized strand and continues with polymerization. This ultimately leads to a long strand with a sequence which is the repeated complement of T.

As depicted in Figure 2 A, the resulting single strand with periodic sequence can be transformed into a double strand by hybridizing it to the complement of the repeat unit (or appropriate subunits or multiples of that). If the complementary strands are functionalized, this leads to a periodic one-dimensional arrangement of the functional group.

The result of the RCA reaction was monitored by agarose gel electrophoresis (Figure 3). Gel lane a contains strands T

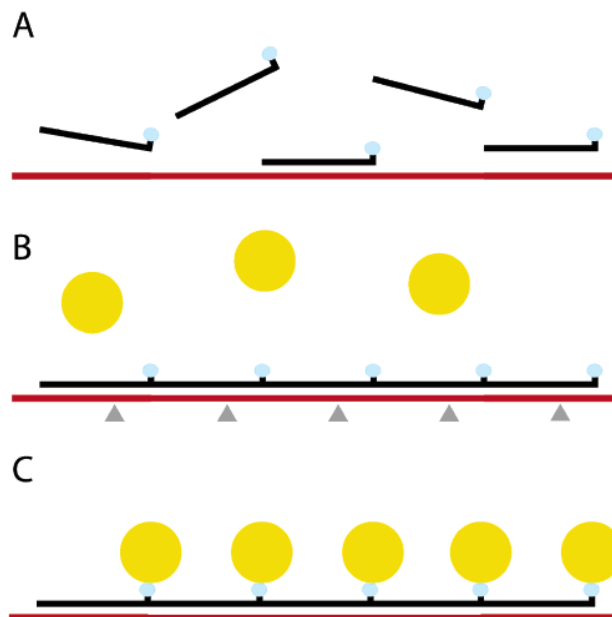


Figure 2. (A) The single-stranded templates (red) can be hybridized to short single strands with the same sequence as the original template T to produce long periodic double-strands. The short strands may be functionalized as indicated, which leads to a periodic arrangement of the functional group. (B and C) As an example, streptavidin-coated gold nanoparticles can be added to an RCA-synthesized template with periodically attached biotin, leading to a one-dimensional organization of the nanoparticles. The gray triangles in B indicate periodically arranged restriction sites that have been incorporated for characterization purposes (see text).

and P after the ligation reaction. Circularization is not complete. The lower band corresponds to unhybridized P, whereas the upper band contains circularized and noncircular T–P. The latter two species are not resolved in this gel. Circularization was checked, however, using lambda exonuclease, which only digests noncircular DNA strands (not shown). Lane b contains the result of the subsequent RCA reaction. The RCA product forms a sharp band with high molecular weight. If either no dNTPs, $\phi 29$ DNA polymerase, or templates were added to the reaction, no such band was observed. Heat inactivation of the polymerase or skipping the ligation step during template preparation impeded the RCA as well. The length of the resulting single strand was not dependent on the amount of additional primers, dNTPs, or polymerase. Test series with different concentrations of these reactants always resulted in single strands of the same length. This is consistent with earlier findings by other groups. The length of the product can only be varied by stopping the reaction within the first 20 min.²⁹ Gel lane c contains the result of a hybridization reaction between the RCA product and DNA strands complementary to the repeat unit. A smeared band develops, corresponding to a length of about 10 kbp as judged from a comparison with the 2-Log size standard ladder in lane e. The smearing probably occurs due to imperfect hybridization (not all of the repeat units are hybridized to their complement) and due to cross-linking of several RCA products by the complementary strands. To prove that lane c indeed contains a double-stranded product with a repeating sequence, a restriction site for endonuclease

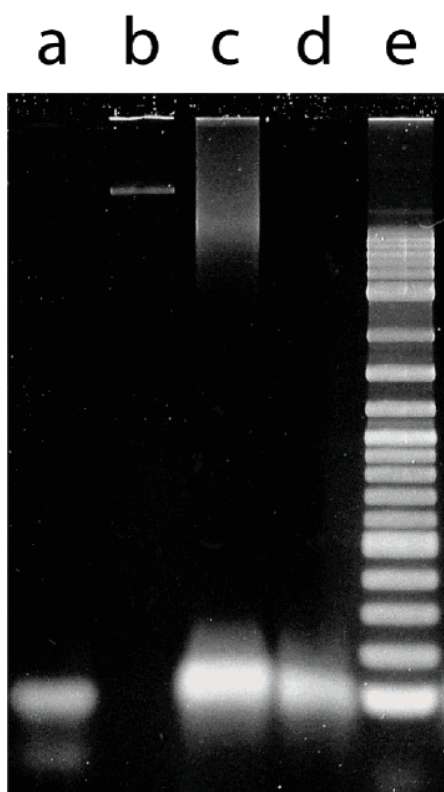


Figure 3. Characterization of the assembly procedure by agarose gel electrophoresis. Lane a contains strands T and P after the ligation procedure. The lower band corresponds to unhybridized P. The upper band contains both ligated and nonligated T–P hybrids, which are not resolved in this gel. Lane b contains the result of the RCA procedure. The amount of circular templates used for the reaction is 1/50 of the amount loaded into lane a. In lane c, the RCA product has been hybridized with an excess of strand T. The hybridization product shows up as a smeared band at around 10 kbp, the unhybridized T is on the bottom of the lane. In lane d, the contents of lane c have been digested with the restriction endonuclease HindIII. The high molecular weight product disappears and the cleavage product shows up at the bottom of the gel. Into lane e, a 2-Log DNA ladder has been loaded for comparison. The lowest band is 100 bp, the highest is 10 kbp long. Exact amounts of material loaded into the gel are given in the Supporting Information.

HindIII was incorporated into the template strands (also indicated in Figure 2 B). Lane d contains the product of a digestion reaction with the contents of lane c. The disappearance of the high molecular weight smeared band indeed proves that lane c contained long double stranded reaction products.

The RCA products were further characterized by atomic force microscopy (AFM). For Figure 4, the RCA product was hybridized to the complementary strand T. The resulting nicks were closed by ligation. The AFM image shows DNA strands with lengths of several hundred nanometers up to a few micrometers, demonstrating the successful generation of long DNA templates with defined sequence from a starting template of only ~25 nm length. For the one-dimensional organization of nanoparticles, the single-stranded periodic DNA template was hybridized to biotinylated DNA strands T-bt with the same sequence as strand T as schematically depicted in Figure 2. Subsequent incubation of the sample

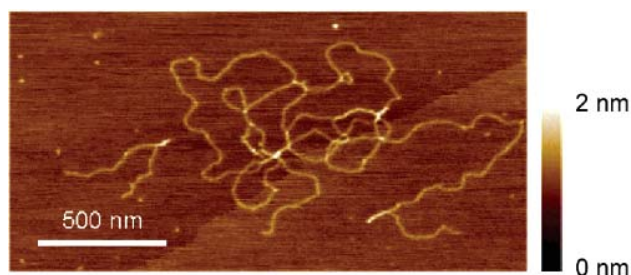


Figure 4. AFM image of the RCA product hybridized to the original template T deposited on mica. The DNA strands have lengths of at least several hundred nanometers. Bright regions (larger height) correspond to several DNA strands sticking together.

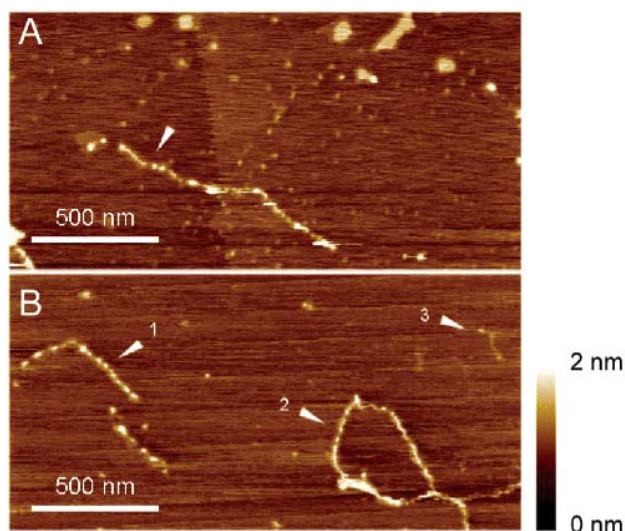


Figure 5. AFM images of the RCA product hybridized to the biotinylated template T-bt and incubated with streptavidin-coated gold nanoparticles with diameter 5 nm. In A, a DNA strand is densely coated with gold nanoparticles with a mutual distance between 30 and 50 nm. In B, densely coated strands can be seen (#1, #2), but also strands which are decorated with only few nanoparticles (#3).

with streptavidin-coated gold nanoparticles with a diameter of 5 nm led to an arrangement of the nanoparticles along the DNA template.³⁷ In Figure 5, several examples of DNA strands uniformly covered with gold nanoparticles are displayed. The distances measured between two particles are typically ~30 nm or ~50 nm, which is consistent with nanoparticles binding to every possible binding site with an occasional gap of one single unoccupied biotin. There are other examples where nanoparticle coverage is rather incomplete (Figure 5a, strand #3) and only few particles bind to the template. In general, coverage with nanoparticles is strongly dependent on the total concentration of DNA templates and nanoparticles, the ratio between these concentrations, and the details of the immobilization procedure. High concentrations can lead to the formation of extensively cross-linked networks, as the streptavidin-coated gold particles can link several templates together. In fact, at the concentrations used here, most of the strands with a length comparable to the undecorated strands shown in Figure 4 participate in agglomerated structures. Only shorter strands

as shown in Figure 5 could be imaged isolated from other structures. This problem could be circumvented, however, by using nanoparticles functionalized with a single antibiotic antibody.

In summary, we have shown how an enzymatic method, rolling circle amplification, can be used to produce single-stranded DNA templates with a length of several hundred nanometers which have a repeating sequence with a freely chosen repeat unit of approximately 100 nucleotides. By hybridization to the biotinylated complement of the repeat unit, the templates can be used to periodically arrange streptavidin-coated nanoparticles, or, in principle, any other nanoobject or functional group attached to the appropriate DNA sequence. The resulting 1D structures are, by their very nature, much less complex than the two-dimensional DNA lattices based on multiple crossover molecules or triangular building blocks. As some two-dimensional lattices composed of branched DNA junctions can be constructed from four sets of long periodic DNA strands, e.g., the Winfree tiling of the DAO-E type,⁵ it is conceivable that the RCA procedure could even be adapted for the self-assembly of 2D structures. The complexity of one-dimensional structures, however, is already sufficient for many applications and they are relatively simple to produce. One-dimensional chains of nanoparticles can serve as catalysts for subsequent localized materials deposition.¹⁸ Moreover, chains of metal particles with a defined separation are highly interesting in the context of plasmon waveguides.³⁸ In combination with sequence specific lithography,²³ the periodic templates could be used to produce wires with alternating material composition, e.g., semiconductor islands connected by metal contacts. Finally, an enzyme-based method offers the possibility of in situ synthesis of nanostructures starting from immobilized templates.³² This could be very helpful for the construction of hybrid systems in which a biomolecular nanostructure has to be embedded into a lithographically defined environment.

Acknowledgment. The authors thank Jörg P. Kotthaus for his continuous support and for hosting the biomolecular nanoscience group in his labs. The authors gratefully acknowledge financial support by the Deutsche Forschungsgemeinschaft (Emmy Noether program, SI 761/2-1 and -2).

Supporting Information Available: DNA sequences, details on the reaction conditions, AFM imaging procedures (PDF). This material is available free of charge via the Internet at <http://pubs.acs.org>.

References

- Chen, J. H.; Seeman, N. C. *Nature* **1991**, 350(6319), 631–633.
- Zhang, Y. W.; Seeman, N. C. *J. Am. Chem. Soc.* **1994**, 116(5), 1661–1669.
- Mao, C. D.; Sun, W. Q.; Seeman, N. C. *Nature* **1997**, 386(6621), 137–138.
- Shih, W. M.; Quispe, J. D.; Joyce, G. F. *Nature* **2004**, 427(6975), 618–621.
- Winfree, E.; Liu, F. R.; Wenzler, L. A.; Seeman, N. C. *Nature* **1998**, 394(6693), 539–544.
- Feng, L. P.; Park, S. H.; Reif, J. H.; Yan, H. *Angew. Chem., Int. Ed.* **2003**, 42(36), 4342–4346.
- Yan, H.; LaBean, T. H.; Feng, L. P.; Reif, J. H. *Proc. Natl. Acad. Sci. U.S.A.* **2003**, 100(14), 8103–8108.
- Liu, D.; Wang, M. S.; Deng, Z. X.; Walulu, R.; Mao, C. D. *J. Am. Chem. Soc.* **2004**, 126(8), 2324–2325.
- Xiao, S. J.; Liu, F. R.; Rosen, A. E.; Hainfeld, J. F.; Seeman, N. C.; Musier-Forsyth, K.; Kiehl, R. A. *J. Nanopart. Res.* **2002**, 4(4), 313–317.
- Yan, H.; Park, S. H.; Finkelstein, G.; Reif, J. H.; LaBean, T. H. *Science* **2003**, 301(5641), 1882–1884.
- Alivisatos, A. P.; Johnsson, K. P.; Peng, X. G.; Wilson, T. E.; Loweth, C. J.; Bruchez, M. P.; Schultz, P. G. *Nature* **1996**, 382(6592), 609–611.
- Mirkin, C. A.; Letsinger, R. L.; Mucic, R. C.; Storhoff, J. J. *Nature* **1996**, 382(6592), 607–609.
- Mucic, R. C.; Storhoff, J. J.; Mirkin, C. A.; Letsinger, R. L. *J. Am. Chem. Soc.* **1998**, 120(48), 12674–12675.
- Loweth, C. J.; Caldwell, W. B.; Peng, X. G.; Alivisatos, A. P.; Schultz, P. G. *Angew. Chem., Int. Ed.* **1999**, 38(12), 1808–1812.
- Mitchell, G. P.; Mirkin, C. A.; Letsinger, R. L. *J. Am. Chem. Soc.* **1999**, 121(35), 8122–8123.
- Niemeyer, C. M.; Adler, M.; Gao, S.; Chi, L. F. *Angew. Chem., Int. Ed.* **2000**, 39(17), 3055–3059.
- Weizmann, Y.; Patolsky, F.; Popov, I.; Willner, I. *Nano Lett.* **2004**, 4(5), 787–792.
- Patolsky, F.; Weizmann, Y.; Lioubashevski, O.; Willner, I. *Angew. Chem., Int. Ed.* **2002**, 41(13), 2323–2327.
- Braun, E.; Eichen, Y.; Sivan, U.; Ben-Yoseph, G. *Nature* **1998**, 391(6669), 775–778.
- Richter, J.; Seidel, R.; Kirsch, R.; Mertig, M.; Pompe, W.; Plaschke, J.; Schackert, H. K. *Adv. Mater.* **2000**, 12(7), 507.
- Richter, J.; Mertig, M.; Pompe, W.; Monch, I.; Schackert, H. K. *Appl. Phys. Lett.* **2001**, 78(4), 536–538.
- Nickels, P.; Dittmer, W. U.; Beyer, S.; Kotthaus, J. P.; Simmel, F. C. *Nanotechnol.* **2004**, 15, 1524–1529.
- Keren, K.; Krueger, M.; Gilad, R.; Ben-Yoseph, G.; Sivan, U.; Braun, E. *Science* **2002**, 297(5578), 72–75.
- Keren, K.; Berman, R. S.; Buchstab, E.; Sivan, U.; Braun, E. *Science* **2003**, 302(5649), 1380–1382.
- Rudert, W. A.; Trucco, M.; Multimers of specific DNA sequences generated by PCR. In *Genetic Engineering with PCR*; Horton, R. M., Tait, R. C., Eds.; Horizon Scientific Press: Wymondham, 1998; pp. 83–95.
- A related approach based on the enzyme telomerase has been taken by Weizmann et al. (ref 17). Using telomerase, however, one is restricted to a specific, and much shorter, repeat sequence (in this case 5'-TTAGGG-3').
- Fire, A.; Xu, S. Q. *Proc. Natl. Acad. Sci. U.S.A.* **1995**, 92(10), 4641–4645.
- Liu, D. Y.; Daubendiek, S. L.; Zillman, M. A.; Ryan, K.; Kool, E. T. *J. Am. Chem. Soc.* **1996**, 118(7), 1587–1594.
- Lizardi, P. M.; Huang, X. H.; Zhu, Z. R.; Bray-Ward, P.; Thomas, D. C.; Ward, D. C. *Nature Genetics* **1998**, 19(3), 225–232.
- Baner, J.; Nilsson, M.; Mendel-Hartvig, M.; Landegren, U. *Nucl. Acids Res.* **1998**, 26(22), 5073–5078.
- Dahl, F.; Baner, J.; Gullberg, M.; Mendel-Hartvig, M.; Landegren, U.; Nilsson, M. *Proc. Natl. Acad. Sci. U.S.A.* **2004**, 101(13), 4548–4553.
- Chen, Y.; Shortreed, M. R.; Peelen, D.; Lu, M. C.; Smith, L. M. *J. Am. Chem. Soc.* **2004**, 126(10), 3016–3017.
- Schweitzer, B.; Wiltshire, S.; Lambert, J.; O'Malley, S.; Kukanskis, K.; Zhu, Z. R.; Kingsmore, S. F.; Lizardi, P. M.; Ward, D. C. *Proc. Natl. Acad. Sci. U.S.A.* **2000**, 97(18), 10113–10119.
- Schweitzer, B.; Roberts, S.; Grimwade, B.; Shao, W. P.; Wang, M. J.; Fu, Q.; Shu, Q. P.; Laroche, I.; Zhou, Z. M.; Tchernev, V. T.; Christiansen, J.; Velleca, M.; Kingsmore, S. F. *Nature Biotechnol.* **2002**, 20(4), 359–365.
- Branch, A. D.; Robertson, H. D. *Science* **1984**, 223(4635), 450–455.
- Blanco, L.; Bernad, A.; Lazaro, J. M.; Martin, G.; Garmendia, C.; Salas, M. *J. Biol. Chem.* **1989**, 264(15), 8935–8940.
- Niemeyer, C. M.; Ceyhan, B.; Hazarika, P. *Angew. Chem., Int. Ed.* **2003**, 42(46), 5766–5770.
- Maier, S. A.; Kik, P. G.; Atwater, H. A.; Meltzer, S.; Harel, E.; Koel, B. E.; Requicha, A. A. G. *Nature Mater.* **2003**, 2(4), 229–232.

NL050155A

A modular DNA signal translator for the controlled release of a protein by an aptamer

Stefan Beyer and Friedrich C. Simmel*

Department of Physics and Center for Nanoscience, LMU München, Geschwister-Scholl-Platz 1, 80539 München, Germany

Received February 6, 2006; Revised and Accepted March 3, 2006

ABSTRACT

Owing to the intimate linkage of sequence and structure in nucleic acids, DNA is an extremely attractive molecule for the development of molecular devices, in particular when a combination of information processing and chemomechanical tasks is desired. Many of the previously demonstrated devices are driven by hybridization between DNA ‘effector’ strands and specific recognition sequences on the device. For applications it is of great interest to link several of such molecular devices together within artificial reaction cascades. Often it will not be possible to choose DNA sequences freely, e.g. when functional nucleic acids such as aptamers are used. In such cases translation of an arbitrary ‘input’ sequence into a desired effector sequence may be required. Here we demonstrate a molecular ‘translator’ for information encoded in DNA and show how it can be used to control the release of a protein by an aptamer using an arbitrarily chosen DNA input strand. The function of the translator is based on branch migration and the action of the endonuclease FokI. The modular design of the translator facilitates the adaptation of the device to various input or output sequences.

INTRODUCTION

In the past few years, the information encoding and strand recognition capabilities of DNA have been utilized for the realization of a variety of nanoscale DNA-based devices. DNA conformational changes have been shown to result in rotatory (1,2), stretching (3–12), and even translatory (13–18) movements. DNA devices have also been combined with functional nucleic acids such as ribozymes (9,17,19) and aptamers (20,21). Apart from chemomechanical action, DNA has also been demonstrated to be capable of a variety of information

processing tasks (22–28). One of the more recent developments here is the realization of autonomous molecular automata performing, e.g. simple logical computations (29–36).

To implement more complex functions into molecular systems, it is of great interest to combine the computational and chemomechanical capabilities of these devices by linking them together into artificial reaction networks. As one example, we demonstrated recently how the operation of a DNA nanomechanical device can be controlled by mRNA signals transcribed from regulatory ‘genes’ (37,38). However, in this case both the ‘gene’ and the DNA device were artificially constructed and the sequences could be chosen freely. In a more realistic application one would like to trigger the action of a DNA-based device with an arbitrary DNA or RNA input signal. As an example, consider the release of a specific molecule bound to a DNA aptamer in response to the presence of a particular mRNA molecule. In general, the sequence of the mRNA (indicating the expression of a gene) will be completely unrelated to the DNA aptamer sequence. There are several possible solutions to this problem. One solution commonly found in nature is ‘allosteric regulation’. Here two spatially separated binding sites on an enzyme communicate with each other via a conformational change triggered by the binding of an effector to one of the binding sites. Such a principle has been utilized previously for the construction of allosteric ribozymes or aptazymes [e.g. (39–41)], and also recently for the DNA-controlled release of a small molecule by an aptamer (21). In some cases, however, allosteric regulation may not be an option—e.g. when the binding capacity of an aptamer or the activity of a ribozyme is affected too strongly by sequence modifications and the introduction of a regulatory part is not feasible. For ribozyme regulation, one approach is the ‘expansive regulation’ strategy developed by Wang *et al.* (42,43). Here the activity of a ribozyme is regulated by an effector molecule stabilizing the ribozyme–substrate complex. To regulate protein release by an aptamer, in the present work an alternative approach is taken in which a DNA or RNA input signal is translated into the desired output signal by a molecular translation device. One possible realization of such a translator is the molecular automaton recently

*To whom correspondence should be addressed. Tel: +49 89 21805793; Fax: +49 89 21803182; Email: simmel@lmu.de

© The Author 2006. Published by Oxford University Press. All rights reserved.

The online version of this article has been published under an open access model. Users are entitled to use, reproduce, disseminate, or display the open access version of this article for non-commercial purposes provided that: the original authorship is properly and fully attributed; the Journal and Oxford University Press are attributed as the original place of publication with the correct citation details given; if an article is subsequently reproduced or disseminated not in its entirety but only in part or as a derivative work this must be clearly indicated. For commercial re-use, please contact journals.permissions@oxfordjournals.org

introduced by Benenson *et al.* (31) which is based on the action of the restriction endonuclease FokI. As a type II-S endonuclease, FokI cuts 9 and 13 nt away from its 5 nt recognition sequence, and therefore the 4 nt sticky end created by this process is unrelated to the recognition sequence itself. In Ref. (31), the recognition sequence for FokI was hidden within an internal loop of a DNA double strand. In the presence of input strands ('disease indicators'), the FokI recognition site was completed and a DNA 'drug'—the product of cleavage by FokI—was administered. We here use the FokI system as a DNA signal translator to trigger the release of a protein by an aptamer device using an arbitrarily chosen DNA input signal. In contrast to Ref. (29), the DNA signal translator used here consists of two hairpin structures which contain the FokI recognition site and the effector sequence, respectively. The FokI site is inactivated by initially hybridizing the hairpin to a 'protection' strand. The translator is activated through the removal of the protection strand by a DNA input strand with a sequence completely unrelated to the effector or aptamer sequence.

MATERIALS AND METHODS

Materials

FokI (4 U/ μ l) was obtained from New England Biolabs, human α -thrombin in solution (200 μ M) from Cell Systems, Germany. SYBR Gold nucleic acid stain was from Molecular Probes (Invitrogen), all other chemicals mentioned from Sigma-Aldrich. DNA strands were synthesized by biomers.net, Germany. The sequences of the oligonucleotides for the construction of the device (IN, CO, PR, OUT, APT) are given in Table 1. For fluorescence measurements a doubly labeled aptamer specific for the protein thrombin and extended by a 12 nt toehold was used (APT), similar to the aptamer device reported before (20,44). DNA strands were designed to minimize cross-hybridization and to have favorable ratios of melting temperatures in the different states of the device. The sequence generator software *DNAStructureCompiler* (45) was used for creating the sequences according to these specifications, the nucleic acids folding program *RNAstructure* (46) for checking the secondary structures.

Device preparation and gel electrophoresis

For gel electrophoresis experiments, DNA strands were diluted to 1 μ M in the hybridization buffer (50 mM potassium

acetate, 20 mM Tris-acetate, 10 mM magnesium acetate, 1 mM DTT, pH 7.9 at 25°C). The concentration of the strands was determined from their OD₂₆₀.

A typical reaction mixture contained 0.5 μ l CO, 2.5 μ l of PR, 4 μ l of OUT and 4 U/10 μ l FokI. The addition of 3 μ l of IN started the reaction. All samples were adjusted to the same volume prior to the FokI reaction. Samples were incubated at 20°C for 2 h and heated to 65°C for 15 min to denature FokI and terminate the reaction. All assays were run on native 18% polyacrylamide gels in TBE (Tris-borate-EDTA, pH 8.3) buffer at 100 V/cm for 1.5–2 h and stained with SYBR Gold using the manufacturer's protocol and imaged under UV illumination.

Fluorescence measurements

Fluorescence resonance energy transfer (FRET) experiments were performed with the doubly labeled DNA aptamer strand APT. In its folded G quadruplex state (compare Figure 5) its two ends are in close proximity and energy transfer from fluorescein to TAMRA occurs efficiently. When APT is stretched due to hybridization with the output strand, FRET between the fluorophores is less efficient and fluorescein fluorescence is increased. The fluorescence signal therefore directly monitors the progress of the hybridization reaction of the output strand with the target strand APT. For the fluorescence experiments, all DNA strands were initially diluted to 10 μ M. For the enzyme reaction, buffer composition, ratio of the strands, time and temperature was the same as for the gel assays. The FokI reaction was performed in a volume of 50 μ l containing 20 U of FokI and terminated before the FRET measurements.

For the measurements, the aptamer strands were diluted in 1 ml aptamer buffer (20 mM Tris-HCl, 150 mM NaCl, 10 mM MgCl₂ and 10 mM KCl, pH 8.0) to a final concentration of 75 nM.

FRET measurements were performed on a spectrofluorometer (Fluorolog-3, Jobin-Yvon, Munich, Germany). Fluorescence was excited at 490 nm and recorded at 515 nm, with excitation and emission bandwidths of 10 nm. The temperature was kept constant at 23°C.

Thrombin-aptamer complexes

For experiments with thrombin, the aptamer strand was mixed with thrombin in a ratio of 1:2. Aptamer and thrombin were incubated for 30 min at 23°C in a reaction volume of 50 μ l before FRET measurements were conducted in a sample volume of 1 ml.

Table 1. Sequences of the DNA strands used

Strand	Sequence (5'–3')
IN	GATTGCGGAAAGAAGGTATGAGATAATGTCAC
CO	GCTTGCATCCGATTGCGGAAAGAAGGTATGAGATCGG ATG
PR	GTGACATTATCTCATACCTTCTTTCCGCAATCGGA
OUT-1	CAAGCAAGTCGCATTCATCCACCAACCGAGATGAATGCG ACTT
OUT-1*	CGCATTATCCACCAACCGAGATGAA
OUT-2	CAAGCAGTGC GACTAACCAACCAACCGAGATGAACTTA GTCGCACT
OUT-2*	CGACTAACCAACCAACCGAGATGAACTTA
OUT-3	CAAGCTTAGCGACCAACCGAGATTTGGTTCGCTAA
OUT-3*	CGACCAACCGAGATTTG
APT	TAAGTTCATCTCGGTTGGTGTGGTTGG

RESULTS AND DISCUSSION

Operation principle of the DNA transducer

The operation principle of the transducer is schematically depicted in Figure 1. It is based on three processes which have been utilized previously for the operation of other DNA nanodevices and automata: (i) DNA branch migration (3); (ii) the specific DNA cleaving properties of the restriction endonuclease FokI (29); and (iii) the inhibition of hybridization between complementary strands by secondary structure formation (47). As shown in Figure 1A, the DNA output signal

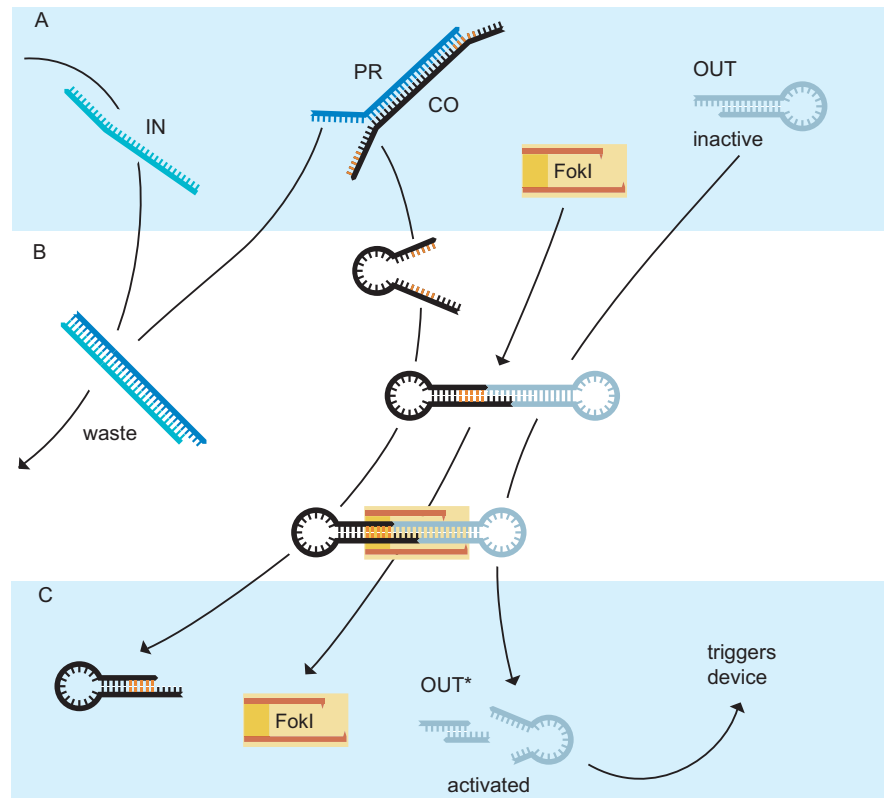


Figure 1. Operation principle of the DNA translator. (A) Initially, the output signal (OUT) is present in an inactive stem–hairpin loop conformation. Hybridization with the sequence hidden in the loop is kinetically inhibited. Also present is a ‘connector strand’ (CO) partially hybridized to a protection strand (PR) which in turn is complementary to the input signal strand. When added to the reaction, the input strand (IN) binds to the unhybridized ‘toehold’ section of the protection strand and displaces the connector through a branch migration process. (B) The connector is now able to fold into its hairpin configuration, the two halves of the FokI recognition site are united and are recognized by the enzyme. Together with the protected output signal strand, the connector forms a dumbbell shaped dimer and the FokI enzyme cuts the output strand 9 and 13 bases downstream of the recognition site, across the unligated nicks. The waste product formed by the input and protection strand is very stable and does not participate in the further reaction. (C) The stability of the remaining short stem of the output strand is too low to keep the loop closed and so the activated output signal OUT* can bind to other DNA-based devices to start or inhibit a reaction.

(OUT) initially is in an inactive state—it is forced into a small hairpin loop in which hybridization with its complement is inhibited (31,47). The stem of the hairpin has a sticky end which is complementary to the sticky end of a ‘connector strand’ (CO) which can also assume a hairpin conformation. However, initially the connector strand is forced into a duplex structure by a ‘protection strand’ (PR) in which it cannot hybridize to the inactive output strand. The protection strand in turn is equipped with a single-stranded ‘toehold’ (3) at which the input DNA strand (IN)—which is to be translated into an active output strand—can attach. The input strand can displace the protection strand from the connector strand by branch migration, producing a double-stranded waste product (IN-PR, Figure 1B). The released connector strand can now fold into its hairpin structure and hybridize to the inactive output signal. The sequence of the connector strand CO is chosen in such a way that in the folded state it contains the FokI recognition sequence (5′-GGATG-3′/3′-CCTAC-5′). FokI binds to the complex formed by connector and inactive output and cleaves the output strand 9 and 13 bases downstream from the FokI recognition site. As has been shown previously by Benenson *et al.* (30), FokI can cleave such a construct even without ligation of the two substrate duplexes. The result of the cleavage reaction is shown in Figure 1C.

The connector strand leaves the reaction unaltered, whereas the stem of the output signal strand has been shortened (OUT becomes OUT*). The loop conformation of the output strand is therefore less stable and breaks open which makes the output DNA sequence available for hybridization with a downstream target sequence. In the present example, the activated output signal can bind to an aptamer-based DNA device and trigger the release of the protein thrombin. The release of the protein is achieved by the competition for binding between the output strand and the protein to the aptamer. The output strand sequence therefore necessarily has to be chosen (at least partly) complementary to the aptamer sequence. Using the DNA translator, an arbitrarily chosen DNA input strand can be translated into this specific output strand.

Design of the input section

The various sections of the transduction device are indicated in Figure 2. In order to emphasize the modularity and generality of our approach, we here describe the design of the input and output sections in terms of an ‘algorithm’. (i) Given is the input signal strand IN which is to be transduced into a different sequence. This input signal can be of any sequence with length of >20 nt, it does not have to be extended

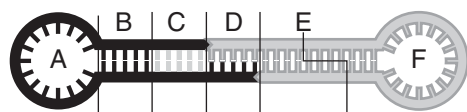


Figure 2. Core of the device composed of strands CO and OUT from Figure 1. Section A contains the part that is complementary to the protection strand PR. C is the FokI recognition sequence, spacer section B is needed to ensure that the binding of the enzyme is not disturbed by the loop A. Section D connects the two loops, it should be short and rich in GC pairs to improve FokI performance across the nicks. Line E indicates the FokI cleavage site, with the output F as result of the translation process.

or altered. (ii) The protection strand PR is the complement of strand IN and has to be augmented at the 3' end with the three bases 'GGA' contained in the FokI recognition sequence. This prevents the binding of FokI to dimers which may be formed by two protected connector strands in the inactive state of the device. (iii) The connector hairpin loop CO can be derived from IN in the following way: cut off 8–10 bases from the 3' end of IN, as they are used as toehold sequence for the displacement of PR from CO. (iv) Add the reverse complement of the first three bases of the 5' end to the 3' end, this acts as a spacer between the FokI binding site and the loop (compare section B of Figure 2). We experimentally verified that binding of FokI is obstructed if <3 bp are located upstream between the recognition sequence and the first bases of the loop. (v) Next add the FokI recognition sequences to the ends: CATCC to the 5' end and GGATG to the 3' end (C in Figure 2). (vi) As a last step, a sticky end has to be added to the connector hairpin (D in Figure 2). Since FokI cleaves asymmetrically with an overhang of 4 bases at the 5' end, it is best to attach the sticky end at the 5' end as well. The lower limit of the length of the sticky is set by the temperature at which the intermediate dumbbell structure (Figures 1B and 2) has to be stable. The upper limit is given by the distance between the recognition and the restriction site of FokI on the 5' end, i.e. 13 bases. Reasonable values are between 4 and 8 bases (compare next paragraph).

Design of the output section

The complement of the sequence of the target strand (e.g. an aptamer-based device) has to be incorporated into the stem and/or the loop of the output section (E and F in Figure 2). In the inactive state (before cleavage by FokI), hybridization between the output loop and the target strand should be kinetically inhibited, whereas in the active state this reaction should be fast. The stem of the output loop (E in Figure 2) therefore has to be sufficiently long to be stable in its uncleaved form and short enough to break open after restriction by FokI. Furthermore, the opening of the loop (F in Figure 2) has to be kept small enough to prevent the complementary strand from threading through (47). Several design variations based on these considerations are described below. The design of the sticky end connecting the input and output section of the device (D in Figure 2) has to ensure efficient cleavage by FokI. As described in Ref. (30), cleavage without prior ligation is possible for short sticky ends with a high CG-content. In experiments at various temperatures we found that the restriction reaction was successful with a 5 nt sticky end for temperatures up to 20°C. It has been found previously (30) that

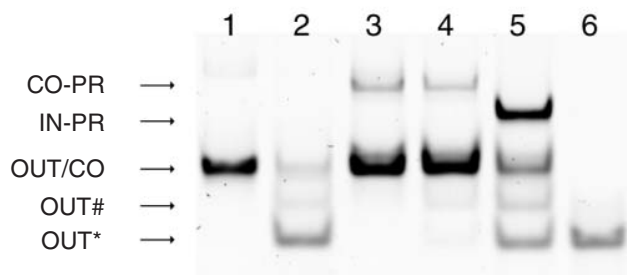


Figure 3. Operation of the device characterized by gel electrophoresis. Lane 1 contains output (OUT) and connector (CO) strand in the absence of FokI. Lane 2 contains OUT and CO with FokI added, leading to the appearance of the cleavage products OUT*, OUT#. The latter is due to incomplete cleavage of the output strand (see text). Lane 3 contains protected connector strand (CO-PR) and OUT in the absence of FokI; lane 4 contains the same strands plus FokI added. Almost no cleavage reaction occurs in this situation. In lane 5, the input strand IN was added to the mixture contained in lane 4, leading to cleavage of the output strand. A new band appears for the 'waste' product IN-PR. Lane 6 contains the pre-cleaved output strand OUT* for comparison.

with increasing length of the sticky ends, FokI tends to cut only one strand of the helix. This reaction results in an additional band in the gel assay (band OUT# in Figure 3). For efficient cleavage at relatively high temperatures, 4 or 5 bases are the best choices for the length of the sticky ends.

Experimental proof of the mechanism

The basic operation of the DNA translator was characterized in gel electrophoresis experiments. The gel image displayed in Figure 3 clearly demonstrates that FokI can cleave the output loop OUT in the presence of the connector loop CO even without ligation. It also shows that cleavage is inhibited when the connector strand CO is bound to the protection strand PR. When a removal strand IN is added to the reaction mixture, the protection strand is displaced from the input loop by branch migration and the restriction reaction starts. This can be monitored by the appearance of a band for the 'waste' duplex (IN-PR) and for the restricted output strand OUT*. The intensity of these bands can also be used to obtain the transfer function of the device which relates the concentration of the output strand to that of the input strand (Figure 4). For the strand concentrations used in this particular experiment (compare Materials and Methods), the I/O relation is slightly sigmoidal (Figure 4B). The linear relationship between band intensity and DNA concentration in the relevant concentration range used was verified in a separate experiment.

Influence of design parameters

As described above, several design parameters are critical for the operation of the DNA transducer: On the input side, the length of the spacer sequence (section B in Figure 2) is important. When shorter than 2 bp, the distance of the FokI recognition site and the loop is too small to accommodate the FokI enzyme. When larger than 4 bp, the formation of dimers between protected input strands leads to false positive reactions. The ideal length therefore turns out to be 3 bp. To reduce side reactions due to dimer formation, it is necessary that the protection strand not only overlaps with one side of the spacer sequence (B in Figure 2), but also with part of the recognition site (C in Figure 2). The length of the linker sequence

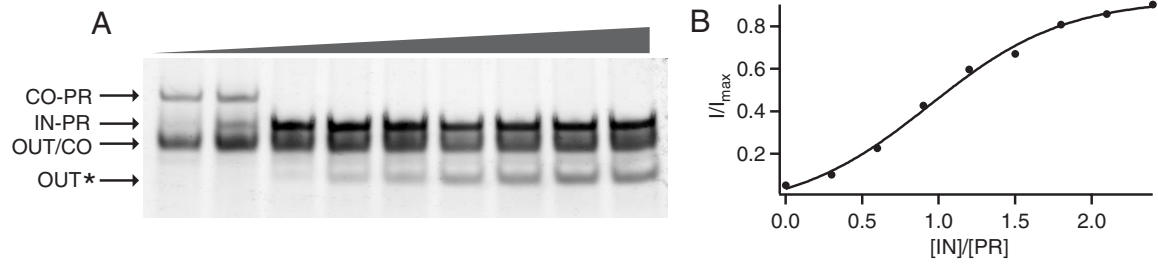


Figure 4. The response of the device depending on the input strand concentration. (A) Gel analysis of the device with different input signal amounts, ranging from 0 to 6 μ l of 1 μ M concentration. This highest value corresponds to 2.4 times the concentration of the protection strand, which was kept constant in all lanes. (B) A plot of the intensity of the product band as a function of input strand concentration.

(D in Figure 2) influences the temperature at which the device performs correctly. To be able to work at room temperature, an overlap of 5 bases was used in all cases.

The details of the design of the output end strongly influence the hybridization behavior of the device in the presence of the target DNA sequence. Ideally, in the inactive state, no hybridization between output loops and target DNA should occur. On the other hand, after activation of the translator by an input strand, hybridization of the target with the FokI cleavage product should occur efficiently. Experimentally, three different designs for the output section with different stem lengths and loop sizes were studied [OUT-1, 14 bp stem before, 6 bp stem after cleavage/10 nt loop; OUT-2, 11 bp (3 bp) stem/20 nt loop; OUT-3, 11 bp (3 bp) stem, 7 nt loop, (for sequences see Table 1)]. To study the hybridization kinetics, we first performed experiments with synthesized output strands with appropriately shortened sequences to mimic the behavior of the FokI reaction products. The hybridization kinetics of the three different output loops in their cleaved and uncleaved form was determined in FRET measurements. In all cases the target sequence for hybridization was the doubly labeled aptamer strand APT. Hybridization between the output strand and APT results in a strong increase in fluorescence, as the FRET donor (fluorescein) and acceptor (TAMRA) are spatially more separated from each other in the duplex form than in the folded single-stranded G quadruplex form of APT. As can be judged from Figure 5, the three different designs for the output section result in completely different hybridization kinetics. This is due mainly to two effects. First, hybridization of a DNA strand with a stable DNA hairpin loop is extremely slow. To form a double helix, the DNA strand has to form a few initial base pairs with bases in the loop and then wind through the loop hole. Depending on the size of the loop, this can be very slow or even impossible on an experimental time scale. It also has to be considered that hybridization of a DNA strand to a hairpin loop structure is reduced even further when no end of the strand is able to bind within the loop and break open the stem through branch migration (47).

The second important parameter—the stem length—has influence on the stability of the loop conformation. A short stem will break open occasionally and make the DNA loop sequence more accessible for hybridization with its complement. Similar effects have been studied extensively in the context of molecular beacons and also as a concept for fueling free-running DNA nanomachines.

OUT-2 and OUT-3 have the same stem lengths and different loop sizes, whereas OUT-1 and OUT-3 have different stem

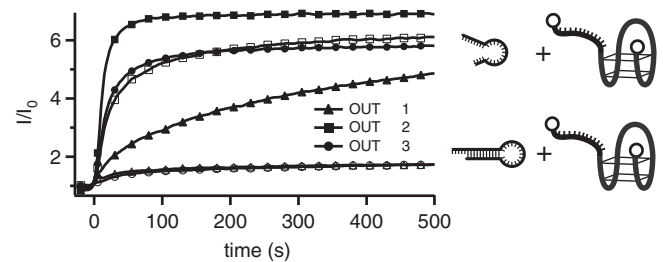


Figure 5. Binding kinetics of processed (closed symbols) and unprocessed (open symbols) output strands to the aptamer beacon APT, measured by FRET. The three strand designs differ in stem length and loop sizes (triangles, OUT-1, 14 bp stem/10 nt loop, OUT-1*, 6 bp stem/10 nt loop; squares, OUT-2, 11 bp stem/20 nt loop, OUT-2*, 3 bp stem/20 nt loop; circles, OUT-3, 11 bp stem/7 nt loop, OUT-3*, 3 bp stem/7 nt loop). Larger loop sizes lead to stronger unwanted interactions with the aptamer. The stem size further regulates the hybridization rate after output strand cleavage.

lengths and comparable loop sizes. As can be seen in Figure 5, owing to its 20 nt long loop region, OUT-2 already strongly hybridizes with the target sequence in the 'inactive' state before cleavage by FokI. In contrast OUT-1 and OUT-3—with the small loops—only show a low level of unwanted hybridization with the target. After cleavage, all output strands hybridize well with the target sequence. Here, OUT-1* displays slower hybridization kinetics than OUT-2* and OUT-3* as it still has a considerable stem length (6 bp) after cleavage.

Performance of the device

In Figure 6, the hybridization kinetics of the full translation device containing FokI, PR, CO, OUT-3 with the target strand APT is shown. Before the addition of the input signal IN, the spurious hybridization reactions are at roughly the same level as in a 'clean' system containing only OUT-3. After addition of the input signal strand IN, the degree of hybridization to the target is enhanced several fold, showing the successful performance of the DNA translation device. The efficiency of hybridization is comparable with that with the pre-cleaved strands OUT-3*. Also shown is a test experiment, in which only the arbitrarily chosen strand IN is added to the aptamer device APT. This input strand in fact does not display any interaction with the target at all. This demonstrates that the device in fact works as a signal translator. By the action of the translator an otherwise non-reactive input strand can influence the hybridization with a target sequence.

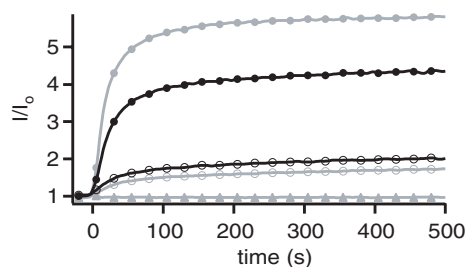


Figure 6. Comparison of the action of an output signal released by the translator device and a synthesized analogous output strand (OUT-3*). The closed circles represent the interaction between the aptamer beacon and the products of the device (solid, active; empty, idle). To examine the deviation from optimal performance, the same experiment was done with the inactive output loops only (gray open circles) and with pre-synthesized output loops (gray solid circles). Also shown is the direct interaction of the input signal with the aptamer beacon (gray triangles). As desired, the addition of the input strand leads to a strong enhancement of the hybridization signal (closed compared with open circles). The performance of the full translator device is almost as good as when only the pre-synthesized OUT-3* is hybridized to APT (gray solid circles).

Translator-controlled release of thrombin by the aptamer device

As an application of the signal translator concept, we demonstrate how the release of a protein by an aptamer-based DNA device can be controlled by an arbitrarily chosen DNA input signal. In Figure 7, the hybridization of the DNA translator reaction mixture with the DNA aptamer device APT bound to the protein thrombin is shown with and without the addition of the input strand IN. The initial fluorescence level is decreased to about 80% in comparison with Figure 6 ($I_{\text{bound}} = 0.78 I_0$), as the folded G quadruplex structure of APT is now bound to the protein, leading to a stronger FRET effect—i.e. APT acts as a sensor for thrombin (48,49). Upon hybridization of the output strands with the aptamer device the fluorescence intensity increases. In a simplified two-state model, the total fluorescence signal is given as $I(t) = \xi(t) I_{\text{released}} + [1 - \xi(t)] I_{\text{bound}}$, where $\xi(t)$ is the fraction of aptamers which have released their protein. I_{released} is the maximum fluorescence value obtained for aptamer beacons completely hybridized to the output strands and can be estimated from the limiting value $I_{\text{released}} = 5.8 I_0$ (from Figure 6), where I_0 is the initial fluorescence value for APT in the absence of protein. In Figure 7, the degree of protein release $\xi(t) = [I(t) - I_{\text{bound}}] / (I_{\text{released}} - I_{\text{bound}})$ is plotted. In the presence of the protein, this process is much slower than the hybridization of output strands with the aptamer without thrombin. The side reaction with the ‘inactive’ output strand OUT-3 already leads to a slight protein release. However, as desired the action of the DNA translator in response to the input strand IN leads to a much more efficient protein release. In principle, the side reaction could be completely suppressed if two distinct input signal strands were used and a correspondingly longer stem region for the inactive output strand (31).

CONCLUSIONS

We have demonstrated how a molecular signal translation device based on DNA hairpin loops and the action of the restriction endonuclease FokI can be used to release a specific

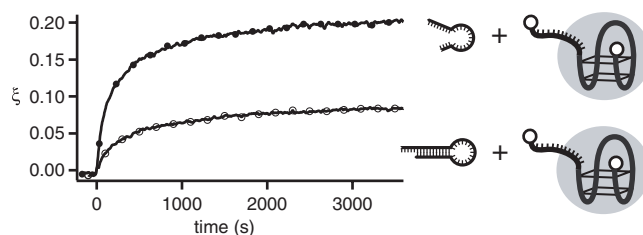


Figure 7. Fraction ξ of released thrombin controlled by the translation device. Closed circles, triggered device; open circles, idle device. The fraction ξ is determined indirectly from the fluorescence of the aptamer device as described in the text. The fact that the protein is initially bound to the aptamer results in a much slower kinetics of the change of the signal than in the absence of the protein.

DNA output strand in response to an arbitrarily chosen input strand. This translator can be used to uncouple nucleic acids-based signal and effector molecules and therefore link together molecular processes which produce or require specific DNA or RNA strands. Such situations may arise in DNA-based self-assembly, when the temporal or logical order of several self-assembly steps is to be controlled or when reaction networks of DNA-based nanodevices are to be constructed. Similar situations are of considerable interest in the context of intelligent biosensing or even drug delivery, when a specific compound is to be released in response to the presence of a certain nucleic acids molecule, e.g. mRNA. As a specific example, we demonstrated how the release of a protein by an aptamer-based nanodevice can be controlled by an arbitrarily chosen DNA strand which is translated by the molecular translator into a protein-releasing effector sequence.

ACKNOWLEDGEMENTS

Continuous support by Jörg P. Kotthaus is acknowledged. The authors acknowledge financial support by the Deutsche Forschungsgemeinschaft (Emmy Noether grant DFG SI 761/2-2). Funding to pay the Open Access publication charges for this article was provided by Nanion Technologies, GmbH, Munich, Germany.

Conflict of interest statement. None declared.

REFERENCES

- Mao, C.D., Sun, W.Q., Shen, Z.Y. and Seeman, N.C. (1999) A nanomechanical device based on the B–Z transition of DNA. *Nature*, **397**, 144–146.
- Yan, H., Zhang, X.P., Shen, Z.Y. and Seeman, N.C. (2002) A robust DNA mechanical device controlled by hybridization topology. *Nature*, **415**, 62–65.
- Yurke, B., Turberfield, A.J., Mills, A.P., Simmel, F.C. and Neumann, J.L. (2000) A DNA-fuelled molecular machine made of DNA. *Nature*, **406**, 605–608.
- Simmel, F.C. and Yurke, B. (2002) A DNA-based molecular device switchable between three distinct mechanical states. *Appl. Phys. Lett.*, **80**, 883–885.
- Li, J.W.J. and Tan, W.H. (2002) A single DNA molecule nanomotor. *Nano Lett.*, **2**, 315–318.
- Alberti, P. and Mergny, J.L. (2003) DNA duplex–quadruplex exchange as the basis for a nanomolecular machine. *Proc. Natl Acad. Sci. USA*, **100**, 1569–1573.
- Liu, D.S. and Balasubramanian, S. (2003) A proton-fuelled DNA nanomachine. *Angew. Chem. Int. Ed. Engl.*, **42**, 5734–5736.

8. Feng, L.P., Park, S.H., Reif, J.H. and Yan, H. (2003) A two-state DNA lattice switched by DNA nanoactuator. *Angew. Chem. Int. Ed. Engl.*, **42**, 4342–4346.
9. Chen, Y., Wang, M.S. and Mao, C.D. (2004) An autonomous DNA nanomotor powered by a DNA enzyme. *Angew. Chem. Int. Ed. Engl.*, **43**, 3554–3557.
10. Chen, Y., Lee, S.H. and Mao, C.D. (2004) A DNA nanomachine based on a duplex–triple transition. *Angew. Chem. Int. Ed. Engl.*, **43**, 5335–5338.
11. Shen, W.Q., Bruist, M.F., Goodman, S.D. and Seeman, N.C. (2004) A protein-driven DNA device that measures the excess binding energy of proteins that distort DNA. *Angew. Chem. Int. Ed. Engl.*, **43**, 4750–4752.
12. Brucalé, M., Zuccheri, G. and Samori, B. (2005) The dynamic properties of an intramolecular transition from DNA duplex to cytosine–thymine motif triplex. *Org. Biomol. Chem.*, **3**, 575–577.
13. Sherman, W.B. and Seeman, N.C. (2004) A precisely controlled DNA biped walking device. *Nano Lett.*, **4**, 1203–1207.
14. Yin, P., Yan, H., Daniell, X.G., Turberfield, A.J. and Reif, J.H. (2004) A unidirectional DNA walker that moves autonomously along a track. *Angew. Chem. Int. Ed. Engl.*, **43**, 4906–4911.
15. Shin, J.S. and Pierce, N.A. (2004) A synthetic DNA walker for molecular transport. *J. Am. Chem. Soc.*, **126**, 10834–10835.
16. Tian, Y. and Mao, C.D. (2004) Molecular gears: a pair of DNA circles continuously rolls against each other. *J. Am. Chem. Soc.*, **126**, 11410–11411.
17. Tian, Y., He, Y., Chen, Y., Yin, P. and Mao, C.D. (2005) Molecular devices—a DNzyme that walks processively and autonomously along a one-dimensional track. *Angew. Chem. Int. Ed. Engl.*, **44**, 4355–4358.
18. Bath, J., Green, S.J. and Turberfield, A.J. (2005) A free-running DNA motor powered by a nicking enzyme. *Angew. Chem. Int. Ed. Engl.*, **44**, 4358–4361.
19. Chen, Y. and Mao, C.D. (2004) Putting a brake on an autonomous DNA nanomotor. *J. Am. Chem. Soc.*, **126**, 8626–8627.
20. Dittmer, W.U., Reuter, A. and Simmel, F.C. (2004) A DNA-based machine that can cyclically bind and release thrombin. *Angew. Chem. Int. Ed. Engl.*, **43**, 3550–3553.
21. Kolpashchikov, D.M. and Stojanovic, M.N. (2005) Boolean control of aptamer binding states. *J. Am. Chem. Soc.*, **127**, 11348–11351.
22. Adleman, L.M. (1994) Molecular computation of solutions to combinatorial problems. *Science*, **266**, 1021–1024.
23. Ouyang, Q., Kaplan, P.D., Liu, S.M. and Libchaber, A. (1997) DNA solution of the maximal clique problem. *Science*, **278**, 446–449.
24. Sakamoto, K., Gouzu, H., Komiya, K., Kiga, D., Yokoyama, S., Yokomori, T. and Hagiya, M. (2000) Molecular computation by DNA hairpin formation. *Science*, **288**, 1223–1226.
25. Faulhammer, D., Cukras, A.R., Lipton, R.J. and Landweber, L.F. (2000) Molecular computation: RNA solutions to chess problems. *Proc. Natl Acad. Sci. USA*, **97**, 1385–1389.
26. Braich, R.S., Chelyapov, N., Johnson, C., Rothmund, P.W.K. and Adleman, L. (2002) Solution of a 20-variable 3-SAT problem on a DNA computer. *Science*, **296**, 499–502.
27. Su, X.P. and Smith, L.M. (2004) Demonstration of a universal surface DNA computer. *Nucleic Acids Res.*, **32**, 3115–3123.
28. Schmidt, K.A., Henkel, C.V., Rozenberg, G. and Spaink, H.P. (2004) DNA computing using single-molecule hybridization detection. *Nucleic Acids Res.*, **32**, 4962–4968.
29. Benenson, Y., Paz-Elizur, T., Adar, R., Keinan, E., Livneh, Z. and Shapiro, E. (2001) Programmable and autonomous computing machine made of biomolecules. *Nature*, **414**, 430–434.
30. Benenson, Y., Adar, R., Paz-Elizur, T., Livneh, Z. and Shapiro, E. (2003) DNA molecule provides a computing machine with both data and fuel. *Proc. Natl Acad. Sci. USA*, **100**, 2191–2196.
31. Benenson, Y., Gil, B., Ben-Dor, U., Adar, R. and Shapiro, E. (2004) An autonomous molecular computer for logical control of gene expression. *Nature*, **429**, 423–429.
32. Adar, R., Benenson, Y., Linshiz, G., Rosner, A., Tishby, N. and Shapiro, E. (2004) Stochastic computing with biomolecular automata. *Proc. Natl Acad. Sci. USA*, **101**, 9960–9965.
33. Stojanovic, M.N., Mitchell, T.E. and Stefanovic, D. (2002) Deoxyribozyme-based logic gates. *J. Am. Chem. Soc.*, **124**, 3555–3561.
34. Stojanovic, M.N. and Stefanovic, D. (2003) Deoxyribozyme-based half-adder. *J. Am. Chem. Soc.*, **125**, 6673–6676.
35. Stojanovic, M.N. and Stefanovic, D. (2003) A deoxyribozyme-based molecular automaton. *Nat. Biotechnol.*, **21**, 1069–1074.
36. Soreni, M., Yogev, S., Kossov, E., Shoham, Y. and Keinan, E. (2005) Parallel biomolecular computation on surfaces with advanced finite automata. *J. Am. Chem. Soc.*, **127**, 3935–3943.
37. Dittmer, W.U. and Simmel, F.C. (2004) Transcriptional control of DNA-based nanomachines. *Nano Lett.*, **4**, 689–691.
38. Dittmer, W.U., Kempter, S., Radler, J.O. and Simmel, F.C. (2005) Using gene regulation to program DNA-based molecular devices. *Small*, **1**, 709–712.
39. Robertson, M.P. and Ellington, A.D. (1999) In vitro selection of an allosteric ribozyme that transduces analytes to amplicons. *Nat. Biotechnol.*, **17**, 62–66.
40. Burgstaller, P., Jenne, A. and Blind, M. (2002) Aptamers and aptazymes: Accelerating small molecule drug discovery. *Curr. Opin. Drug Discov. Dev.*, **5**, 690–700.
41. Liu, J.W. and Lu, Y. (2004) Adenosine-dependent assembly of aptazyme-functionalized gold nanoparticles and its application as a colorimetric biosensor. *Anal. Chem.*, **76**, 1627–1632.
42. Wang, D.Y., Lai, B.H.Y. and Sen, D. (2002) A general strategy for effector-mediated control of RNA-cleaving ribozymes and DNA enzymes. *J. Mol. Biol.*, **318**, 33–43.
43. Wang, D.Y., Lai, B.H.Y., Feldman, A.R. and Sen, D. (2002) A general approach for the use of oligonucleotide effectors to regulate the catalysis of RNA-cleaving ribozymes and DNzymes. *Nucleic Acids Res.*, **30**, 1735–1742.
44. Beyer, S., Dittmer, W.U. and Simmel, F.C. (2005) Design variations for an aptamer-based DNA nanodevice. *J. Biomed. Nanotechnol.*, **1**, 96–101.
45. Feldkamp, U., Saghafi, S., Banzhaf, W. and Rauhe, H. (2001) DNA computing. In Jonoska, N. and Seeman, N.C. (eds), *Proceedings of Seventh International Workshop on DNA-Based Computers, DNA7*. Springer, Tampa, FL, Vol. 2340, pp. 23–32.
46. Mathews, D.H., Disney, M.D., Childs, J.L., Schroeder, S.J., Zuker, M. and Turner, D.H. (2004) Incorporating chemical modification constraints into a dynamic programming algorithm for prediction of RNA secondary structure. *PNAS*, **101**, 7287–7292.
47. Turberfield, A.J., Mitchell, J.C., Yurke, B., Mills, A.P., Blakey, M.I. and Simmel, F.C. (2003) DNA fuel for free-running nanomachines. *Phys. Rev. Lett.*, **90**, 118102.
48. Nutiu, R. and Li, Y.F. (2003) Structure-switching signaling aptamers. *J. Am. Chem. Soc.*, **125**, 4771–4778.
49. Hamaguchi, N., Ellington, A. and Stanton, M. (2001) Aptamer beacons for the direct detection of proteins. *Anal. Biochem.*, **294**, 126–131.

Bibliography

- [1] P. Nickels, W. U. Dittmer, S. Beyer, J. P. Kotthaus, and F. C. Simmel. Polyaniline nanowire synthesis templated by DNA. *Nanotechnology*, pages 1524–1529, 2004.
- [2] S. Beyer, P. Nickels, and F. Simmel. Periodic DNA nanotemplates synthesized by rolling circle amplification. *Nano Letters*, (4):pages 719–722, 2005.
- [3] S. Beyer, W. U. Dittmer, and F. C. Simmel. Design variations for an aptamer based device. *Journal of Biomedical Nanotechnology*, (1):pages 96–101, 2004.
- [4] S. Beyer and F. Simmel. A modular DNA signal transducer for the controlled release of a protein by an aptamer. *Proceedings of the National Academy of Science*, *submitted*.
- [5] S. I. Stupp, V. LeBonheur, K. Walker, L. S. Li, K. E. Huggins, M. Keser, and A. Amstutz. Supramolecular materials: Self-organized nanostructures. *Science*, (5311):pages 384–389, 1997.
- [6] U. B. Sleytr and T. J. Beveridge. Bacterial s-layer. *Trends Microbiol*, (6):pages 253–260, 1999.
- [7] S. Griessl, M. Lackinger, M. Edelwirth, M. Hietschold, and W. M. Heckl. Self-assembled two-dimensional molecular host-guest architectures from trimesic acid. *Single Molecules*, (1):pages 25–31, 2002.
- [8] J. W. Hong and S. R. Quake. Integrated nanoliter systems. *Nature Biotechnology*, pages 1179–1183, 2003.
- [9] C. Meyer, H. Lorenz, and K. Karrai. Optical detection of quasi-static actuation of nanoelectromechanical systems. *Applied Physics Letters*, (12):pages 2420–2422, 2003.
- [10] C. Wilson and J. W. Szostak. *In vitro evolution of a self-alkylating ribozyme*. *Nature*, 374:pages 777–782, 1995.
- [11] V. Balzani, A. Credi, F. M. Raymo, and J. F. Stoddart. *Artificial molecular machines*. *Angewandte Chemie-International Edition*, 39:pages 3348–3391, 2000.

- [12] Y. Shirai, A. J. Osgood, Y. Zhao, K. F. Kelly, and J. M. Tour. *Directional control in thermally driven single-molecule nanocars*. *Nano Letters*, (11):pages 2330–2334, 2005.
- [13] W. U. Dittmer, A. Reuter, and F. C. Simmel. *A DNA-based machine that can cyclically bind and release thrombin*. *Angewandte Chemie-International Edition*, pages 3550–3553, 2004.
- [14] D. L. Nelson and M. M. Cox. *Lehninger Principles of Biochemistry*. *Worth Publishers, New York, 3rd edition, 2000*.
- [15] V. A. Bloomfield, D. M. Cothers, and I. Tinoco. *Nucleic Acids*. *University Science Books, Sausalito, California, 2000*.
- [16] C. Storm and P. C. Nelson. *Theory of high-force DNA stretching and overstretching*. *Physical Review E*, (51906):pages 1–12, 2003.
- [17] C. Bustamante, J. F. Marko, E. D. Siggia, and S. Smith. *Entropic elasticity of lambda-phage DNA*. *Science*, pages 1599–1600, 1994.
- [18] R. B. Wallace, J. Shaffer, R. F. Murphy, J. Bonner, T. Hirose, and K. Itakura. *Hybridization of synthetic oligodeoxyribonucleotides to phi chi 174 DNA: the effect of single base pair mismatch*. *Nucleic Acids Research*, 6(11):pages 3543–3557, 1979.
- [19] P. M. Howley, M. F. Israel, M-F. Law, and M.A. Martin. *A rapid method for detecting and mapping homology between heterologous DNAs*. *Journal of Biological Chemistry*, 254(11):pages 4876–4883, 1979.
- [20] J. SantaLucia and D. Hicks. *The thermodynamics of DNA structural motifs*. *Annual Review Of Biophysics And Biomolecular Struc*, pages 415–440, 2004.
- [21] E. Winfree, F. Liu, L. A. Wenzler, and N. C. Seeman. *Design and self-assembly of two-dimensional DNA crystals*. *Nature*, pages 539–544, 1998.
- [22] E. Braun, Y. Eichen, U. Sivan, and G. Ben-Yoseph. *DNA-templated assembly and electrode attachment of a conducting silver wire*. *Nature*, pages 775–777, 1998.
- [23] D. Porath, A. Bezryadin, S. de Vries, and C. Dekker. *Direct measurement of electrical transport through DNA molecules*. *Nature*, pages 635–638, 2000.
- [24] C. Dekker and M. A. Ratner. *Electronic properties of DNA*. *Physics World*, pages 29–33, 2001.
- [25] L. T. Cai, H. Tabata, and T. Kawai. *Self-assembled DNA networks and their electrical conductivity*. *Applied Physics Letters*, pages 3105–3106, 2000.
- [26] H. W. Fink and C. Schonberger. *Electrical conduction through DNA molecules*. *Nature*, pages 407–410, 1999.

- [27] A. Y. Kasumov, M. Kociak, S. Gueron, B. Reulet, V. T. Volkov, D. V. Klinov, and H. Bouchiat. *Proximity-induced superconductivity in DNA*. *Science*, pages 280–282, 2001.
- [28] K. Keren, R. S. Bergman, E. Buchstab, U. Sivan, and E. Braun. *DNA-templated carbon nanotube field-effect transistor*. *Science*, pages 1380–1382, 2003.
- [29] D. S. Hopkins, D. Pekker, P. M. Goldbart, and A. Bezryadin. *Quantum interference device made by DNA templating of superconducting nanowires*. *Science*, pages 1762–1765, 2005.
- [30] K. Tanaka and M. Shionoya. *Synthesis of a novel nucleoside for alternative DNA base pairing through metal complexation*. *Journal of Organic Chemistry*, pages 5002–5003, 1999.
- [31] H. Weizman and Y. Tor. *2,2'-bipyridine ligandoxide: a novel building block for modifying DNA with intra-duplex metal complexes*. *Journal Of The American Chemical Society*, pages 3375–3376, 2001.
- [32] P. Aich, S. L. Labiuk, L. W. Tari, L. J. T. Delbaere, W. J. Roesler, K. J. Falk, R. P. Steer, and J. S. Lee. *M-DNA: a complex between divalent metal ions and DNA which behaves as a molecular wire*. *Journal of Molecular Biology*, pages 477–485, 1999.
- [33] K. Keren, M. Krueger, R. Gilad, G. BenYoseph, U. Sivan, and E. Braun. *Sequence specific molecular lithography on single DNA molecules*. *Science*, pages 72–75, 2002.
- [34] K. Keren, R. S. Bergman, and E. Braun. *Patterned DNA metallization by sequence-specific localization of a reducing agent*. *Nano Letters*, (2):pages 323–326, 2004.
- [35] J. Richter, R. Seidel, R. Kirsch, M. Mertig, W. Pompe, J. Plaschke, and H. K. Schackert. *Nanoscale palladium metallization of DNA*. *Advanced Materials*, pages 507–510, 2000.
- [36] T. Torimoto, M. Yamashita, S. Kuwabata, T. Sakata, H. Mori, and H. Yoneyama. *Fabrication of cds nanoparticle chains along DNA double strands*. *Journal of Physical Chemistry B*, pages 8799–8803, 1999.
- [37] W. U. Dittmer and F. C. Simmel. *Chains of semiconductor nanoparticles templated on DNA*. *Applied Physics Letters*, (4):pages 3550–3553, 2004.
- [38] N. C. Seeman and N. R. Kallenbach. *Design of immobile nucleic acid junctions*. *Biophysical Journal*, (2):pages 201–209, 1983.
- [39] Y. Wang, J. E. Mueller, B. Kemper, and N. C. Seeman. *The assembly and characterization of 5-arm and 6-arm DNA junctions*. *Biochemistry*, pages 5667–5674, 1991.

- [40] J. Chen and N. C. Seeman. *Synthesis from DNA of a molecule with the connectivity of a cube*. *Nature*, pages 631–633, 1991.
- [41] Y. Zhang and N. C. Seeman. *The construction of a DNA truncated octahedron*. *Journal Of The American Chemical Society*, pages 1661–1669, 1994.
- [42] C. Mao, W. Sun, and N. C. Seeman. *Assembly of borromean rings from DNA*. *Nature*, pages 137–138, 1997.
- [43] J. L. Coffey, S. R. Bigham, X. Li, R. F. Pinizzotto, Y. G. Rho, R. M. Pirtle, and I. L. Pirtle. *Dictation of the shape of mesoscale semiconductor nanoparticle assemblies by plasmid DNA*. *Applied Physics Letters*, pages 3851–3853, 1991.
- [44] C. A. Mirkin, R. L. Letsinger, R. C. Mucic, and J. J. Storhoff. *A DNA-based method for rationally assembling nanoparticles into macroscopic materials*. *Nature*, pages 607–609, 1996.
- [45] C. J. Loweth, W. B. Caldwell, X. G. Peng, A. P. Alivisatos, and P. G. Schultz. *DNA-based assembly of gold nanocrystals*. *Angewandte Chemie-International Edition*, (12):pages 1808–1812, 1999.
- [46] Y. Maeda, H. Tabata, and T. Kawai. *Two-dimensional assembly of gold nanoparticles with a DNA network template*. *Applied Physics Letters*, (8):pages 1181–1183, 2001.
- [47] T. J. Fu and N. C. Seeman. *DNA double-crossover molecules*. *Biochemistry*, pages 3211–3220, 1993.
- [48] T. H. LaBean, H. Yan, J. Kopatsch, F. Liu, E. Winfree, J. H. Reif, and N. C. Seeman. *Construction, analysis, ligation, and self-assembly of DNA triple crossover complexes*. *Journal Of The American Chemical Society*, pages 1848–1860, 2000.
- [49] F. R. Liu, R. J. Sha, and N. C. Seeman. *Modifying the surface features of two-dimensional DNA crystals*. *Journal Of The American Chemical Society*, pages 917–922, 1999.
- [50] W. M. Shih, J. D. Quispe, and G. F. Joyce. *A 1.7-kilobase single-stranded DNA that folds into a nanoscale octahedron*. *Nature*, pages 618–621, 2004.
- [51] D. Liu, S. H. Park, and J. H. Reif and T. H. LaBean. *DNA nanotubes self-assembled from triple-crossover tiles as templates for conductive nanowires*. *Proceedings of the National Academy of Science*, pages 717–722, 2004.
- [52] P. W. Rothmund, A. Ekani-Nkodo, N. Papadakis, A. Kumar, D. k. Fygenson, and E. Winfree. *Design and characterization of programmable DNA nanotubes*. *Journal Of The American Chemical Society*, pages 16344–16352, 2004.

- [53] S. H. Park, R. Barish, H. Li, J. H. Reif, G. Finkelstein, H. Yan, and T. LaBean. *Three bundle DNA tiles self-assemble into 2D lattice or 1d templates for silver nanowires*. Nano Letters, pages 693–696, 2005.
- [54] F. Mathieu, S. Liao, J. Kopatsch, T. Wang, C. Mao, and N. C. Seeman. *Six-helix bundles designed from DNA*. Nano Letters, pages 661–665, 2005.
- [55] P. W. Rothemund, N. Papadakis, and E. Winfree. *Algorithmic self-assembly of DNA sierpinski triangles*. PLoS Biology, (12):page e424, 2004.
- [56] C. Mao, T. H. LaBean, J. H. Reif, and N. C. Seeman. *Logical computation using algorithmic self-assembly of DNA triple-crossover molecules*. Nature, pages 493–496, 2000.
- [57] Z. Deng and C. Mao. *Molecular lithography with DNA nanostructures*. Angewandte Chemie-International Edition, pages 4068–4070, 2004.
- [58] Y. He, Y. Chen., H. Liu and A. E. Ribbe, and C. Mao. *Self-assembly of hexagonal DNA two-dimensional (2D) arrays*. Journal Of The American Chemical Society, pages 12202–12203, 2005.
- [59] S. H. Park, P. Yin, Y. Liu, J. H. Reif, , T. LaBean, and H. Yan. *Programmable DNA self-assemblies for nanoscale organization of ligands and proteins*. Nano Letters, pages 729–733, 2005.
- [60] H. Y. Li, S. H. Park, J. H. Reif, T. H. LaBean, and H. Yan. *DNA-templated self-assembly of protein and nanoparticle linear arrays*. Journal Of The American Chemical Society, pages 418–419, 2004.
- [61] H. Yan, S. H. Park, G. Finkelstein, J. H. Reif, and T. H. LaBean. *DNA-templated self-assembly of protein arrays and highly conductive nanowires*. Journal Of The American Chemical Society, pages 14246–14247, 2003.
- [62] C. M. Niemeyer, M. Adler, S. Gao, and L. F. Chi. *Supramolecular nanocircles consisting of streptavidin and DNA*. Angewandte Chemie International Edition, pages 3055–3059, 2000.
- [63] Y. Li, Y. D. Tseng, S. Y. Kwon, L. D’Espaux, J. S. Bunch, P. L. McEuen, and D. Luo. *Controlled assembly of dendrimer-like DNA*. Nature Materials, (1):pages 38–42, 2004.
- [64] A. Chworos, I. Severcan, A. Y. Koyfman, P. Weinkam, E. Oroudjev, H. G. Hansma, and L. Jaeger. *Building programmable jigsaw puzzles with RNA*. Science, pages 2068–2072, 2004.

- [65] J. Malo, J. C. Mitchell, C. Vnien-Bryan, J. R. Harris, H. Wille, D. J. Sherratt, and A. J. Turberfield. *Engineering a 2D protein-DNA crystal*. *Angewandte Chemie International Edition*, (20):pages 3057–3061, 2005.
- [66] D. Liu, M. S. Wang, Z. X. Deng, R. Walulu, and C. D. Mao. *Tensegrity: Construction of rigid DNA triangles with flexible four-arm DNA junctions*. *Journal Of The American Chemical Society*, pages 2324–2325, 2004.
- [67] Y. Weizmann, F. Patolsky, I. Popov, and I. Willner. *Telomerase generated templates for the growing of metal nanowires*. *Nano Letters*, (4):pages 787–792, 2004.
- [68] A. Fire and S. Xu. *Rolling replication of short DNA circles*. *Proceedings of the National Academy of Science*, (92):pages 4641–4645, 1995.
- [69] J. Banr, M. Nilsson, M. Mendel-Hartvig, and U. Landegren. *Signal amplification of padlock probes by rolling circle replication*. *Nucleic Acids Research*, (22):pages 5073–5078, 1998.
- [70] M. Lizardi, X. H. Huang, Z. R. Zhu, P. Bray-Ward, D. C. Thomas, and D. C. Ward. *Mutation detection and single-molecule counting using isothermal rolling-circle amplification*. *Nature Genetics*, pages 225–232, 1998.
- [71] Z. Deng, Y. Tian, S. H. Lee, A. E. Ribbe, and C. Mao. *DNA-encoded self-assembly of gold nanoparticles into one-dimensional arrays*. *Angewandte Chemie-International Edition*, pages 2–5, 2005.
- [72] D. Lubrich, J. Bath, and A. Turberfield. *Design and assembly of double crossover linear arrays of micrometer length using rolling circle replication*. *Nanotechnology*, pages 1574–1577, 2005.
- [73] M. Zivarts, Y. Liu, and R. R. Breaker. *Engineered allosteric ribozymes that respond to specific divalent metal ions*. *Nucleic Acids Research*, (2):pages 622–631, 2005.
- [74] M. N. Stojanovic, P. De Prada, and D. W. Landry. *Aptamer-based folding fluorescent sensor for cocaine*. *Journal Of The American Chemical Society*, pages 4928–4931, 2001.
- [75] L. C. Bock, L. C. Griffin, J. A. Latham, E. H. Vermaas, and J. J. Toole. *Selection of single-stranded-DNA molecules that bind and inhibit human thrombin*. *Nature*, pages 564–566, 1992.
- [76] D. Grate and C. Wilson. *Laser-mediated, site-specific inactivation of RNA transcripts*. *Proceedings of the National Academy of Science*, (11):pages 6131–6136, 1999.

- [77] O. Kensch, B. A. Connolly, H. J. Steinhoff, A. McGregor, R. S. Goody, and T. Restle. *Hiv-1 reverse transcriptase-pseudoknot RNA aptamer interaction has a binding affinity in the low picomolar range coupled with high specificity*. *Journal of Biological Chemistry*, (24):pages 18271–18278, 2000.
- [78] L. Gold. *Oligonucleotides as research, diagnostic, and therapeutic agents*. *Journal of Biological Chemistry*, (23):pages 13581–13584, 1995.
- [79] C. P. Rusconi, J. D. Roberts, G. A. Pitoc, S. M. Nimjee, R. R. White, G. Quick, E. Scardino, W. P. Fay, and B. A. Sullenger. *Antidote-mediated control of an anti-coagulant aptamer in vivo*. *Nature Biotechnology*, pages 1423–1428, 2004.
- [80] C. Mao, W. Sun, Z. Shen, and N. C. Seeman. *A nanomechanical device based on the b-z transition of DNA*. *Nature*, pages 144–146, 1999.
- [81] D. S. Liu and S. Balasubramanian. *A proton-fuelled DNA nanomachine*. *Angewandte Chemie-International Edition*, pages 5734–5736, 2003.
- [82] Y. Chen, S-H. Lee, and C. Mao. *A DNA nanomachine based on a duplex-triplex transition*. *Angewandte Chemie International Edition*, pages 5535–5538, 2004.
- [83] R. P. Fahlman, M. Hsing, C. S. Sporer-Tuhten, and D. Sen. *Duplex pinching: A structural switch suitable for contractile DNA nanoconstructions*. *Nano Letters*, pages 1073–1078, 2003.
- [84] B. Yurke, A. J. Turberfield, Mills and Jr. and A. P., F. C. Simmel, and J. L. Neumann. *A DNA-fuelled molecular machine made of DNA*. *Nature*, pages 605–608, 2000.
- [85] F. C. Simmel and B. Yurke. *A DNA-based molecular device switchable between three distinct mechanical states*. *Applied Physics Letters*, pages 883–885, 2002.
- [86] W. U. Dittmer, S. Kempter, J. O. Radler, and F. C. Simmel. *Using gene regulation to program DNA-based molecular devices*. *Small*, pages 709–712, 2005.
- [87] L. M. Adleman. *Molecular computation of solutions to combinatorial problems*. *Science*, 266:pages 1021–1024, 1994.
- [88] M. N. Stojanovic and D. Stefanovic. *A desoxyribozyme-based molecular automaton*. *Nature Biotechnology*, pages 1069–1074, 2003.
- [89] M. N. Stojanovic, T. E. Mitchell, and D. Stefanovic. *Desoxyribozyme-based logic gates*. *Journal Of The American Chemical Society*, pages 3555–3561, 2002.
- [90] Y. Benenson, T. Paz-Elizur, R. Adar, E. Keinan, Z. Livneh, and E. Shapiro. *Programmable and autonomous computing machine made of biomolecules*. *Nature*, pages 430–434, 2001.

- [91] Y. Benenson, R. Adar, T. Paz-Elizur, Z. Livneh, and E. Shapiro. *DNA molecule provides a computing machine with both data and fuel*. Proceedings of the National Academy of Science, (5):pages 2191–2196, 2003.
- [92] Y. Chen, M. Wang, and C. Mao. *An autonomous DNA nanomotor powered by a DNA enzyme*. Angewandte Chemie International Edition, pages 3638–3641, 2004.
- [93] W. B. Sherman and N. C. Seeman. *A precisely controlled DNA biped walking device*. Nano Letters, (7):pages 1203–1207, 2004.
- [94] J. S. Shin and N. A. Pierce. *A synthetic DNA walker for molecular transport*. Journal Of The American Chemical Society, pages 10834–10835, 2004.
- [95] J. Bath, S. J. Green, and A. J. Turberfield. *A free-running DNA motor powered by a nicking enzyme*. Angewandte Chemie-International Edition, pages 4358–4361, 2005.
- [96] Y. Tian, Y He, Y. Chen, and C. Mao. *A DNzyme walks processively and autonomously along a one-dimensional track*. Angewandte Chemie-International Edition, pages 4355–4358, 2005.
- [97] R. D. Vale, T. S. Reese, and M. P. Sheetz. *Identification of a novel force-generating protein, kinesin, involved in microtubule-based motility*. Cell, pages 39–50, 1985.
- [98] R. Nutiu and Y. Li. *Structure-switching aptamers*. Journal Of The American Chemical Society, pages 4771–4778, 2003.
- [99] G. A. Soukup and R. R. Braker. *Engineering precision molecular switches*. Proceedings of the National Academy of Science, pages 3584–3589, 1999.
- [100] D. M. Kolpashchikov and M. N. Stojanovic. *Boolean control of aptamer binding states*. Journal Of The American Chemical Society, pages 11348–11351, 2005.
- [101] Y. Liu, C. X. Lin, H. Y. Li, and H. Yan. *Protein nanoarrays - aptamer-directed self-assembly of protein arrays on a DNA nanostructure*. Angewandte Chemie-International Edition, pages 4333–4338, 2005.
- [102] D. M. Tasset, M. F. Kubik, and W. Steiner. *Oligonucleotide inhibitors of human thrombin that bind distinct epitopes*. Journal of Molecular Biology, pages 688–698, 1997.
- [103] C. V. Miduturu and S. K. Silverman. *DNA constraints allow rational control of macromolecular conformation*. Journal Of The American Chemical Society, 127:pages 10144–10145, 2005.
- [104] Y. Benenson, B. Gil, U. Ben-Dor, R. Adar, and E. Shapiro. *An autonomous molecular computer for logical control of gene expression*. Nature, pages 423–429, 2004.

[105] *H. Yan, T. H. LaBean, L. P. Feng, and J. H. Reif. Directed nucleation assembly of DNA tile complexes for barcode-patterned lattices. Proceedings of the National Academy of Science, pages 8103–8108, 2003.*

Danksagung

Mein herzlicher Dank geht an alle, die zum Gelingen der Arbeit beigetragen haben:

- Prof. Jörg P. Kotthaus, für die Möglichkeit an seinem Lehrstuhl forschen zu dürfen. Es war außerordentlich angenehm in dieser Atmosphäre aus Forscherdrang und Gelassenheit zu arbeiten und zu wissen, dass Du kompromisslos hinter Deinen Leuten stehst.
- Fritz Simmel, für die Auswahl meines Themas, das bis zum Ende interessant und fordernd geblieben ist. Danke für die super Betreuung, die kreativen Ideen und Diskussionen, und die Zeit und Geduld, die Du mir gewidmet hast.
- Wendy Dittmer, Partick Nickels und Ralph Sperling, für die Unterstützung bei der Übernahme der Weltherrschaft mit Hilfe von Nanomaschinen.
- der gesamten Arbeitsgruppe, Andreas Reuter, Michael Olapinski, Tim Liedl und Eike Friedrichs für die gute Zusammenarbeit und das angenehme Arbeitsklima.
- Christine Meyer und Marion Hochrein, für die Unterstützung bei Lithographie und Mikroskopie.
- Stefan Schöffberger, Alex Paul, Armin Kriele und Klaus Wehrhahn, für Euren unermüdlichen Einsatz im Reinraum.
- Bert Lorenz, Wolfgang Kurpas, Stefan Manus und Pit Kiermeier, für Eure Hilfe bei vielen kleinen und großen Problemen.
- Martina Jüttner, für die freundliche Unterstützung bei allem, was mit Physik nicht mehr zu bewältigen ist, z. B. der Kampf mit der Verwaltung.
- Susi Kempfer und Gerlinde Schwake, für die unermüdliche Rettung von Physikern aus den Strudeln der Biochemie.
- Den ehemaligen und aktuellen Hinterzimmerinsassen für die gute Stimmung im Büro und Einblick in andere Forschungsgebiete.
- meiner Familie, für ihre moralische Unterstützung.
- Denise, dafür dass Du mich während der stressigen Zeit unterstützt und ertragen hast und meine Arbeit in eine Form gebracht hast, die nicht nur Physiker anspricht.

Lebenslauf

Stefan Christoph Beyer, geboren am 30.09.1975 in Gräfelfing, ledig

Ab 2002

Wissenschaftlicher Mitarbeiter der Ludwig-Maximilians Universität München
am Lehrstuhl für angewandte Physik (Prof. J. P. Kotthaus)

Januar 2002

Physik-Diplom an der technischen Universität München
Lehrstuhl für Physik (Prof. E. Sackmann)

2001- 2002

Diplomarbeit bei der Firma Zyomyx, Hayward, Kalifornien, USA
Diplomarbeitsthema: Schnelle Impedanzspektroskopie von
substratgestützten Lipidmembranen.

1995-2002

Studium der Physik an der technischen Universität München

1986-1995

Gymnasium Geretsried
Abschluss: Abitur

1982-1986

Grundschule Waldram

München, der 23.12.2005